Behavior of Reinforced Concrete Beams Strengthened Using CFRP Sheets with Superior Anchorage Devices

by

Mohammed Ameen Zaki

B.S., University of Technology, Baghdad, 2007
M.S., University of Massachusetts Amherst, 2016

AN ABSTRACT OF A DISSERTATION

submitted in partial fulfillment of the requirements for the degree

DOCTOR OF PHILOSOPHY

Department of Civil Engineering
Collage of Engineering

KANSAS STATE UNIVERSITY
Manhattan, Kansas

2018

Abstract

The use of carbon fiber reinforced polymer (CFRP) anchors can improve the performance of reinforced concrete (RC) beams strengthened in flexure with CFRP sheets. This improvement results from delaying or controlling the debonding of FRP sheets at failure. In this research, six full-scale T beams and six full-scale rectangular beams are prepared and tested as two separate series. All the specimens are strengthened identically using three layers of unidirectional CFRP sheets and one layer of bidirectional CFRP sheet. The first strengthened beam in each series is anchored with side GFRP bars inserted longitudinally to both sides of the beam. The second strengthened beam in each series is anchored with GFRP patches applied to both sides of the beam. CFRP spike anchors are utilized for the other beams in the two series. The third beam in each series is secured with CFRP spike anchors of 16 mm diameter at 140 mm spacing along the shear span. The fourth strengthened beam in each series is anchored with CFRP spike anchors of 19 mm diameter at 203 mm spacing along the shear span. Four CFRP anchors are applied to each shear span of the fifth beam in each series with 16 mm- diameter (spaced at 406 mm) to secure the flexural CFRP sheets. An end CFRP anchorage technique is considered for the last beam in each series, which includes installing one CFRP spike anchor placed at 76 mm from the free edge of CFRP sheets. The beams were tested under four-point bending until failure and the results for each series are evaluated. In addition, the outcome is compared with other anchorage techniques that have been examined by some researchers utilizing the same beam geometry and properties. The experimental testing and nonlinear analysis showed improvement in the flexural performance of anchored beams compared with those strengthened beams without anchorage. By attaining debonding or rupture failure modes for the T beams and concrete crushing failure mode for the

rectangular specimens, the ultimate sectional force capacity is achieved. Accordingly, the results prove that the anchors offer an effective solution against premature debonding failure.

Behavior of Reinforced Concrete Beams Strengthened Using CFRP Sheets with Superior Anchorage Devices

by

Mohammed Ameen Zaki

B.S., University of Technology, Baghdad, 2007
M.S., University of Massachusetts Amherst, 2016

A DISSERTATION

submitted in partial fulfillment of the requirements for the degree

DOCTOR OF PHILOSOPHY

Department of Civil Engineering
Collage of Engineering

KANSAS STATE UNIVERSITY
Manhattan, Kansas

2018

Approved by:

Major Professor
Hayder A. Rasheed

Copyright

Abstract

The use of carbon fiber reinforced polymer (CFRP) anchors can improve the performance of reinforced concrete (RC) beams strengthened in flexure with CFRP sheets. This improvement results from delaying or controlling the debonding of FRP sheets at failure. In this research, six full-scale T beams and six full-scale rectangular beams are prepared and tested as two separate series. All the specimens are strengthened identically using three layers of unidirectional CFRP sheets and one layer of bidirectional CFRP sheet. The first strengthened beam in each series is anchored with side GFRP bars inserted longitudinally to both sides of the beam. The second strengthened beam in each series is anchored with GFRP patches applied to both sides of the beam. CFRP spike anchors are utilized for the other beams in the two series. The third beam in each series is secured with CFRP spike anchors of 16 mm diameter at 140 mm spacing along the shear span. The fourth strengthened beam in each series is anchored with CFRP spike anchors of 19 mm diameter at 203 mm spacing along the shear span. Four CFRP anchors are applied to each shear span of the fifth beam in each series with 16 mm- diameter (spaced at 406 mm) to secure the flexural CFRP sheets. An end CFRP anchorage technique is considered for the last beam in each series, which includes installing one CFRP spike anchor placed at 76 mm from the free edge of CFRP sheets.

The beams were tested under four-point bending until failure and the results for each series are evaluated. In addition, the outcome is compared with other anchorage techniques that have been examined by some researchers utilizing the same beam geometry and properties. The experimental testing and nonlinear analysis showed improvement in the flexural performance of anchored beams compared with those strengthened beams without anchorage. By attaining debonding or rupture failure modes for the T beams and concrete crushing failure mode for the

rectangular specimens, the ultimate sectional force capacity is achieved. Accordingly, the results prove that the anchors offer an effective solution against premature debonding failure.

Table of Contents

List of Figures

List of Tables

Acknowledgements

I would like to thank and acknowledge all the following people who helped make this dissertation possible and an unforgettable experience for me.

I would like to express my sincere gratitude and special appreciate to my major advisor Prof. Hayder Rasheed for his continuous support of my Ph.D study and research, for his patience, motivation, enthusiasm and immense knowledge. His guidance helped me throughout the research and writing of this dissertation. I cannot imagine having a better advisor and mentor for my Ph.D. study than Dr. Rashheed. I am blessed to have him as my doctoral advisor.

I would also like to thank my committee members, Dr. Hani Melhem, Dr. Christopher Jones, and Dr. Bacim Alali for their willingness to serve on my supervisory committee and provide me with their wise comments and recommendations.

I am grateful to the research technologists Cody Delaney for helping me to manage building the beams and Ben Thurlow for setting up the beams and running the testing equipment. In addition, I would like to acknowledge Ambassador Steel (Harris Rebar) for donating the steel reinforcement material. Thanks also are extended to Structural Technologies for donating the CFRP sheets and fiber anchors and to KL Structures for donating the CFRP dowel anchors.

My gratitude goes to my dear friend Marty Klein, for his support and careful attention. Marty, you have never hesitated to do your best to provide me with any help I would need. You are really my “American uncle!” as you said many years ago.

Most importantly, I am very thankful to my parents, my brothers and sisters for their loving support and for inspiring me to follow my dreams.

Dedication

To my parents and my lovely fiancée

for their constant support and unconditional love.

I love you all dearly

Chapter 1 - Introduction

1.1 General

The externally bonded FRP composite systems have been considered over the last few decades in the repair and strengthening of existing RC members. To date, several studies have been conducted using RC beams strengthened with carbon fiber reinforced polymer (CFRP) and/or glass fiber reinforced polymer (Arrari et al. 2012, Dong et al. 2013, Smith et al. 2013, and Zhang et al. 2017). These studies concluded that the FRP applications improve the strength, stiffness, ductility, and durability. However, premature failure of the strengthened beams may occur in concrete beams at the plate end due to stress concentrations or debonding (local failure). Normal stress concentrations and shear around flexural cracks or at the cut-off point are the main reason for local failures (Saadatmanesh and Malek 1998).

A large number of studies have observed that the FRP debonds at strains below its rupture strain. Using anchorage systems offer an efficient solution to avoid this type of undesirable failure by providing an extra support to delay or shift the FRP debonding. Various types of anchorage systems have been studied such as using metallic anchors (Duthinh and Starnes 2001), utilizing U-jacket FRP anchors (Al-Amery and Al-Mahaidi 2006), adopting near surface mounted rods (Zhang and Smith 2012), and applying distributed CFRP U-Wraps (Rasheed et al. 2015). It was found that the FRP anchors are preferable anchorage system since they are non-corrosive materials and they can be applied to wide dimensioned elements such as beams, slabs and walls (Kalfat et al. 2011). FRP anchors are typically made from glass or carbon fibers in such a way the fiber sheets are folded or rolled (Smith et al. 2011). FRP sheets can also be used as an anchorage by wrapping the tension face of structural members, forming as a U-shape anchorage or using FRP patches to secure the flexural CFRP layers.

In this research, an experimental study is conducted to examine the behavior of the reinforced concrete beams strengthened with CFRP sheets and anchored using superior anchorage devices. Twelve RC beams were tested, six of them with T-shaped section (series 1) and the other six with rectangular cross-section (series 2). The T and rectangular beams had the same span length of 4478 mm. All the specimens are strengthened identically using three layers of unidirectional CFRP sheets and one layer of bidirectional CFRP sheet. The bidirectional CFRP layer was used to provide transverse fibers that support the side anchorage systems. One of each of the beam types (series 1 and series 2) is referred herein as set. Thus, set one (one T beam plus one rectangular beam) is secured with 13 mm diameter of side GFRP bars inserted longitudinally to both sides of the beam. The second set is anchored with GFRP patches applied to both sides of the beam. Two GFRP patches are applied for the T beams, while one GFRP patch is installed for the rectangular beams since the failure mode in T-beams is expected to be FRP rupture or debonding rather than concrete crushing.

CFRP spike anchors are utilized for the other sets of beams. The third set is bonded using 9 CFRP spike anchors with 19 mm diameter spaced at 203 mm along the shear span. The fourth set is anchored using 12 CFRP spike anchors with 16 mm diameter at 140 mm spacing per shear span. Set 3 and 4 have exactly equivalent amount of carbon fiber per shear span. Four CFRP anchors are applied to each shear span of the fifth set with 16 mm- diameter spaced at 406 mm. The design of last set (set 6) included applying one CFRP spike anchor placed at 76 mm from the free edge of CFRP sheets. The flexural teats for the beams were performed in the structural testing lab at Kansas State University using four-point loading. The results are evaluated and compared with utilizing the U-wrap anchorage technique (Rasheed et al. 2015). It is concluded from the

experimental tests that the flexural performance of RC anchored beams significantly enhancement over those strengthened but unanchored beams.

1.2 Objectives

The main objective of this research is to evaluate the behavior of reinforced concrete beams retrofitted with externally CFRP sheets and anchored using superior anchorage devices.

1.3 Organization of Dissertation

The research work in this dissertation includes a literature review about the use of CFRP sheets and different anchorage techniques, which are described in chapter two. Specimen design and material properties are explained in chapter three. Specimen construction details are covered in chapter four. Behavior of reinforced concrete beams strengthened using CFRP sheets with innovative anchorage devices is presented in chapter five. Superior performance of CFRP-strengthened concrete beams fastened with distributed CFRP spike anchors is studied in chapter six. Flexural behavior of strengthened reinforced concrete beams with CFRP sheets and bonded using CFRP spike anchors is investigated in chapter seven. Finally, the summary and conclusion are addressed in chapter eight.

1.4 References

Al-Amery, R., & Al-Mahaidi, R. (2006). Coupled flexural–shear retrofitting of RC beams using CFRP straps. *Composite Structures*, *75*(1-4), 457-464.

Attari, N., Amziane, S., & Chemrouk, M. (2012). Flexural strengthening of concrete beams using CFRP, GFRP and hybrid FRP sheets. *Construction and Building Materials*, *37*, 746-757.

Dong, J., Wang, Q., & Guan, Z. (2013). Structural behaviour of RC beams with external flexural and flexural–shear strengthening by FRP sheets. Composites Part B: Engineering, 44(1), 604-612.

Duthinh, D., & Starnes, M. A. (2001). *Strengthening of reinforced concrete beams with carbon FRP* (No. Journal of Composites for Construction).

Kalfat, R., Al-Mahaidi, R., & Smith, S. T. (2011). Anchorage devices used to improve the performance of reinforced concrete beams retrofitted with FRP composites: State-of-the-art review. *Journal of Composites for Construction*, *17*(1), 14-33.

Rasheed, H. A., Decker, B. R., Esmaeily, A., Peterman, R. J., & Melhem, H. G. (2015). The influence of CFRP anchorage on achieving sectional flexural capacity of strengthened concrete beams. *Fibers*, *3*(4), 539-559.

Saadatmanesh, H., & Malek, A. M. (1998). Design guidelines for flexural strengthening of RC beams with FRP plates. *Journal of composites for construction*, *2*(4), 158-164.

Smith, S. T., Hu, S., Kim, S. J., & Seracino, R. (2011). FRP-strengthened RC slabs anchored with FRP anchors. *Engineering Structures*, *33*(4), 1075-1087.

Smith, S. T., Zhang, H., & Wang, Z. (2013). Influence of FRP anchors on the strength and ductility of FRP-strengthened RC slabs. *Construction and Building Materials*, *49*, 998-1012.

Zhang, H. W., & Smith, S. T. (2012). FRP-to-concrete joint assemblages anchored with multiple FRP anchors. *Composite Structures*, *94*(2), 403-414.

Zhang, H., & Smith, S. T. (2017). Influence of plate length and anchor position on FRP-to-concrete joints anchored with FRP anchors. *Composite Structures*, *159*, 615-624.

Chapter 2 - Literature Review

2.1 Background

FRP is a composite material which mostly consists of high strength that made from glass, aramid, or carbon fibers in a polymeric matrix. The fibers may be in the form of preformed laminates or flexible sheets that can be used to strengthen RC components (beams, girders, and slabs). The laminates are stiff plates that are pre-cured and installed by bonding them externally to the tension face of the RC concrete members using a resin. The sheets are dry or pre-impregnated with resin. These sheets are cured after installation on the tension face of the concrete structure, which is known as wet lay-up technique. FRP materials offer a desired combination of physical and mechanical properties, such as high tensile strength, high stiffness, high fatigue strength, and light weight. Also, FRP materials are an excellent choice for external reinforcement since these systems are non-corrosive, and chemical resistance (Sundarraja and Rajamohan 2008).

One of the earliest techniques for strengthening and repair of concrete structures started in 1970s, which involved utilizing epoxy-bonded external steel plates (Dussek 1980). Even though the external steel plate technique increased the strength of the plated member, durability studies found that corrosion of external steel pales is a restrictive factor for this type of strengthening (Van Gemert and Van den Bosch 1985). To avoid corrosion, a new technique of using FRP in new concrete structures has begun with replacement of steel bars with FRP bars. FRP is non-corrosion material and has high strength-to-weight and high stiffness-to-weight ratios that provide efficient designs and ease of application (Rasheed 2015). As a result, a numerous research in FRP strengthening technique has developed since 1987.

2.2 Previous Researches on Using FRP Composite Sheets and Anchors

(Meier 1987) introduced the use of externally bonding of FRP reinforcement to the tension face of concrete beams to increase the flexural capacity as a replacement of the external steel plate. Since then, numerous studies have been conducted to prove the effectiveness of the FRP system. This technique of using FRP material has been extended to include near-surface-mounted FRP bars and strips (Alkhrdaji et al. 2000). The extension has been more developed to involve using FRP anchorage to secure the external bonded FRP sheets.

(Grace et al. 1999) conducted an experimental study to examine the effect of using FRP strengthening systems and to evaluate the ductility of strengthened beams with FRP. They utilized a different pattern of FRP in strengthening the RC beams. In that study, 14 simply supported concrete beams were tested. All beams had a rectangular cross section with the same dimensions and the same flexural and shear reinforcements. Five different types of FRP were used in their research project, namely two types of CFRP sheets, bidirectional GFRP sheet, unidirectional GFRP sheet, and CFRP plates. Four different types of epoxies were also utilized in these systems. Some beams were retrofitted with CFRP sheets in flexural only, while other specimens were strengthened in flexural and shear by applying the flexural CFRP layers plus U-wrap anchorage along the entire span. Furthermore, an end anchorage of CFRP U-wraps was considered for one of the beams to secure the flexural sheets around the beam cross section.

First, all beams were cracked by applying a mid-span load of 44.8 kN (10 kips). After cracking level was reached, each beam was strengthened with FRP laminates with different techniques, layers, and type of epoxy. Then, the beams were tested with a concentrated load applied at midspan until the complete failure. The authors concluded that the longitudinal FRP layers plus the U-wrap anchorage significantly reduce beam deflections and increase load carrying

capacity of beams. Also, applying vertical FRP sheets along the entire span length supports the longitudinal sheets and eliminates the potential rupture of the flexural sheets. The ultimate load carrying capacity of the beam was doubled by using the combination of vertical and horizontal sheets, together with a proper epoxy.

(Attari et al. 2012) investigated the efficiency of RC beams strengthened with external FRP fabric (Glass–Carbon). The authors considered different strengthening configurations using separate unidirectional glass and carbon fibres with U-anchorages or bidirectional glass–carbon fiber hybrid fabric. Seven simply supported concrete beams were strengthened in flexure and tested under repeated loading sequences using a four-point bending. All beams had the identical dimensions and the same flexural and shear reinforcements. A displacement control at a constant rate of 0.02 mm/s was followed throughout the testing process. Two displacement transducers (LVDT) were placed on the specimens to measure the mid-span deflection.

The following conclusions were reached by the authors,

- Utilizing a twin layer of glass–carbon fibers for strengthening RC beams is very efficient. The strengthened specimens had an increase of 114% in strength capacity compared with the control beam.
- The use of U-anchorage strengthening improves the flexural strength.
- The ductility can be improved by using a strengthening composite material in glass fibers alone or as a single-layered hybrid composite having a good elongation at rupture.

(Ceroni 2010) illustrated the experimental results of RC beams retrofitted externally with carbon fiber reinforced sheets (FRP) laminates. The near surface mounted (NSM) FRP technique using carbon bars was also examined. Furthermore, end or distributed FRP U-wrap anchorage was

applied to the strengthened beams with FRP sheets. Monotonic and cyclic loading have been considered using a four-point test as two concentrated loads located at a distance of 120 mm from each side of the mid-span. Twenty-one (21) RC beams were tested using load control method process. The specimens were divided into 2 series (A and B). All beams had the same dimensions and the same compression steel, whereas series A and B had various internal tensile steel reinforcements and different span lengths. One beam from each of the series A and B was tested as control beam (A1 and B1), and 16 beams were externally retrofitted with carbon fiber reinforce polymer (CFRP) sheets. The remaining three beams were strengthened with two CFRP bars of 8 mm diameter that were placed into the two grooves on the bottom face of the beams, forming the NSM technique. These grooves were filled with an epoxy paste.

The obtained conclusions from this experimental study proved the efficiency of using FRP materials as externally bonded reinforcement. For the retrofired beams with FRP sheets, the increase in the load capacity was 26%-50% and 17%-33% for lowest and highest steel percentage 1% and 1.5%, respectively. Using NSM bars enhanced the performance of the failure load and ductility in comparison with the beams strengthened with an equivalent amount of externally bonded reinforcement (EBR). The failure mode in the strengthened beams with NSM technique was concrete crushing in compression joined to the separation of the inferior concrete cover. It was also found that the distributed FRP U-wrap strips along the beam span is efficient to avoid or delay the debonding.

(Dong et al. 2012) conducted experimental study on reinforced concrete (RC) beams strengthened externally in flexural and flexural–shear with carbon and glass fiber reinforced polymer (CFRP and GFRP) sheets. The structural behavior of the combined flexural–shear was evaluated. The CFRP sheets were applied to the tension face of the beam for the flexural

strengthening, then the sheets were strengthened in shear by retrofitting GFRP or CFRP sheets using U or L configurations. One specimen was left and tested as a control beam. Other six beams were strengthened and tested with either a single layer or two layers of CFRP sheets to investigate the effectiveness of the one extra layer on the crack load, ultimate load, strains and deflection of the strengthened beams. Two strips of CFRP U-wraps were applied on both sides of the beam near the supports to serve as external end anchorage. The rationale behind that was to reduce the stress concentration at the free edges of CFRP layers and to prevent the delamination of CFRP sheets. All the beams were simply supported over a clear span length of 1.5 m and tested under four-point bending.

The experimental study showed that the cracks were delayed for the strengthened beams with one or two layers of CFRP sheets. The crack width and the inter space between cracks were also reduced. The use of external CFRP or GFRP sheets onto bottom and/or lateral faces of the beams significantly improved the flexural and shear capacity. Also, the strength, stiffness, and ductility increased for strengthened beams using FRP sheets. Much more significant enhancement on load carrying capacity was found when the flexural–shear strengthening was used.

(Rahimi and Hutchinson 2001) researched the structural behavior of RC beams strengthened using adhesively bonded FRP. They used three different types of external reinforcements, namely GFRP, CFRP, and external mild steel. All types of reinforcement were bonded by utilizing a two-part epoxy adhesive. The beams were simply supported and tested under four-point bending loading. The failure mode depended on the type and thickness of the reinforcement. The strengthened beams with thin laminates failed in concrete cover close to the applied loads. However, the strengthened beams with thicker laminates failed at plate ends. The failure mode of the reinforced beams by using external mild steel was steel yielding followed by plate debonding

that occurred at the ends of plate. The ultimate load capacity of the strengthened beams with a composite plate was significantly increased in terms of stiffness and strength over those strengthened beams with mild steel. The capacity was up to 230% over the unplated ones.

(Smith et al. 2011) reported experimental results of a series tests on one-way simply supported RC slabs. Eight identical slabs were cast with the same geometry and same steel reinforcements. These slabs were strengthened in flexure with FRP composite and anchored using different anchorage arrangements. Two slabs were tested as control specimens (S1 and S2). S1 slab was left as a control specimen, and S2 was strengthened in flexure with three layers of CFRP sheets without any anchorage (strengthened control). The other six slabs were strengthened with the same three layers of CFRP sheets and anchored with different arrangements and types of FRP anchors. The positioning and type of the CFRP anchors were the variables in that study.

The results of these eight slabs showed the following conclusions,

- Using FRP anchorage improved the strength and the deflection of the RC slabs/ beams.
- Positioning the anchors in the shear span was found to be very effective. However, anchors installed in the constant moment region were mostly ineffective.
- Utilizing closer spaced anchors reduced the rate of debonding crack propagation and enabled higher deflections to be achieved.
- Spacing the anchors at large distances increased the deflection but reduced the strength capacity.
- The greatest improvement in strength with significant deflection capacity was obtained using anchors of greater fiber content installed closer to the ultimate bending moment region along with anchors of lesser fiber content but installed close together near the free ends of the FRP plate.

(Smith at al. 2013) verified the work of (Smith, Kim, and Seracino 2011) by considering the application of FRP anchors to RC flexural members. They prepared and tested ten simply supported one-way RC slabs. All the slabs were constructed as identical dimensions with a total span length of 2.7 meters. Also, the compression steel reinforcements were the same for all the beams. The tensile steel bars were 0.33% on effective depth and 0.26% on total depth. One slab tested without FRP as a control and another one slab tested as strengthened control specimen with three layers of FRP plates (without anchors). The remaining eight slabs were flexurally strengthened using three layers of FPR plates and anchored with different FRP anchorage arrangements. That arrangements included the number of FRP anchors per shear span, anchor fiber contents, anchor diameters, and the position of the anchors. Based on this study, the authors are made the following conclusions.

- The use of FRP anchors can significantly enhance the load and deflection.
- The greatest increase in the ultimate load capacity and deflection over the unanchored control slab was 44% and 216%, respectively.
- Greater peak load capacity and plate capacity were obtained by using smaller but more numerous anchors.
- Much greater anchor fiber contents enabled to achieve the greatest increase in deflection.

(Rasheed et al. 2015) Conducted an experimental study to examine the beneficial use of distributed U-wrap CFRP anchors to delay or shift the premature debonding of the RC beams in flexure. Three T beams and three rectangular beams were tested. The T beams had web dimensions of 152 mm x 305 mm with the depth extending through the flange thickness. The flange dimensions were 406 mm width and 102 mm thickness. The rectangular beams had 152 mm width

and 305 mm depth. Two 16 mm steel bars were used in the tension zone for all T and rectangular beams. The compression steel bars included utilizing four 10 mm diameter of steel bars for the T beams, while two 10 mm diameter were used for the rectangular beams. All the beams had a clear span length of 4724 mm, and they were loaded in four-point bending. One from each types of the beams (T and rectangular beams) was tested as a control beam (T1 and R1). The next specimen from each type of the beams (T2 and R2) was strengthened in flexure with five layers of CFRP (C100) on the bottomed face of the beam in the longitudinal direction. The last specimen from each types of the beams was strengthened in flexure with the same five layers of CFRP (C100) that used in second specimens (T2 and R2) and anchored with distributed U-wrap anchors. Two layers of U-wraps around the web were used for the T beams with 127 mm wide spacing at 305 mm on center. For rectangular specimens, one layer of U-wraps was utilized with 140 mm wide spaced at 305 mm on center.

It was found from the results that the strengthened but unanchored T and rectangular beams failed in debonding. On the other hand, the strengthened and anchored T beam with U-wraps failed in CFRP rupture with about 30% increase in the ultimate load capacity as unanchored beam. The strengthened and anchored rectangular beam U-wraps failed in concrete crushing with 10% increase in the strength over the unanchored beam. That was an excellent proof that the U-wrap anchorage was successfully helped providing resistance to debonding by shear friction.

(Zhang and Smith 2016) investigated the influence of FRP anchors to enhance the bond capacity and the ductility of the strengthened RC slabs with FRP. Also, they evaluated the behavior of FRP-to-concrete bonded interfaces and the influence of crack position on the efficiency of strengthened RC members (FRP) and anchored with FRP anchors. To study the properties of FRP-to-concrete bonded interfaces, single-shear FRP-to-concrete joints system were used. The

influence of plate length on FRP-to-concrete joints anchored with FRP anchors had been considered.

The experimental and analytical test results demonstrated the following observations. All control joints unanchored with FRP anchors failed by debonding between FRP plates and concrete interface. For all anchored joints, three levels of load-slip response modes were observed. These are, pre-debonding (linear portion), debonding propagation, and post-debonding level. The linear level (pre-debonding) behaved in a similar manner to the control joints since the debonding load for the anchored joints and the control joints were similar. Whereas, the obtained corresponding slip debonding was greater for the unanchored control joints. Moreover, the length of plate between the FRP anchor and unloaded plate end had greater influence on the ultimate strength of joint than positioning of anchor relative to the loaded bonded plate end. Also, plate strain for anchored joints increased 32% compared with unanchored joints).

2.3 References

Attari, N., Amziane, S., & Chemrouk, M. (2012). Flexural strengthening of concrete beams using CFRP, GFRP and hybrid FRP sheets. *Construction and Building Materials, 37*, 746-757.

Alkhrdaji, T., Nanni, A., & Mayo, R. (2000). Upgrading Missouri transportation infrastructure: Solid reinforced-concrete decks strengthened with fiber-reinforced polymer systems. *Transportation Research Record: Journal of the Transportation Research Board*, (1740), 157-163.

Ceroni, F. (2010). Experimental performances of RC beams strengthened with FRP materials. *Construction and Building Materials*, 24(9), 1547-1559.

Dussek, I. J. (1980). Strengthening of bridge beams and similar structures by means of epoxy-resin-bonded external reinforcement. *Transportation Research Record*, (785).

Dong, J., Wang, Q., & Guan, Z. (2013). Structural behaviour of RC beams with external flexural and flexural–shear strengthening by FRP sheets. *Composites Part B: Engineering*, *44*(1), 604-612.

Grace, N. F., Sayed, G. A., Soliman, A. K., & Saleh, K. R. (1999). Strengthening reinforced concrete beams using fiber reinforced polymer (FRP) laminates. *ACI Structural Journal-American Concrete Institute*, 96(5), 865-874.

Meier, U. (1987). Bridge repair with high performance composite materials. *Material und Technik, 4*, 125-128.

Rasheed, H. A. (2014). *Strengthening design of reinforced concrete with FRP*. CRC Press.

Rasheed, H., Decker, B., Esmaeily, A., Peterman, R., & Melhem, H. (2015). The influence of CFRP anchorage on achieving sectional flexural capacity of strengthened concrete beams. *Fibers, 3*(4), 539-559.

Rahimi, H., & Hutchinson, A. (2001). Concrete beams strengthened with externally bonded FRP plates. *Journal of composites for construction, 5*(1), 44-56.

Smith, S. T., Hu, S., Kim, S. J., & Seracino, R. (2011). FRP-strengthened RC slabs anchored with FRP anchors. *Engineering Structures, 33*(4), 1075-1087.

Sundarraja, M. C., & Rajamohan, S. (2008). Flexural strengthening effect on RC beams by bonded composite fabrics. *Journal of reinforced Plastics and Composites, 27*(14), 1497-1513.

Smith, S. T., Zhang, H., & Wang, Z. (2013). Influence of FRP anchors on the strength and ductility of FRP-strengthened RC slabs. *Construction and Building Materials, 49,* 998-1012.

Zhang, H., & Smith, S. T. (2017). Influence of plate length and anchor position on FRP-to-concrete joints anchored with FRP anchors. *Composite Structures, 159,* 615-624.

Chapter 3 - Design of Specimens

3.1 General

The experimental program consists of designing and testing twelve (12) reinforced concrete (RC) beams. Six full-scale T beams (series 1) are strengthened with CFRP sheets and anchored with different types and arrangements of FRP anchors. The other six full scale rectangular beams (series 2) were strengthened in an identical manner to that of the T beams. The purpose of maintaining the same identical designs was to perform one on one comparisons between the T and rectangular beams.

3.2 Beam Geometry

The T- beams have a 152 mm x 305 mm web dimensions with the depth extending through the flange thickness, Figure 3-1(a). The flange dimensions are 406 mm in width and 102 in thickness. The main flexural reinforcement consists of 2 Φ16 steel bars. The compression steel includes 4 Φ10 bars to hold the shear reinforcement caging with Φ10 hanger bars spaced at 127 mm along the span length, Figure 3-1 (a). The rectangular beams have a cross section of 152 mm x 305 mm, Figure 3-1(b). The main flexural reinforcement is identical to that of the T beams, which includes using 2 Φ10 bars for the compression steel just to provide a caging framework for the shear reinforcement, as shown in Figure 3-1(b). The beams have shear reinforcements consisting of Φ10 stirrups at 127 mm on center, Figure 3-1. All specimens have a span length of 4877 mm with a clear span of 4724 mm.

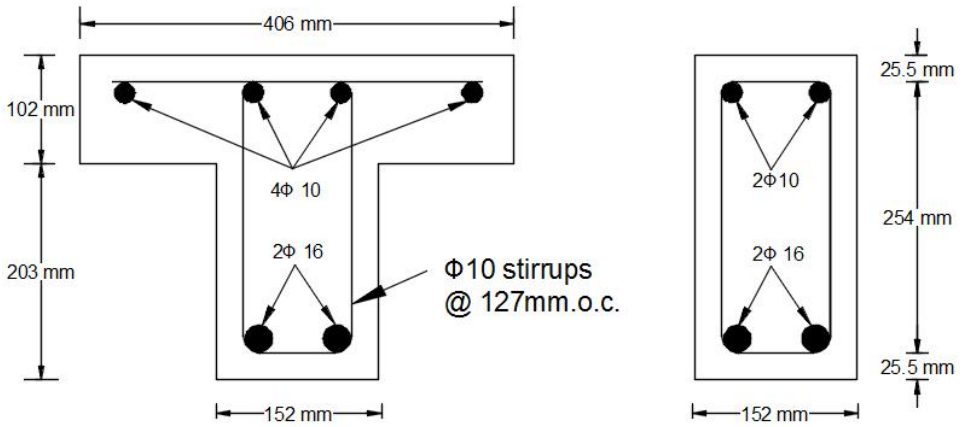

(a) (b)

Figure 3-1 Beam cross section details (a) T-beam; (b) rectangular beam

3.3 Material Properties

3.3.1 Concrete

The concrete that was used in casting the twelve (12) beams is composed of Portland cement Type I, water, sand, gravel, and crushed stone delivered by a ready-mix company on 8/24/2017. The mix design nominal strength was 35.0 MPa. While casting the beams, 12 cylinders were taken for compressive strength test. The 102 mm. x 203 mm cylinders were prepared and tested according to ASTM C39 (ASTM 2011) using compressive strength testing machine in the department of Civil Engineering lab at Kansas State university as shown in Figure 3-2 a-b. The average compressive strength (f'c) of 28 days was found to be 38.0 MPa. Table 3-1 shows the results of the cylinder tests.

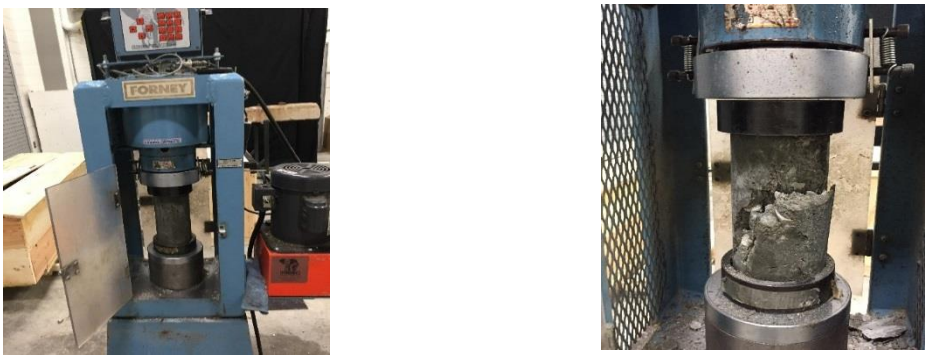

(a) (b)

Figure 3-2 Testing the cylinders (a) before testing; (b) after testing

Table 3-1 The results of the cylinder tests

Nu	Ultimate load (kN)	Compressive strength, (MPa)	Nu	Ultimate load, (kN)	Compressive strength, (MPa)
1	315.86	38.96	7	317.82	39.20
2	301.77	37.22	8	320.70	39.55
3	322.83	39.81	9	295.90	36.49
4	323.67	39.92	10	288.40	35.57
5	319.25	39.37	11	292.16	36.03
6	318.42	39.27	12	290.30	35.80
Ave (MPa):		**38**			

3.3.2 Steel Reinforcement

The actual tensile testing of 8-inch long bar specimens was performed by research lab at Kansas Department of Transportation (KDOT). The test was conducted according to ASTM E8/E8M (ASTM 2009) The modulus of elasticity and yield strength of the Φ 16 mm steel bars were 211 GPa and 488 MPa, respectively. For Φ 10 steel bars, the modulus of elasticity was 200 GPa and the yield strength was 470 MPa. These values represent the average test results of 3 samples. Figures 3-3 (a-b) were taken during the tensile test at KDOT. Figures 3-4 (a-b) show the load-displacement diagrams of the Φ16 mm and Φ10 mm bars.

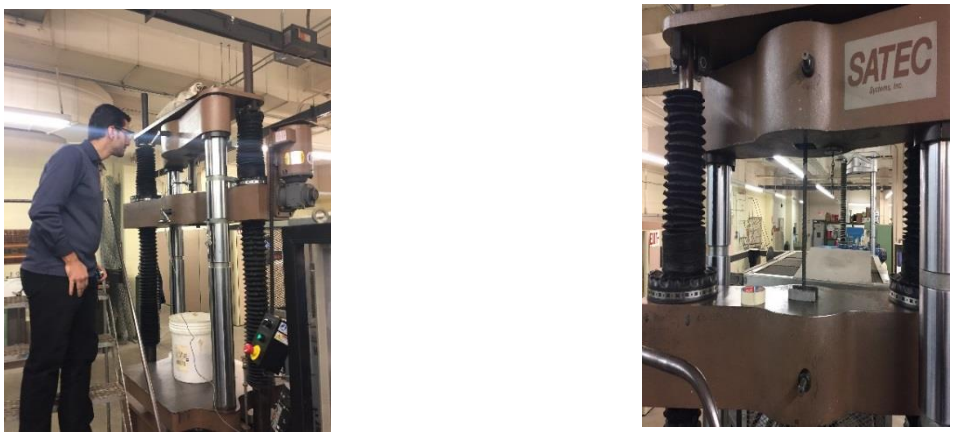

(a) (b)

Figure 3-3 Running tensile test (a) before the test; (b) after yielding of the specimen

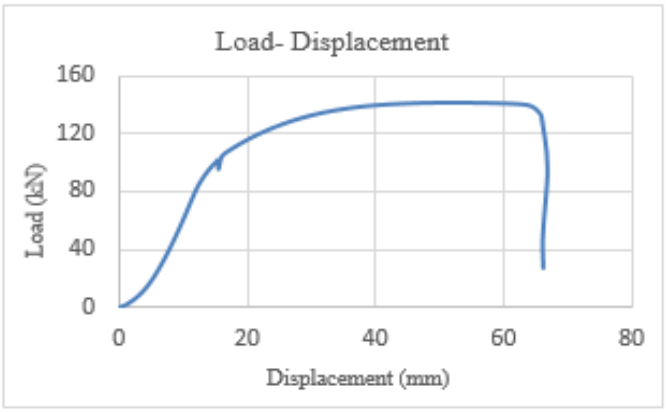

(a)

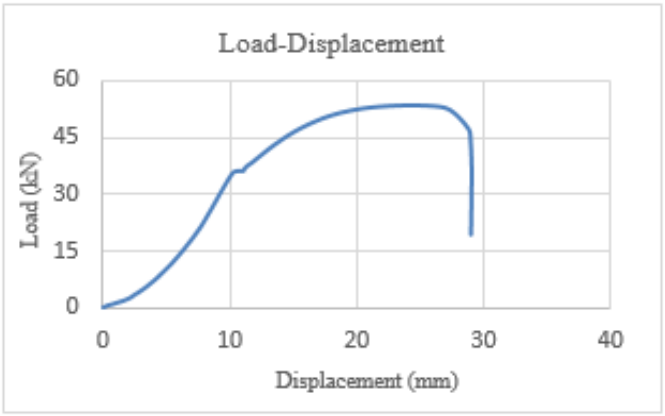

(b)

Figure 3-4 Load-displacement diagram (a) Φ 16 mm steel bars; (b) Φ 10 mm steel bars

3.3.3 Fiber Reinforced Polymer (FRP)

Reinforced concrete members can be strengthened by bonding external tensile reinforcements such as steel plates, bars, or cables. However, the use of fiber reinforced polymer (FRP) composites have become popular due to their light weight, flexibility, and resistance to corrosion (Orton et al. 2008). FRP composites have been used to increase the flexural capacity of reinforced concrete (RC) beams since the 1980s (Teng et al. 2002). Three different types of FRP materials are used in this research for strengthening the twelve RC beams. These types are, uni-directional carbon fiber reinforced polymer (CFRP) identifies as V-Wrap C100 (Figure 3-5 a), bi-directional CRFP identifies as V-Wrap C220B (Figure 3-5 b), and glass fiber reinforced polymer

(GFRP) identifies as EG-50B (Figure 3-5 c). The CFRP fibers of C100 sheets are oriented longitudinally along one direction of the beam axis only (0°). While, the CFRP fibers for the C220B sheets are oriented in both directions longitudinally and transversely (0° and 90°). Furthermore, GFRP is a bidirectional glass fiber fabric with fiber oriented in the ±45° directions. The material properties are provided by the manufacturer and listed in table 3-2.

(a) (b) (c)

Figure 3-5 FRP sheets (a) unidirectional CFRP-C100; (b) bidirectional CFRP-C220B; (c) bidirectional GFRP-EG50B

Table 3-2 Properties of CFRP and GFRP sheets

Properties	0° Unidirectional CFRP (V-Wrap C100)	0/90° Bidirectional CFRP (V-Wrap C220B)	±45° Bidirectional GFRP (V-Wrap EG50-B)
Tensile Strength	966 MPa	1068 MPa	279 MPa
Tensile Modulus	66.19 GPa	96.53 GPa	18.6 GPa
Thickness	0.584 mm	0.51 mm (each direction)	0.864 mm (each direction)

3.3.4 Epoxy Adhesive

The epoxy resin V-Wrap 770 is used for saturating the carbon fiber and bonding it to the concrete surface. V-Wrap 770 is a multi-use epoxy that performs as a primer tack coat and saturating resin for the V-Wrap carbon and glass fiber systems. This epoxy consists of two parts A and B (Figure 3-6) that is mixed together according to manufacture proportions to achieve a high strength composite bonding, Figure 3-7. The epoxy physical properties and packaging are

shown in table 3-3. In addition, an epoxy putty filler V-Wrap PF is also used to fill and cover the grooves that have been made on both sides of two out of twelve RC beams. The V-Wrap PF is a two-part epoxy for high strength composite bonding applications. This epoxy putty filler has a tensile strength of 3380 psi and tensile modules of 367800 psi.

Figure 3-7 Part A and B of the epoxy

Figure 3-6 Mixing the epoxy

Table 3-3 Physical properties and packing of the epoxy

Physical properties	**Psi**	**MPa**
Tensile Strength (ASTM D638)	8800	60.7
Tensile Modulus (ASTM D638)	400000	2760
Elongation at Break (ASTM D638	4.4%	-
Flexure Strength (ASTM D790)	13780	95
Flexure Modulus (ASTM D790)	380000	2620
Compressive Strength (ASTM D695)	12450	85.8
Compressive Strength (ASTM D695)	387000	2670
Epoxy Shear Strength		

Density		**Packaging**		
		Volume	**Weight**	**Package**
Part A	9.7 Ibs/gal (1.16 kg/L)	2.8 gal	27.3 gal	5 gal pail
Part B	7.9 Ibs/gal (0.95 kg/L)	1.15 gal	9.1 Ibs	5 gal pail

3.4 FRP Anchors

Externally bonded (RC) members strengthened with FRP composites are vulnerable to premature failure by debonding of the FRP. An effective way to delay or avoid the propagation of the FRP debonding is by anchorage of the FRP strengthening members with FRP anchors (Zhang et al. 2012). Accordingly, all the beams herein are anchored with different anchorage devices such as using the GFRP side rebars, GFRP side patches, and spike CFRP anchors to secure the flexural CFRP sheets. The spike CFRP anchors are made from carbon fibers in which the fiber sheets are rolled, or lose fibers are bundled together, Figure 3-8 (a-b). Also, the CFRP or GFRP sheets can be also as U-wraps to anchor the FRP sheets.

(a) (b)

Figure 3-8 CFRP anchors (a) bundled fiber anchors; (b) dowel anchors

3.5 References

American Society for Testing and Materials. Committee C-9 on Concrete and Concrete Aggregates. (2011). *Standard test method for compressive strength of cylindrical concrete specimens*. ASTM International.

ASTM American Society for Testing and Materials. (2009). *Standard test methods for tension testing of metallic materials*. ASTM international.

Orton, S. L., Jirsa, J. O., & Bayrak, O. (2008). Design considerations of carbon fiber anchors. *Journal of Composites for Construction, 12*(6), 608-616.

Teng, J. G., Chen, J. F., Smith, S. T., & Lam, L. (2002). FRP: strengthened RC structures. *Frontiers in Physics*, 266.

Zhang, H. W., Smith, S. T., & Kim, S. J. (2012). Optimisation of carbon and glass FRP anchor design. *Construction and Building Materials, 32*, 1-12.

Chapter 4 - Specimen Construction

4.1 Construction of Formwork and Caging

The fabrication of wooden formwork and steel rebar caging were performed in the Civil Engineering wood and steel shops at Kansas State University. The forms had to be fabricated in two halves that combined to create a 4877 mm long form since the plywood is available in the shop market only in 1219 mm x 2439 mm sheets. The steel stirrups for shear reinforcement were bent to the specified dimensions. Also, the longitudinal reinforcement and the stirrups were tied together by hand using rebar ties. Figure 4-1 and 4-2 show the fabricated rebar cage used for the T and rectangular beams.

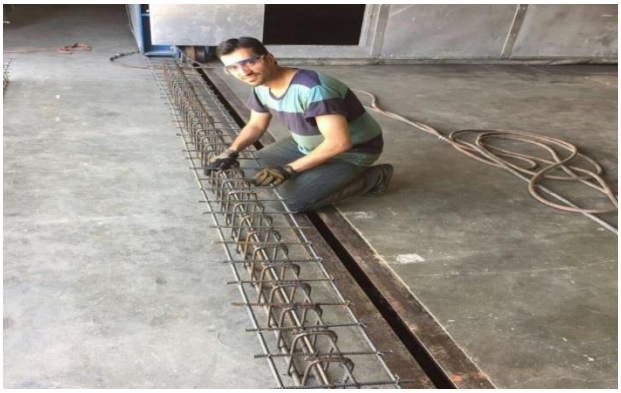

Figure 4-1 Fabricating the steel rebar caging

Figure 4-2 Rebar cages for the T and rectangular beams

To measure the strain results in the rebar during testing process, strain gages were placed on the rebar to be embedded in the concrete. Two strain gages with 5% capacity were installed in each beam, at the midspan of each bottom reinforcement bar as shown in Figure 4-3. The strain gage wires were taped to the stirrup all the way to the top of formwork to avoid being damaged during concrete casting, Figure 4-3.

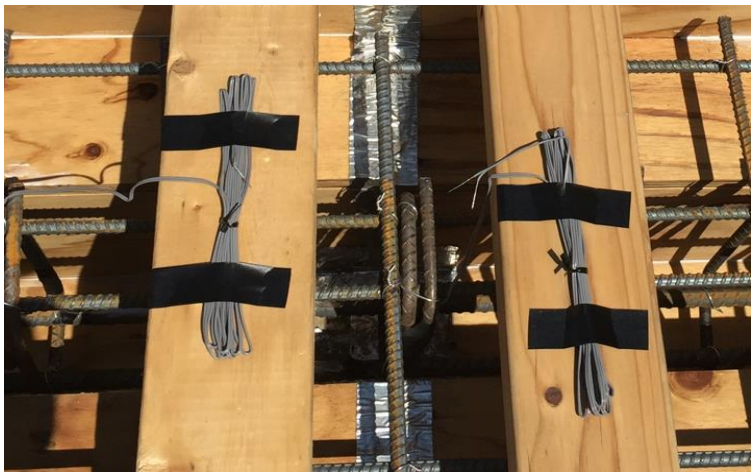

Figure 4-3 Installed strain gages on flexural steel reinforcement

4.2 Preparing the RC Specimens

After the construction of formwork and steel rebars caging, the formwork release oil was applied on the formwork surface prior casting the concrete in order to facilitate easy removal the formwork. Then, the steel cages were positioned inside the formwork. Furthermore, cubic concrete spacers (small blocks) of 25 mm x 25 mm x 25 mm were placed between the formwork and the reinforcement cages to provide the required concrete cover (25 mm). Figures 4-4 and 4-5 show the formwork after the fabrication and prior casting the concrete.

Figure 4-4 Placing the spacers

Figure 4-5 Getting ready to cast the concrete

4.3 Casting the RC Specimens

The specimens were cast using 35 MPa (5000 psi) ready-mix concrete provided by Midwest Concrete Materials, a local concrete provider. Along with casting the beam specimens, twelve concrete cylinders were prepared. The beams and cylinders were allowed to cure for 28 days to reach their appropriate strength. Curing of the beams was done by lightly spraying water to the concrete each day and covering them with plastic to keep the moisture from evaporating. The cylinders were kept in a moisture room (in the new concrete lab of Civil Engineering

Department at Kansas State University) for 28 days and then tested to determine the average compressive strength of the concrete. Figure 4-6 presents the casting of the specimens.

Figure 4-6 RC Specimens after casting the concrete

4.4 Surface Preparation

The bonding surface of the concrete specimens were prepared according to ACI 440.2R-17. To avoid stress concentrations at the corners, the beams were rounded off to approximately a 13-mm radius using a grinder. In order to get efficient bond and avoid premature failure debonding, the surface of the concrete beams have to be adequately cleaned and roughened. Three different techniques was used to rough the bonding surface. These are grinding (Figure 4-7 a), sandblasting (Figure 4-7 b), and water-blasting (Figure 4-7 c). First, a grinder was considered, but it was found that this approach takes a long time to get the work done. Then, sandblasting the surface was followed using a portable sandblaster attached to an air compressor. Black Blast is the type of sand that was used to operate the sandblaster, Figure 4-7 d.

The sandblasting technique is faster than utilizing a grinder. However, it was noticed that the sandblasting is an extremely dusty process especially for indoor applications. Sand dust was extensively spread out everywhere from the work area which requires using full safety suit as well as abrasive blasting hood. Therefore, the water-blasting technique was finally utilized with 24 MPa pressure washing since it is a fast, clean, and safer way to rough and clean the bonding surface. Figure 4-8 shows the beam before and after the rounding and sandblasting. Using spike CFRP anchors is one of anchorage technique that was considered in this research study. Accordingly, an electrical drill was utilized to prepare the holes into the concrete at their specific locations. Then, the predrilled holes were cleaned with compressed air to remove the dust and debris before inserting the CFRP anchors, Figure 4-8.

(a) (b) (c) (d)

Figure 4-7 Tools and materials used for roughening the surface (a) a grinder; (b) sandblaster; (c) pressure washer; abrasive blasting sand

(a) (b) (c) d)

Figure 4-8 Surface preparation (a) before the preparation; (b) after rounding and roughening the surface; (c) drilling the hole; and (d) cleaning the holes

4.5 FRP Preparation

The uni-directional (V-Wrap C100) and bi-directional (V-Wrap B220) CFRP, that are used for strengthening of the specimens, are high strength carbon fibers. These materials are provided by Structural Technologist (LLC). The FRP come in a roll of 610 mm wide and 1270 mm long. The flexural uni-directional CFRP was cut to the appropriate size of 152.4 mm -254 mm wide by 4572 mm long. This length of 4572 was used to stop the FRP at 76 mm from the free end of the clear span to allow adequate room for placing the bearing plates during testing. The flexural bi-directional CFRP size was cut depending on the arrangement and design of the beams to cover the 152 mm of tension face plus the both sides of the beam to have overall 89 mm high from each side.

4.6 FRP Installation

Before applying the CFRP strengthening system to the beams, all the specimens were first flipped upside-down using steel rebars that had been already installed at the centroid of the beam cross sections on each side, Figure 4-9 (a-b). This step had been done after removing the formwork to be easy doing the surface preparations. This is not how the system would be applied in the field since it is not practically possible. However, due to safety concerns in the lab we did not want anyone underneath the specimen while the CFRP and GFRP were being applied. After the beams flipped upside-down and surface preparations were completed, the FRP applications are ready to be applied. The specimens are divided into a number of series, each series includes a one rectangular beam and a one T- shaped beam.

(a) (b)

Figure 4-9 Flipping the beams upside-down (a) before flipping the beams; (b) after flipping the specimens one by one

4.7 Epoxy Preparation

The two part of V-wrap 770 epoxy that is used for saturating the CFRP and GFRP and bonding them to the surface of beams. The epoxy is mixed by volume as 3 from part A to 1 from part B as required by the manufacture. The epoxy was applied using a 150 mm plastic roller frame with roller cover pack, Figure 4-10 a. A wooden roller was also used (Figure 4-10 b) to press the FRP sheets into the resin and to eliminate any air bubbles entrapped between the epoxy/concrete or epoxy/fabric interface.

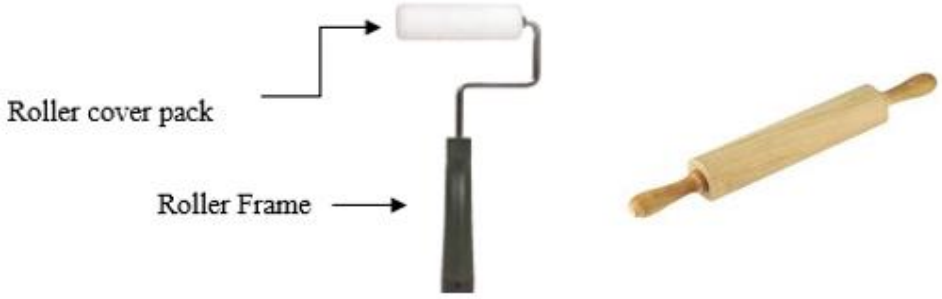

(a) (b)

Figure 4-10 Roller frames (a) the plastic roller; (b) the wooden roller

Chapter 5 - Behavior of Reinforced Concrete Beams Strengthened Using CFRP Sheets with Innovative Anchorage Devices

The objective of this experimental study is to assess the effect of new flexural anchorage devices on improving the performance of strengthened reinforced concrete beams in flexure. Six reinforced concrete (RC) beams were prepared and tested. Three of them with identical rectangular cross-sectional area and the other three with identical T-shaped section. The first beam in each series was tested as a control beam. The second beam in each series was strengthened using four layers of flexural CFRP in addition to side GFRP bars inserted longitudinally to the both sides of the beam through side grooves at the level of primary steel reinforcement. The last beam in each series was strengthened in flexure using identical four layers of CFRP plus one layer of GFRP patches installed to both sides of the rectangular beam. Furthermore, two identical layers of GFRP patches were applied to the T beam on each side. The beams were tested under four-point bending load until failure and the results for each series are evaluated. In addition, the outcome is compared with other anchorage techniques that have been examined by some researchers**.** It was concluded that using CFRP sheets increased the flexural capacity and the results indicated the use of GFRP sidebars or GFRP side patches for T beams significantly enhanced the strength of the tested beams to reach their ultimate sectional capacity before the failure.

5.1 Introduction

Externally bonded fiber reinforced polymer (FRP) composite systems have become a topic of extensive research over the last few decades. FRP applications can be used in the repair and strengthening of existing reinforced concrete structural components. This strengthening technique involves epoxy bonding of FRP sheets or plates to the tension face of the beam to increase the

flexural resistance of RC members such as beams, girders, and slabs. Full composite action is usually assumed between the bonding surface of the beams and FRP materials. The perfect bond, however, depends on the shear stiffness of the adhesive [1]. Excellent bond characteristics may be achieved by most resin adhesives. Yet some epoxy resins have low shear stiffness that cause bond slip between FRP and concrete beams which in return reduces the composite action [1-2].

In order to improve the strength, stiffness, ductility, and durability, several studies have been conducted using RC beams strengthened with carbon fiber reinforced polymer (CFRP) and glass fiber reinforced polymer (GFRP), [3-9]. For typical flexural strengthening procedure, the FRP fibers are oriented longitudinally along the beam axis to increase the flexural capacity. Thus, the stiffness mismatch between the high modulus FRP layer and low modulus concrete substrate promotes the dominance of FRP debonding. The failure usually initiates at the base of flexural and flexural-shear cracks along the span of the member, called intermediate crack debonding or at the FRP plate end, called concrete cover delamination [10-11]. This premature failure of the strengthened concrete members yields an inefficient use of the strength and strain capacity of the FRP. Using FRP anchorage offers an efficient solution to the debonding problem by providing an extra mechanical support that delays FRP debonding to higher level of strain [12-20]. In this study, two innovative anchorage devices are considered to examine the improvement in flexural capacity of RC beams. These anchorage systems were tested for the first time and they consist of utilizing side GFRP bars applied to two beams and side ±45° GFRP patches installed to two other specimens as anchorage devices for the flexural CFRP sheets. The experimental and analytical results of using flexural CFRP with aforementioned anchorage types are evaluated. In addition, the outcome of this study is compared with identical RC beams strengthened with equivalent flexural CFRP sheets

only as well as with distributed transverse CFRP U-wraps that were tested by Rasheed et al, 2015 [21].

5.2 Beam Geometry

The T- beams had a 152 mm x 305 mm web dimensions with the depth extending through the flange thickness that had 406 mm width and 102 mm thickness. The main flexural reinforcement consisted of two Φ 16 mm bars while four Φ 10 mm bars were used for the compression steel as shown in Figure 5-1-a. The rectangular beams had a 152 mm x 305 mm in cross section and the bottom flexural reinforcement was identical to that of the T-beams, Figure 5-1-b. On the other hand, the compression steel included two Φ 10 mm bars to support the shear reinforcement caging. Also, Φ 10 mm stirrups at 127 mm on center was applied as shear reinforcement for both the T and rectangular beams. All beams had a total length of 4877 mm.

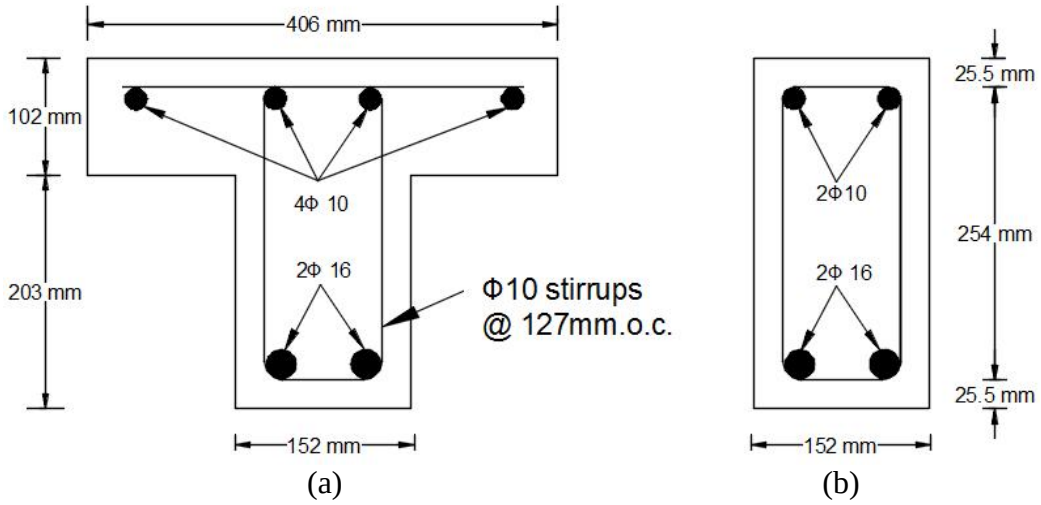

Figure 5-1 Beam cross section details (a) T beam; (b) rectangular beam

5.3 Materials

Twelve cylinders were prepared according to ASTM C39 [22] and tested in the concrete lab at Kansas State University. The average compressive strength at 28 days was 38 MPa as shown

in the Table 5-1. The actual tensile testing of 203-mm long bar specimens was performed by material research lab at Kansas Department of Transportation (KDOT). The modulus of elasticity and yield strength of the Φ 16 mm bars were 211 GPa and 488 MPa, respectively. Whereas, the modulus of elasticity for Φ 10 mm was 200 GPa and the yield strength was 470 MPa. These values represent the average test results of three specimens. The material properties for CFRP and GFRP were provided by the manufacturer and they are listed in the Table 5-2. GFRP is a bidirectional glass fiber fabric with fiber oriented in the ±45° directions. The epoxy resin (V-Wrap 770) consists of part A and part B that were mixed according to the manufacturer proportions.

Table 5-1 The results of the cylinder tests

Num	Ultimate Laod, (kN)	Compressive Strength, (MPa)
1	315.86	38.96
2	301.77	37.22
3	322.83	39.81
4	323.67	39.92
5	319.25	39.37
6	318.42	39.27
7	317.82	39.20
8	320.70	39.55
9	295.90	36.49
10	288.40	35.57
11	292.16	36.03
12	290.30	35.80
-	**Ave:**	**38**

Table 5-2 CFRP and GFRP properties

0° Unidirectional CFRP (V-Wrap C100)	
Tensile Strength	966 MPa
Tensile Modulus	66.19 GPa
Thickness	0.584 mm
0/90° Bidirectional CFRP (V-Wrap C220B)	
Tensile Strength	1068 MPa
Tensile Modulus	96.53 GPa
Thickness (each direction)	0.51 mm
±45° Bidirectional GFRP (V-Wrap EG50-B)	
Tensile Strength	279 MPa
Tensile Modulus	18.6 GPa
Thickness (each direction)	0.864 mm

5.4 Surface Preparation

Surface preparation was performed according to ACI 440.2R-17 [23]. Prior to applying the CFRP sheets and side anchors, the bottom-side corners of the beams were carefully rounded off to approximately a 13-mm radius using a grinder. The bonding surface of the beams was roughened using three different techniques, namely grinding, sandblasting, and water-blasting. First, a grinder with concrete diamond grinding disk was considered, but it was found that this approach takes a long time to get the work done. Then, sandblasting the surface using a portable sandblaster attached to an air compressor was followed. Even though this technique is faster than utilizing a grinder, it was noticed that the sandblasting is an extremely dusty process especially for indoor applications. Sand dust was extensively spread out everywhere from the work area which necessitates using abrasive blasting hood and a full body abrasive blast suit to protect the operator. In addition, this approach requires a big clean up job. Therefore, the water-blasting technique was finally utilized since it is a fast, clean, and safer way that may be considered for this purpose. Using 24 MPa pressure washing helped in cleaning the surface from any dirt, dust or oil as well as roughening the bond surface through water pressure. Figure 5-2 (a-b) shows the beam before and after the rounding and sandblasting.

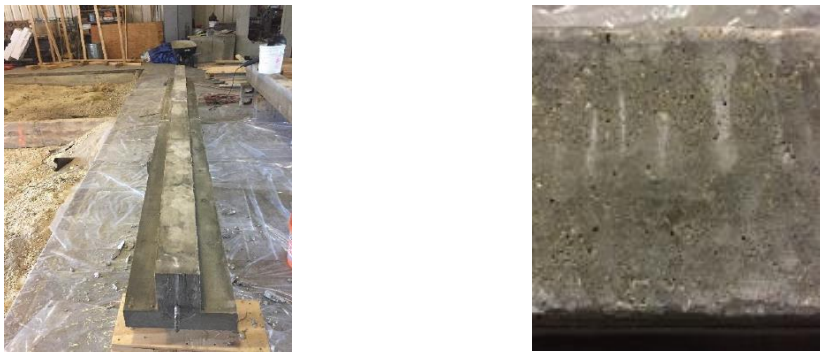

(a) (b)

Figure 5-2 Surface preparation for the beams (a) before surface preparation; (b) after rounding and water-blasting the surface

5.5 Experimental Program

5.5.1 Layout and Application of CFRP Sheets to Beams

A series of three rectangular and three T beams were prepared and tested. One of each of the beam types (set 1) was tested as a control specimen, Figure 5-1. The remaining of RC beams (sets 2-3) were strengthened in flexure with CFRP sheets.

5.5.1.1 Layout and Application of FRP Sheets for Set 2

The second beam in each series (set 2) was cast with grooves on both sides of beams. These grooves had a dimension of 25x25 mm along the span length (4877 mm) and were located at 51 mm up from the soffit of the beam, Figure 5-3. The RC specimens were strengthened with two layers of unidirectional CFRP (V-Wrap C100) applied to the bottom face of beams only, followed by a third layer of CFRP (V-Wrap C100) installed to the bottom face and wrapped 51 mm up the sides from the soffit. Then, a one layer of 0/90° bidirectional CFRP (V-Wrap C220B) sheet was applied on top of the previous 3 sheets, Figure 5-3 section a-a. This last layer of C220B was wrapped up the sides from the soffit and inserted through the premade grooves to cover its perimeter, and continue 12.7 mm above the grooves level with a total length of 89 mm from the soffit on each side, Figure 3 section a-a. Finally, glass (GFRP) bars with diameter of 13 mm were inserted into the grooves that were filled with high strength of epoxy putty filler. Figure 5-4 shows the application of CFRP sheets and GFRP bars. It is important to mention that the bidirectional CFRP layer was intentionally used to provide transverse fibers that support the side anchorage systems. If V-Wrap C100 unidirectional sheets were used for all layers instead, these fibers would have easily separated and detached from the side anchorage prematurely.

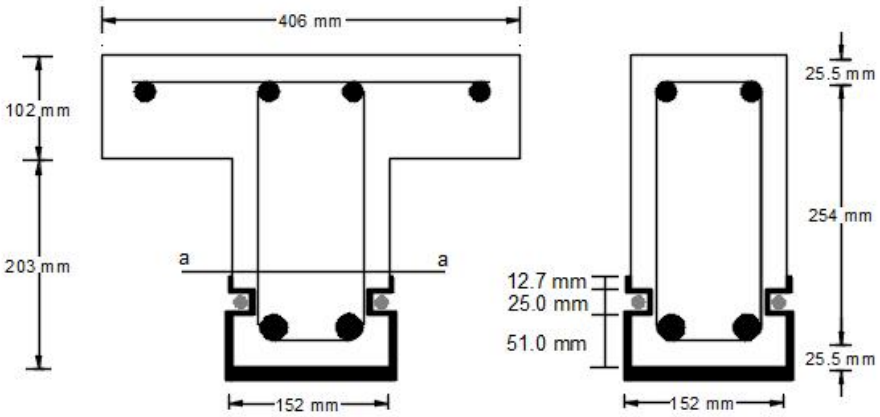

(a) (b)

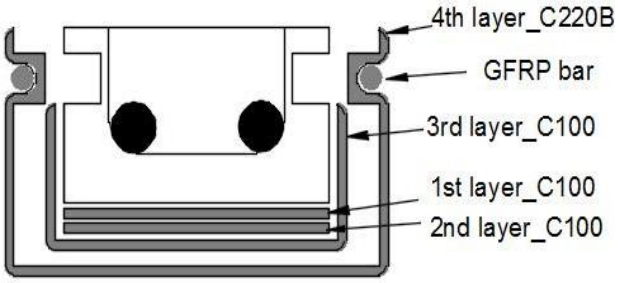

Section a-a

Figure 5-3 Beam cross section details for set 2 (a) T beam; (b) rectangular beam

(a) (b)

Figure 5-4 CFRP applications of set 2 (a) filling the grooves with epoxy putty; (b) inserting the GFRP bars into the grooves

5.5.1.2 Layout and Application of FRP Sheets for Set 3

The third beam in each series (set 3) had no grooves and was strengthened in flexural with the same 3 layers of unidirectional CFRP (V-Wrap C100) and one layer of bidirectional CFRP (V-Wrap C220B) that was installed for set 2 specimens. In addition, the four CFRP sheets were anchored with side ±45° bidirectional GFRP (V-Wrap EG50-B) patches. A one layer of GFRP patch with a total height of 127 mm was used on both sides for the rectangular beam and applied with an overlap of 64 mm on the bidirectional CFRP (C220B) sheet and an overlap of 64 mm on the side web surface of concrete, Figure 5-5. Furthermore, two patches with the same dimensions were utilized for the T-beam since the failure mode in T-beams is expected to be FRP rupture or debonding rather than concrete crushing. The patches were installed as the same heights of those in the rectangular beam. Figure 5-6 shows the application of CFRP sheets and GFRP patches.

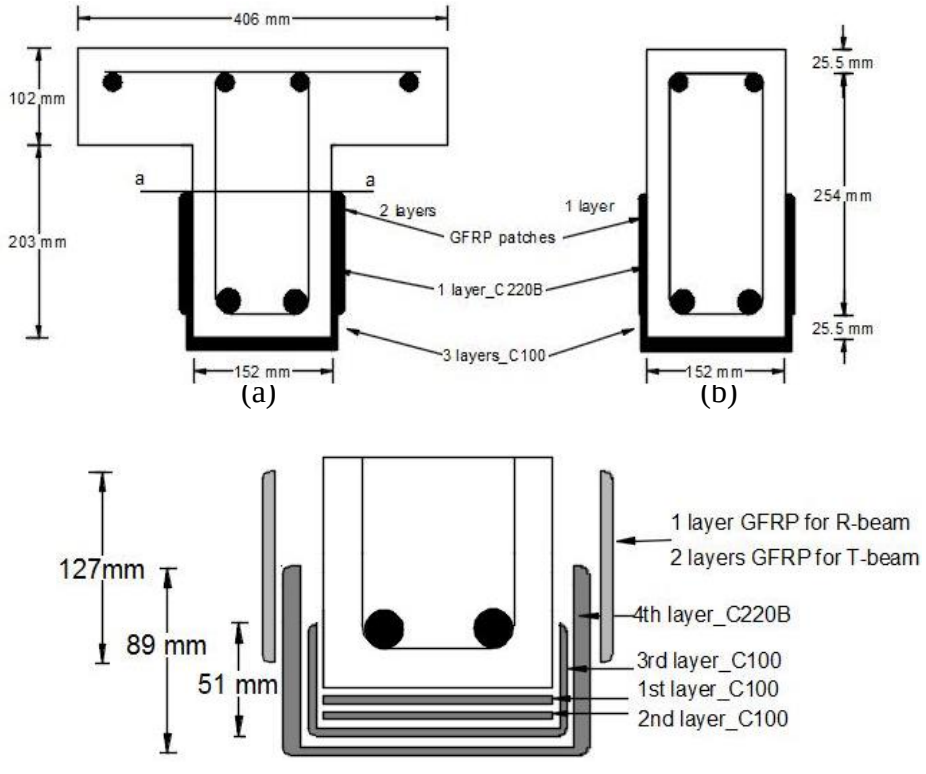

Figure 5-5 Beam cross section details for set 3 (a) T beam; (b) rectangular beam

(a) (b)

Figure 5-6 CFRP Applications of set 3 (a) applying the side GFRP patches; (b) pressing the patches into the resin using a wooden roller

5.6 Test Setup and Data Acquisition

The flexural tests were performed in the structural testing lab at Kansas State University. The beams were tested in four-point bending using a steel spreader beam that was 1219 mm long and a 222-kN hydraulic actuator, Figure 5-7. All the beams were simply supported (pinned sport at one end and roller support at the other end). The supports were placed at 76 mm from the edges of the beams, providing a clear span of 4724 mm. The shear span on each side of the applied load was 1753 mm, Figure 5-7. Two linear variable displacement transducers (LVDTs) were placed at midspan to measure the deflection. Two strain gages were mounted on the main flexural bars at mid span that were embedded into the concrete before casting to measure the strains for steel reinforcement. Another two strain gages were installed at mid-span on the top of beams to monitor the critical compressive strain of concrete. Additionally, two more strain gages were installed at the bottom of mid-span critical section to measure the strain on the CFRP sheets. Displacement control protocol was followed throughout the testing process at a rate of 2.54 mm per minute.

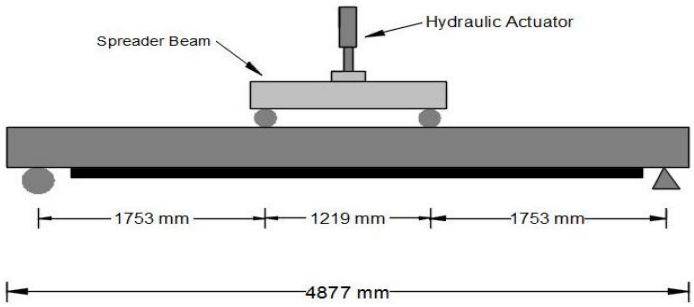

Figure 5-7 Beam details and experimental test setup

5.6.1 Numerical Analysis

5.6.1.1 Computer Program

An Excel analysis program that was developed earlier at Kansas State University was considered to compare the experimental load-deflection and load-strain response to numerical predictions. The program uses strain compatibility and force equilibrium to determine the flexural response, ultimate flexural capacity and the flexural failure mode of the specimen. From the flexural analysis, the program determines a moment curvature relationship as well as load deflection response, Figure 5-8. Furthermore, the program accounts for the nonlinearity of concrete in compression by using the Hognestad's parabola. Tension stiffening effect is also treated after concrete cracking. The stress strain curve of the internal steel reinforcement is assumed to be elastic-perfectly plastic. The program assumes perfect bond between the concrete substrate and FRP sheets. Mormont curvature relationship is computed using the incremental deformation technique. In this technique, the external compression fiber strain is increased between zero and 0.003. Under each strain value, iterations are made to determine the concrete depth of neutral axis once force equilibrium is satisfied. Then, the moment curvature point for that strain is recorded. Load-deflection response is computed utilizing a numerical integration of the deflection expression by dividing the shear span into 50 different segments and using the moment curvature response to perform the numerical deflection calculation.

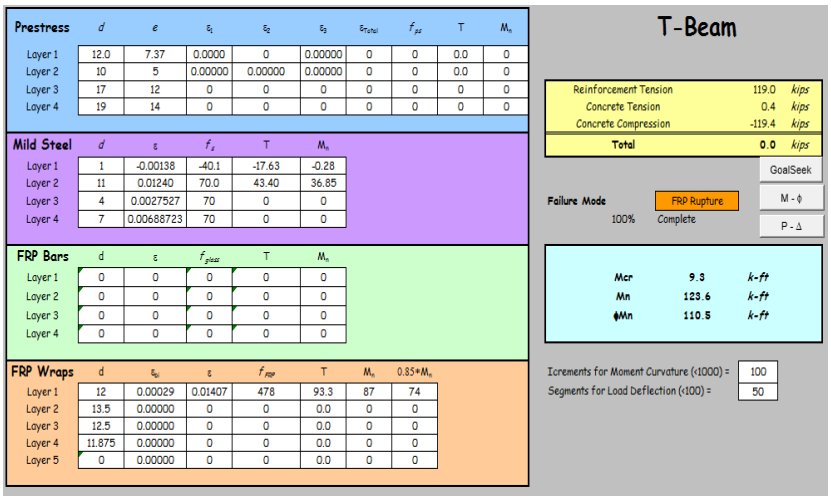

Figure 5-8 Output interface for the analysis program

5.7 Results and Discussion

One of each of the beam types was tested as a control specimen (Set 1, Beams T1 and R1). The remaining RC beam sets 2-3 (Beams T2, T3, R2, and R3). were strengthened in flexure with CFRP sheets plus side GFRP bars or side GFRP patches in order to provide external anchorage reinforcement and anchor the bidirectional side layers of CFRP, Figures 5-3 and 5-5. The results of sets 2 and 3 are further compared with equivalent RC beams strengthened using equivalent flexural CFRP sheets at the soffit only (Beams T4 and R4) and using flexural CFRP sheets plus distributed U-wrap anchorage (Beams T5 and R5).

The latter beams were prepared and tested by Rasheed et al. [21]. The specimens without anchorage (T4 and R4) were reinforced in flexural with five layers of V-Wrap C100 CFRP applied to the bottom face of the beams only. On the other hand, the beams with U-wrap anchors (T5 and R5) had the same five flexural layers of CFRP besides using U-wraps. The beam T5 had two layers of transverse U-wraps with 127 mm width spaced at 305 mm on center. The beam R5 had one layer of transverse U-wraps with 140 mm width spaced on 305 mm on center. The geometry (cross sectional dimensions and span length), and material properties (compressive strength for concrete, yielding strength of steel, modulus of elasticity of steel, number and size of top and bottom rebars)

were exactly identical. In addition, the contribution of V-wrap C100 flexural CFRP sheets (five layers) of the beams tested by Rasheed et al. [21] were designed to be exactly equivalent to the four flexural CFRP layers composed of V-Wrap C100 and V-wrap C220B (Appendix A). Furthermore, the epoxy used in both experimental programs was identical (V-wrap 770). Accordingly, the comparison between the results of T2-T5 and R2-R5 specimens is relevant.

5.7.1 Control T-Beam (T1)

The first specimen in the series of T-shaped beams was tested as a control beam. The beam was loaded in displacement control at a rate of 2.54 mm per minute. Using the analytical program, the predicted failure load for the beam was found to be 57.70 kN. The beam failed at a load of 71.0 kN, which is higher than the theoretical ultimate load. This is attributed to assuming elastic-perfectly plastic response of steel in addition to a maximum useful compressive strain of 0.003 in the analysis. Also, the deflection at mid-span corresponding to maximum load was 165.34 mm and the failure mode was concrete crushing, Figure 5-9. The experimental load level for steel yielding occurred at around 50.14 kN, close to the predicted load from the analysis (49.0 kN). Figure 5-10 shows the load deflection comparisons between the analysis program and the experimental results. Also, the comparison between the theoretical and experimental results of load-strain at the extreme compression fiber is shown in Figure 5-11. The readings of the strain gauges from the main tension reinforcement were unexpectedly lost during the test.

Figure 5-9 Control beam T1 after the test

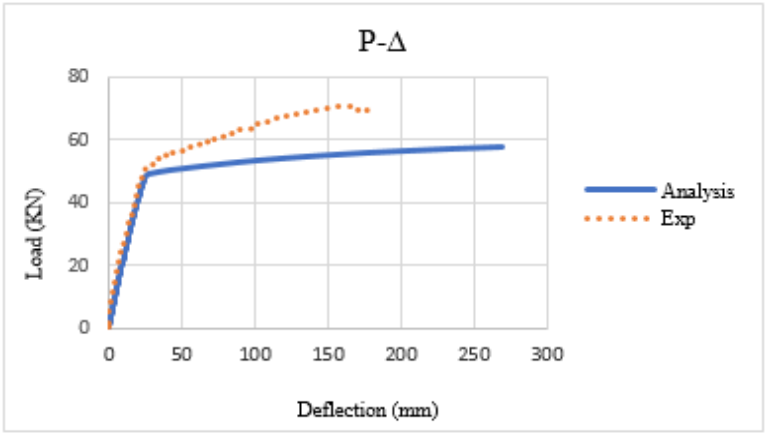

Figure 5-10 Comparison of test and analysis response of control beam T1

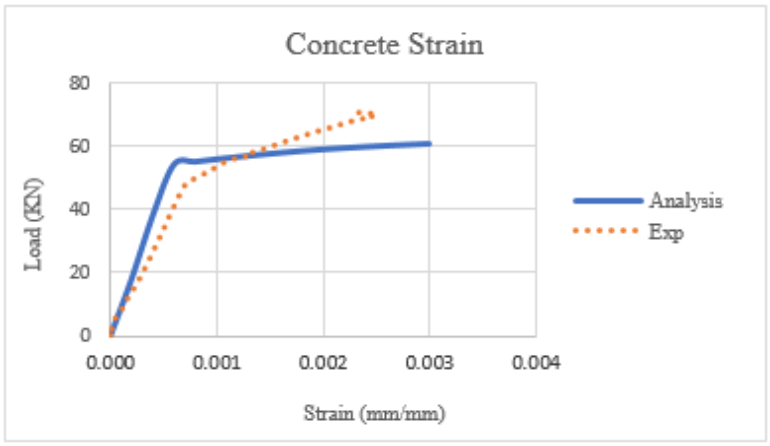

Figure 5-11 Comparison of the load- strain at the top concrete surface of beam T1

5.7.2 T-Beam with Flexural CFRP and GFRP Sidebars (T2)

The second specimen in the series of T-shaped beams was strengthened with flexural CFRP sheets on the bottom face of the beam with at least the last layer wrapped around the sides and anchored longitudinally with glass (GFRP) bars on both sides as explained in section 5.1.1, Figure 5-3. The ultimate load capacity of 199.6 kN, with maximum deflection of 93.03 mm, was predicted by the analysis program with a failure mode of CFRP rupture. The test results show that the beam failed at a load of 197.27 kN with a maximum deflection of 88.36 mm, very similar to the analysis values. The failure mode was a combination of debonding and cover separation, Figure 5-12. This

confirms that this anchorage technique is very effective in securing the ultimate sectional capacity without a loss of strength. On the other hand, the identical T beam (T4) strengthened with equivalent CFRP sheets without anchorage and tested by Rasheed et al. [21] yielded a lower peak load of 113.7 kN with a maximum deflection of 50.1 mm. The beam T4 failed in debonding of CFRP sheets (Figure 5-13) at 57.5% of the ultimate load capacity of beam T2. Furthermore, the beam (T5) with the distributed U-wrap anchorage, tested by Rasheed et al. [21], reached an ultimate load of 148.6 kN when the flexural CFRP sheets ruptured, Figure 5-14. However, the increase in load over that of beam T4 is still significantly lower than the 197.27 kN obtained from beam T2. In other words, the ultimate capacity of beam T5 is only 76% of the ultimate load of beam T2 tested herein. It may be noted that the contribution of the GFRP sidebars was taking into account in the theoretical analysis.

Figure 5-15 shows the load deflection comparisons between the analytical and experimental results of beam T2 alongside the experimental response for the control beam T1, the beam T4 strengthened in flexure only, and the beam T5 with distributed CFRP U-wraps. It is clear from Figure 5-15 that the experimental results for beam T2 (using side GFRP bars) is in excellent agreement with the analysis results since the beam reached its ultimate capacity before failure. That indicates the huge benefit of using side GFRP bars to anchor the flexural CFRP sheets in order to increase the flexural capacity of RC beams. Figure 5-16, 5-17, and 5-18 show the comparison of the load versus strain between the experimental and analytical results at the top concrete surface, on the main tension rebars, and on the flexural CFRP, respectively. Up to the yielding level, the experimental strains for concrete, steel, and CFRP are similar to the predicted response from the analysis. After steel yielding level, the experimental response shows stiffer trend

compared to the analysis curve indicating that the strain gauge locations are relatively far from the induced flexural cracks.

Figure 5-12 Beam T2 after the failure

Figure 5-13 Beam T4 after the failure

Figure 5-14 Failure of the beam T5 with U-wrap anchorage

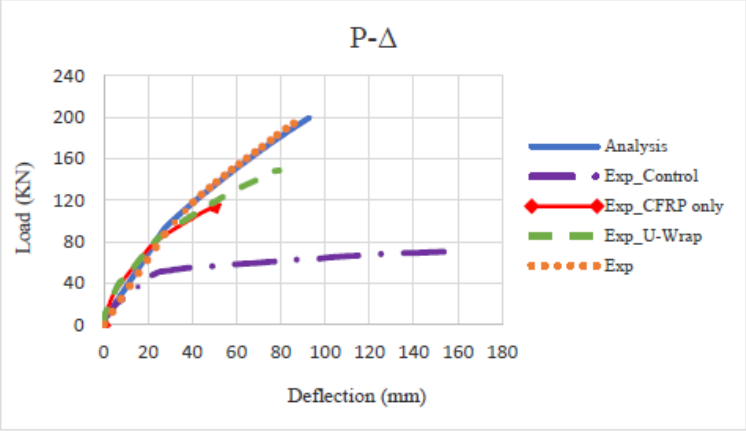

Figure 5-15 Comparison of the load-deflection of beam T2 and comparable beams

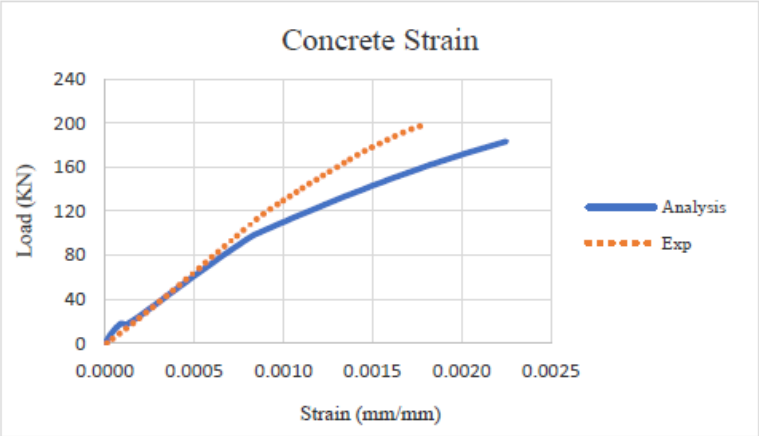

Figure 5-16 Comparison of the load- strain at the top concrete surface of T2

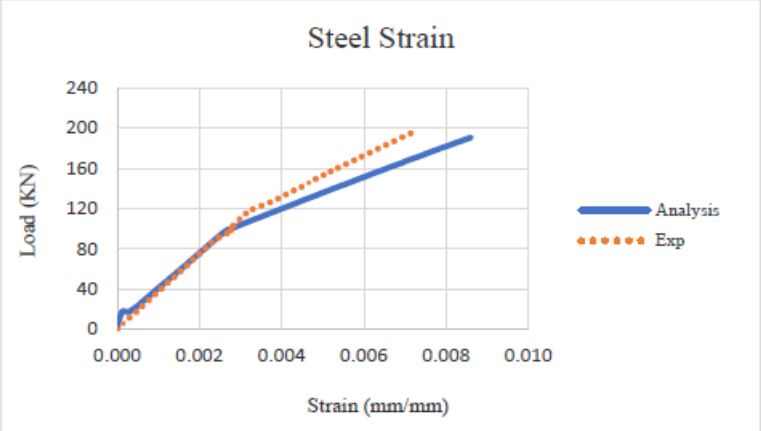

Figure 5-17 Comparison of the load-strain in the main rebars of T2

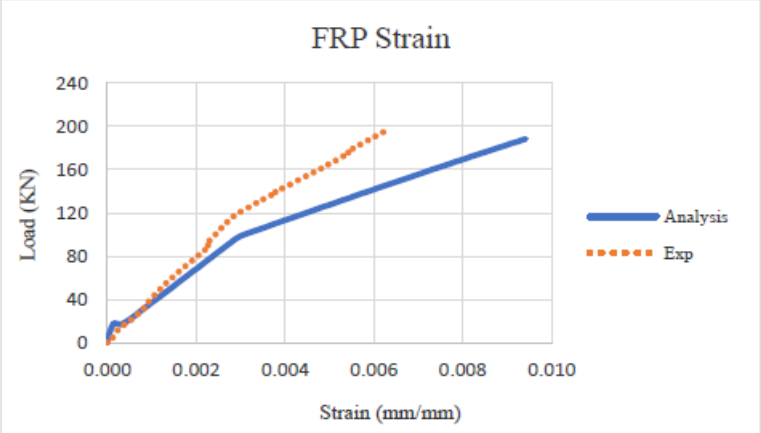

Figure 5-18 Comparison of the load-strain in the CFRP sheets of T2

5.7.3 T-Beam with Flexural CFRP and GFRP Side Patches (T3)

As elaborated in section 5.1.2 and Figure 5-5, the last specimen in the series of T beams was strengthened with flexural CFRP sheets on the bottom face of the beam with at least the last layer wrapped around the sides and anchored longitudinally with ±45° glass patches on both sides of the beam. From the analysis program, the ultimate load of 182.4 kN with a maximum deflection of 86.90 mm were predicted. The experimental results show that the beam reached an ultimate load of 178.2 kN with a maximum deflection 80.3 mm when the CFRP sheets and side GFRP patches completely debonded, Figure 5-19. The load deflection comparisons between the analysis results of the beam T3 and the experimental response for, the control beam T1, the beam T3 with side GFRP patches, the beam T4 with flexural CFRP only [21], and the beam T5 with distributed CFRP U-wraps [21] are shown in Figure 5-20.

It can be clearly observed that the experimental and theoretical load-deflection responses for beam T3 are very similar. That verifies the beneficial use of side GFRP patches for anchoring the flexural CFRP sheets to enhance the flexural capacity of RC beams. Even though the beam T5 with distributed CFRP U-wrap anchorage improved the flexural capacity compared to beam T4, the specimen T5 did not achieve the ultimate sectional capacity (182.4 kN) since it failed at a load of 148.6 kN [21]. On the other hand, using the side GFRP patches significantly increased the strength (178.2 kN) to reach very close to the experimental peak load capacity. The comparison of the load versus strain between the experimental and analytical results at the top concrete surface and in the main tension rebars (steel), at mid-span, are favorably presented in Figure 5-21 and 5-22. Figure 5-23 shows the experimental and theoretical strain responses that were experienced in the CFRP. It seems that there was local debonding in the critical region (constant moment region) between the CFRP sheets and concrete substrate causing strain lag in the experimental graph close to the yielding level at a load of approximately 80 kN. It is evident that the experimental curve right after

this strain lag is parallel to the analysis curve assuming perfect bond. It may be noted that the contribution of the GFRP side patches was taken into account in the theoretical analysis.

Figure 5-19 Beam T3 after the failure

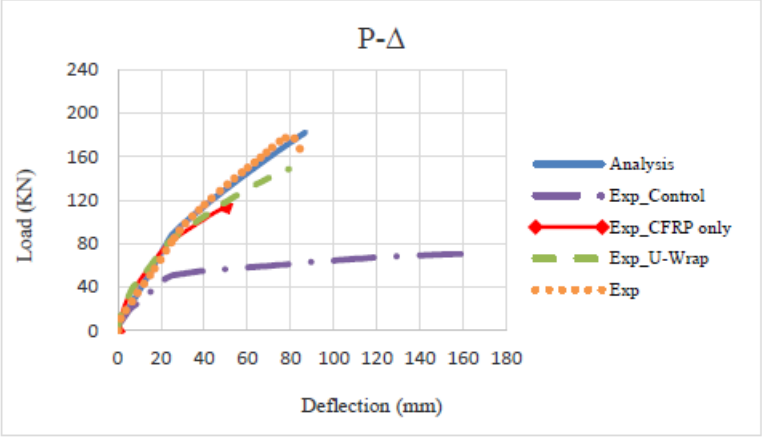

Figure 5-20 Comparison of the load-deflection of beam T3 and comparable beams

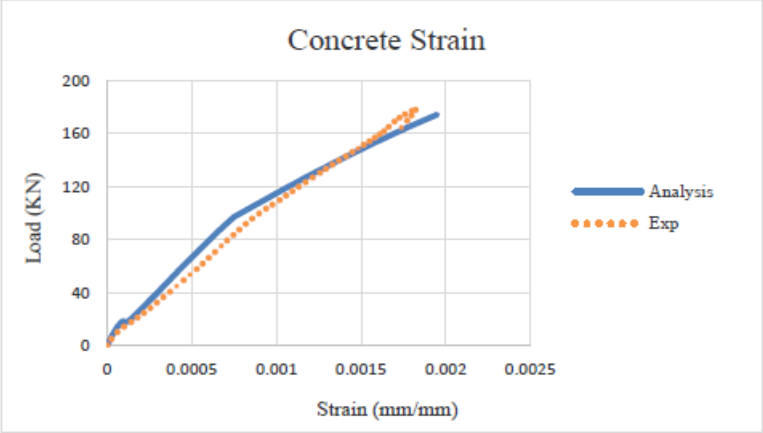

Figure 5-21 Comparison of the load-strain at the top concrete surface of T3

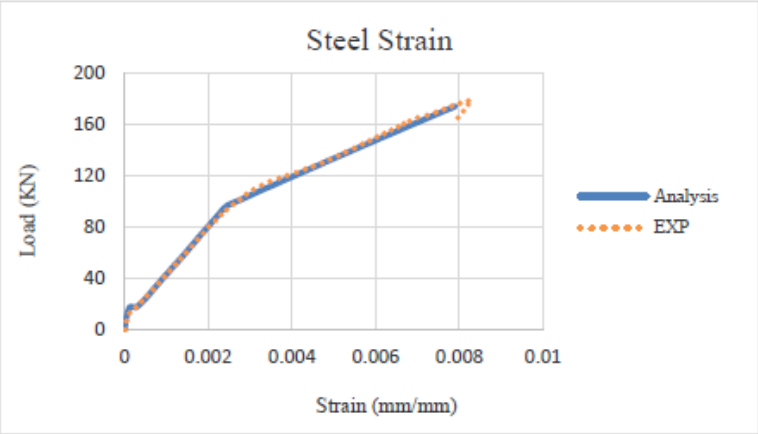

Figure 5-22 Comparison of the load-strain in the main rebars of T3

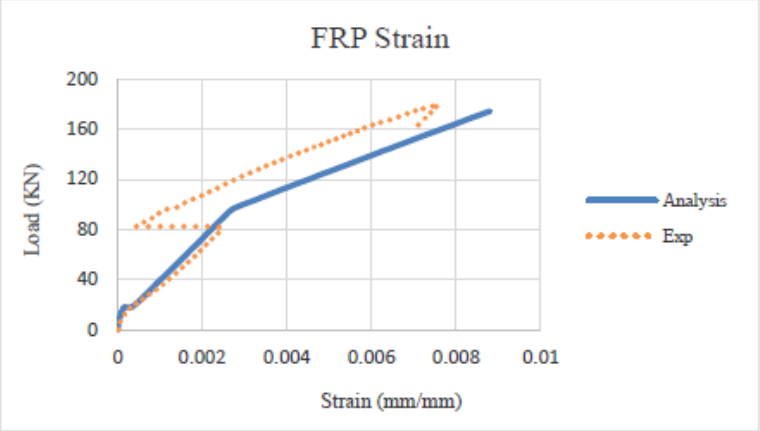

Figure 5-23 Comparison of the load-strain in the CFRP sheets of T3

5.7.4 Rectangular Control Beam (R1)

The first rectangular beam in the series one (set 1) was tested as a control beam. It was determined from the flexural analysis program that the beam would fail at a load of 50.0 kN. The test results indicated the beam failed at a load of 54.7 kN, very similar to the theoretical value that was predicted from the analytical program. Figure 5-24 shows the failure mode of the beam R1, which was initiated by steel yielding followed by concrete crushing. The mid-span deflection at the ultimate load was 79.7 mm. In addition, the steel yielding occurred at a load of 48.9 kN, almost the same as that determined from the analysis (48.6 kN). Figure 5-25 shows the load deflection

comparisons between the analytical and the experimental results, which are matching very well. Also, there were very good agreements between the analysis and experimental results of the load versus strain in top concrete and in steel rebars, Figures 5-26, 5-26, and 5-27.

Figure 5-24 Control beam R1 after the test

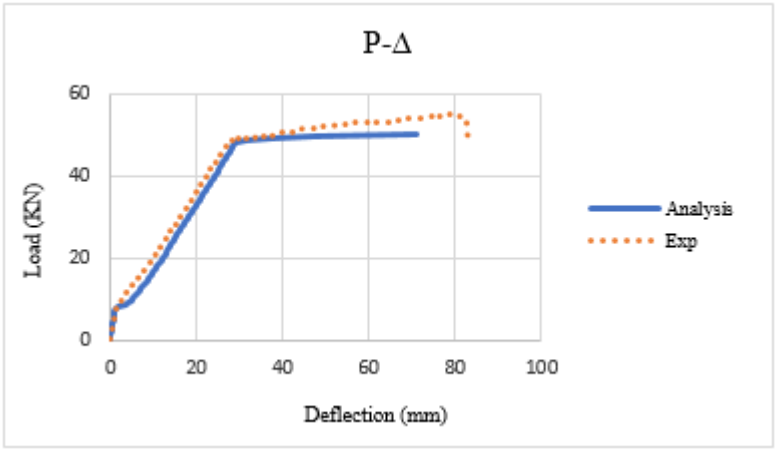

Figure 5-25 Comparison of test and analysis response of control R1 beam

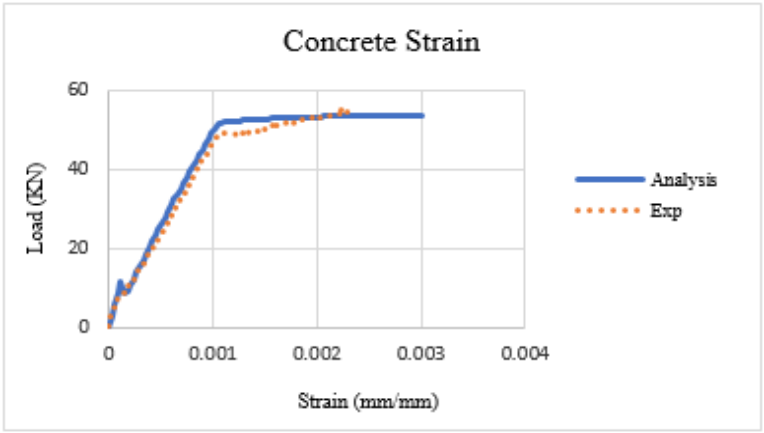

Figure 5-26 Comparison of the load-strain at the top concrete surface of beam R1

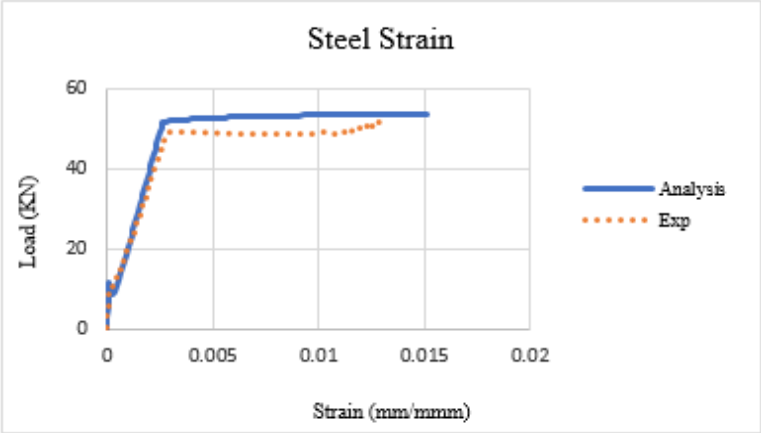

Figure 5-27 Comparison of the load-strain in the main rebars of R1

5.7.5 R-Beam with Flexural CFRP and GFRP Sidebars (R2)

Similar to beam T2, the second specimen in the series of rectangular beams was strengthened with flexural CFRP sheets and anchored using glass bars (GFRP) on both sides of the beams (section 5.1.1, Figure 5-3). A 119.1 kN ultimate load with a maximum deflection of 58.23 mm were estimated by the analysis program. The beam failed in concrete crushing (Figure 5-28) at a load of 103.5 kN with a mid-span deflection of 69.9 mm, less than the predicted load value. The rectangular beam strengthened with CFRP sheets only (R4) reached an ultimate load of 109.4 kN when the FRP debonded from the beam at a deflection of 59.69 mm. The rectangular beam with distributed U-warps (R5) reached an ultimate load of 120.4 kN before the rupture of CFRP caused by concrete crushing and excessive curvature at the critical region as observed in Figure 5-29 [21]. The load-deflection comparisons between the analytical results of the R2 and the experimental values for, the control beam R1, the beam R2 with side GFRP rebars, the specimen R4 with flexure CFRP only [21], and the beam R5 with distributed CFRP U-wraps [21], are shown in Figure 5-30.

The beam R2 did not reach the estimated ultimate load due to concrete crushing that took place early within the constant moment region, which may be attributed to a void in concrete because of

poor vibration near the top surface. This conclusion was further supported by the observation that beam R2 sprung back once the load was removed indicating a high elastic energy content. There are good agreements between the experimental and analytical results for the strains at the top concrete surface and in the steel rebars, Figure 5-31 and 5-32. Also, the experimental and analytical strain response of the CFRP is shown in Figure 5-33. From this graph, a local debonding of FRP at critical section can be noticed before the yielding level. It may be noted that the contribution of the GFRP sidebars was taking into account in the theoretical analysis.

Figure 5-28 Beam R2 after the failure

Figure 5-29 Beam R5 after the failure

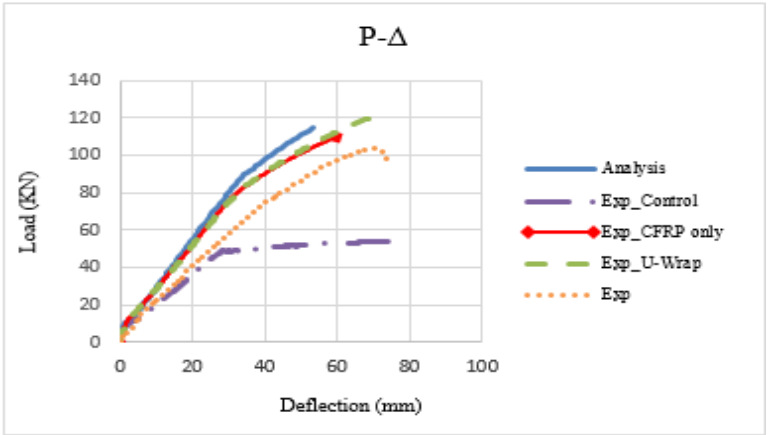

Figure 5-30 Comparison of test and analysis response of beam R2 and comparable beams

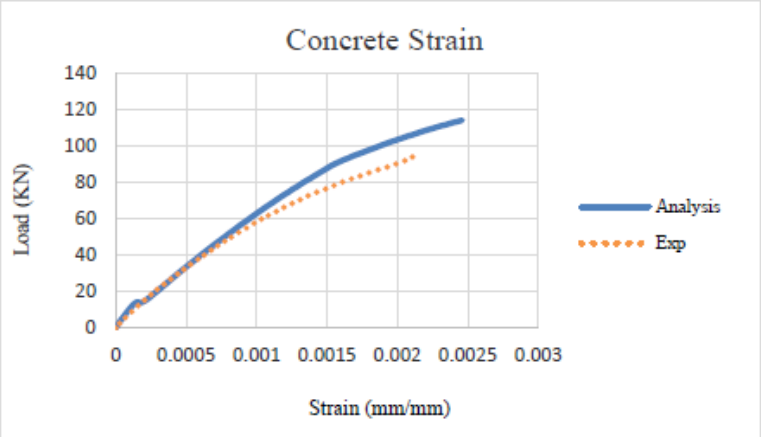

Figure 5-31 Comparison of the load-strain at the top concrete surface of beam R2

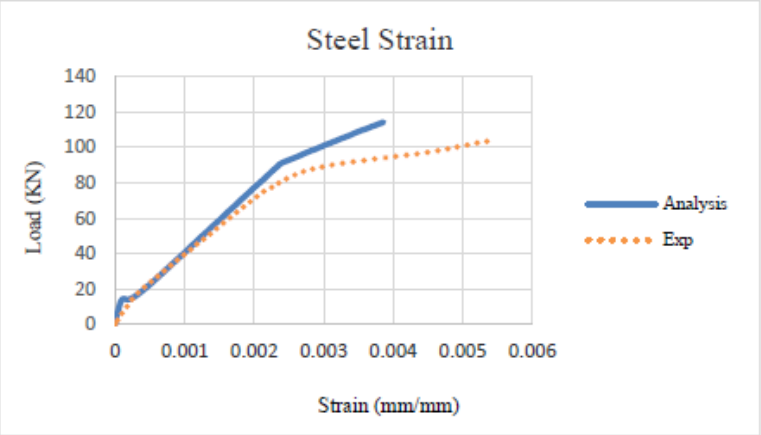

Figure 5-32 Comparison of the load-strain in the main rebars of beam R2

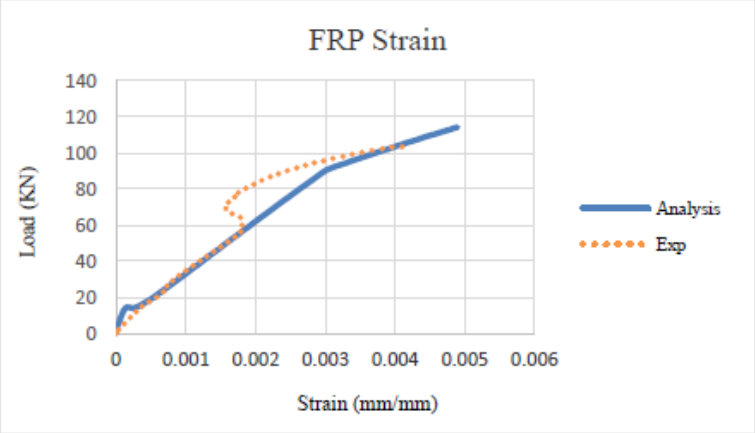

Figure 5-33 Comparison of the load-strain in the CFRP sheets of beam R2

5.7.6 R-Beam with Flexural CFRP and GFRP Side Patches (R3)

Like T3 beam, the last specimen in the series of rectangular beams was strengthened with flexural CFRP sheets and secured with side GFRP patches (section 5.1.2, Figure 5-5). The analysis program calculated the ultimate load of R3 to be 115.3 kN with a central deflection of 60.9 mm. Unfortunately, the beam failed early at a load of 97.1 kN, by concrete crushing at a distance of 1219 mm from the support (outside of the constant moment region) where the steel rebar hook was placed, Figure 5-34. This failure is unusual to occur there since the beam is simply supported inducing much higher moment in the constant moment region, which in turn remained intact. This could be attributed to lack of good vibration inside the concrete near the hook that lead to the early failure there. Figure 5-35 shows the load-deflection comparisons between the analysis results of the beam R3 and the experimental response for, the control beam R1, the beam R3 with side GFRP patches, the specimen R4 with flexure CFRP only [21], and the beam R5 with distributed CFRP U-wraps [21]. The analytical results for R3 and experimental responses for beams R2, R3 and R5 are in excellent agreement, but the beam R3 did not reach to the higher load level due to the early failure. At 1219 mm from the support, the maximum strain at the top of concrete surface reached 0.0014 level analytically at the actual experimental failure load, lower than the crushing strain of concrete (0.003), Figure 5-36. This verifies there was a defect at that section where the failure happened. The experimental and analytical strain relationship for the steel is identical, Figure 5-37. Moreover, the comparison of the strain that was experienced in the CFRP is shown in Figure 5-38. It appears from this figure that the experimental curve diverts from the theoretical one because of local debonding that is expected to have occurred early on after cracking level. Table 5-3 provides a detailed summary of the results for all the tested RC beams (T1 through T5 and R1 through R5). It may be noted that the contribution of the GFRP side patches was taking into account in the theoretical analysis.

Figure 5-34 Beam R3 after the failure

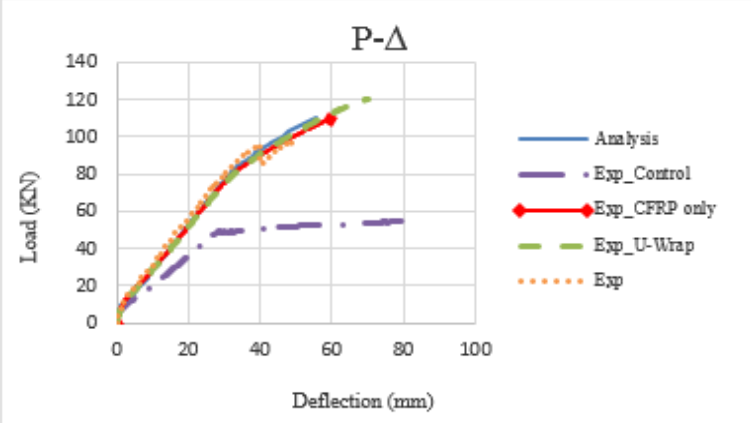

Figure 5-35 Comparison of test and analysis response of beam R3 comparable beams

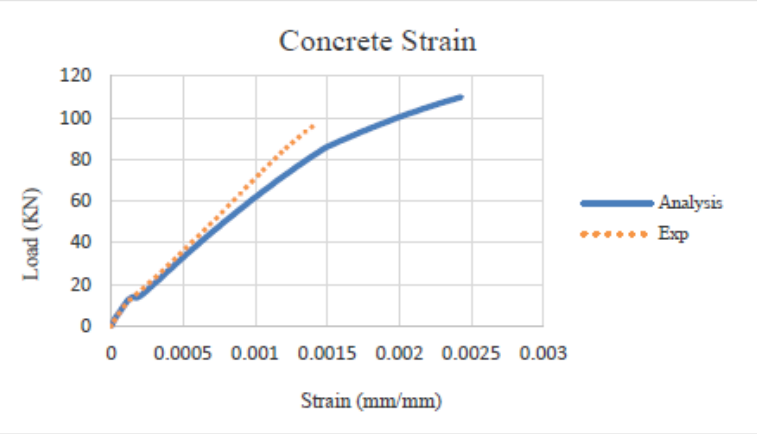

Figure 5-36 Comparison of the load-strain at the top concrete surface of beam R3

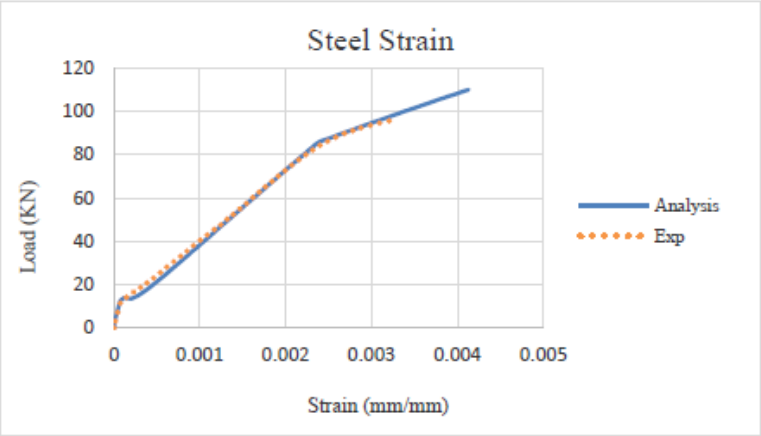

Figure 5-37 Comparison of the load-strain in the main rebars of beam R3

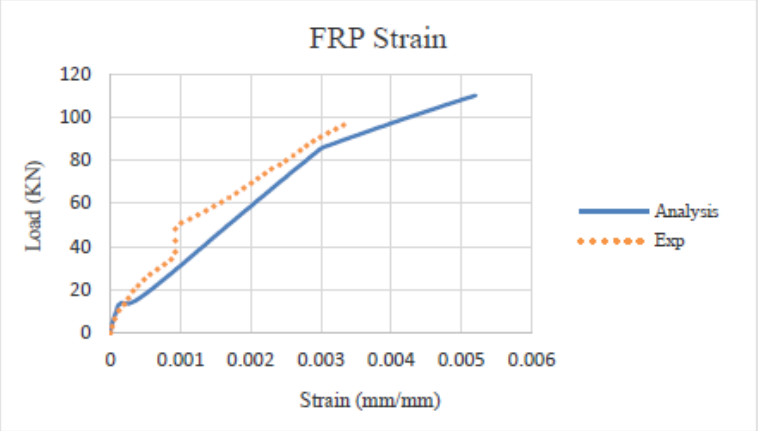

Figure 5-38 Comparison of the load-strain in the CFRP sheets of beam R3

Table 5-3 Summary of the Tested RC Beams

Beam	Type of FRP anchors (mm)	FRP anchorage per span length	Ultimate Experimental load capacity (kN)
T1	Control	Control	71.0
T2	GFRP side bars	One longitudinal GFRP bar with 13 mm diameter on each side of the beam	197.27
T3	GFRP side patches	Two longitudinal GFRP patches with 127 mm height on each side of the beam	178.2
T4	Flexural Layers only	No anchorage	113.7 Rasheed et al [21]
T5	Distributed U-wraps	Two U-wraps with 127 mm width spaced at 305 mm	148.6 Rasheed et al [21]
R1	Control	Control	54.7
R2	GFRP side bars	One longitudinal GFRP bar with 13 mm diameter on each side of the beam	103.5
R3	GFRP side patches	One longitudinal GFRP patch with 127 mm height on each side of the beam	97.1
R4	Flexural Layers only	No anchorage	109.4 Rasheed et al [21]
R5	Distributed U-wraps	One U-wrap with 140 mm width spaced at 305 mm	120.4 Rasheed et al [21]

5.8 Summary and Conclusions

This study introduces for the first time the effectiveness of two new techniques using GFRP sidebars and GFRP side patches to anchor flexural CFRP sheets applied to strengthen RC beams. It is evident from the results that these two anchorage techniques show a fundamental improvement in the flexural behavior by achieving much higher levels of ultimate strength and deformability. The experimental ultimate load of the T beam strengthened with CFRP only was increased by 31% when flexural CFRP sheets were anchored with distributed U-wraps along the span. In this work, the use of GFRP sidebars increased the baseline strength by 74%, which is comparable to the increase expected from perfect bond analysis to be 76%. Therefore, the first technique was proven to achieve the full sectional capacity of the beam without any reduction due to premature debonding or bond slip. Similarly, anchoring the flexural CFRP with the second technique by using GFRP side patches for T- beams increased the ultimate capacity by 58% compared to 61% resulting from perfect bond analysis.

On the other hand, the maximum deflection of the beam with CFRP only increased by 58% when U-wraps were used. The use of GFRP sidebars caused that increase to go up to 76%. Nevertheless, the increase in maximum deflection was found to be 60% when the GFRP side patches were applied. It is important to note here that both techniques marked failure once the GFRP sidebars or the GFRP side patches gave up simply by delaminating the entire concrete cover and the flexural CFRP sheets. This is an evidence that the flexural strengthening held up to such high load level only because of the existence of these anchoring devices. Furthermore, reduction was observed in load capacity or deformability for rectangular beams strengthened with CFRP sheets and anchored with GFRP sidebars or GFRP side patches compared to the rectangular beam strengthened with CFRP only due to the defective compression zones in these former beams that

lead to premature concrete crushing failure as elaborated earlier in the paper. The authors stress here that in case the anchored rectangular beams were free of defects, the new anchorage systems would have easily shown some increase in capacity and deformability. However, such anticipated increase would have been much lower than those of the T-beams' since the perfect bond failure of the rectangular beams is by concrete crushing while that of T-beams is by mostly CFRP rupture making full utilization of the FRP material.

5.9 References

[1] Rasheed, H. A., & Pervaiz, S. (2002). Bond slip analysis of fiber-reinforced polymer-strengthened beams. *Journal of Engineering Mechanics, 128*(1), 78-86.

[2] Saadatmanesh, H., & Ehsani, M. R. (1990). Fiber composite plates can strengthen beams. *Concrete International, 12*(3), 65-71.

[3] Grace, N. F., Sayed, G. A., Soliman, A. K., & Saleh, K. R. (1999). Strengthening reinforced concrete beams using fiber reinforced polymer (FRP) laminates. *ACI Structural Journal-American Concrete Institute, 96*(5), 865-874.

[4] Sundarraja, M. C., & Rajamohan, S. (2009). Strengthening of RC beams in shear using GFRP inclined strips–An experimental study. *Construction and Building Materials, 23*(2), 856-864.

[5] Attari, N., Amziane, S., & Chemrouk, M. (2012). Flexural strengthening of concrete beams using CFRP, GFRP and hybrid FRP sheets. *Construction and Building Materials, 37*, 746-757.

[6] Ceroni, F. (2010). Experimental performances of RC beams strengthened with FRP materials. *Construction and Building materials, 24*(9), 1547-1559.

[7] Dong, J., Wang, Q., & Guan, Z. (2013). Structural behaviour of RC beams with external flexural and flexural–shear strengthening by FRP sheets. *Composites Part B: Engineering,44*(1), 604-612.

[8] Smith, S. T., Zhang, H., & Wang, Z. (2013). Influence of FRP anchors on the strength and ductility of FRP-strengthened RC slabs. *Construction and Building Materials, 49*, 998-1012.

[9] Zhang, H., & Smith, S. T. (2017). Influence of plate length and anchor position on FRP-to-concrete joints anchored with FRP anchors. *Composite Structures, 159*, 615-624.

[10] Saadatmanesh, H., & Malek, A. M. (1998). Design guidelines for flexural strengthening of RC beams with FRP plates. *Journal of Composites for Construction, 2*(4), 158-164.

[11] Smith, S. T., Hu, S., Kim, S. J., & Seracino, R. (2011). FRP-strengthened RC slabs anchored with FRP anchors. *Engineering Structures, 33*(4), 1075-1087.

[12] Kalfat, R., Al-Mahaidi, R., & Smith, S. T. (2011). Anchorage devices used to improve the performance of reinforced concrete beams retrofitted with FRP composites: State-of-the-art review. *Journal of Composites for Construction, 17*(1), 14-33.

[13] Chahrour, A., & Soudki, K. (2005). Flexural response of reinforced concrete beams strengthened with end-anchored partially bonded carbon fiber-reinforced polymer strips. *Journal of Composites for Construction, 9*(2), 170-177.

[14] Ceroni, F., Pecce, M., Matthys, S., & Taerwe, L. (2008). Debonding strength and anchorage devices for reinforced concrete elements strengthened with FRP sheets. *Composites Part B: Engineering, 39*(3), 429-441.

[15] Grelle, S. V., & Sneed, L. H. (2013). Review of anchorage systems for externally bonded FRP laminates. *International Journal of Concrete Structures and Materials, 7*(1), 17-33.

[16] Ozbakkaloglu, T., & Saatcioglu, M. (2009). Tensile behavior of FRP anchors in concrete. *Journal of Composites for Construction, 13*(2), 82-92.

[17] Oh, H. S., & Sim, J. (2004). Interface debonding failure in beams strengthened with externally bonded GFRP. *Composite Interfaces, 11*(1), 25-42.

[18] Kim, S. J., & Smith, S. T. (2010). Pullout strength models for FRP anchors in uncracked concrete. *Journal of composites for construction, 14*(4), 406-414.

[19] Smith, S. T., Rasheed, H. A., & Kim, S. J. (2017). Full-range load-deflection response of FRP-strengthened RC flexural members anchored with FRP anchors. *Composite Structures, 167*, 207-218.

[20] Orton, S. L., Jirsa, J. O., & Bayrak, O. (2008). Design considerations of carbon fiber anchors. *Journal of Composites for Construction, 12*(6), 608-616.

[21] Rasheed, H. A., Decker, B. R., Esmaeily, A., Peterman, R. J., & Melhem, H. G. (2015). The influence of CFRP anchorage on achieving sectional flexural capacity of strengthened concrete beams. *Fibers, 3*(4), 539-559.

[22] American Society for Testing and Materials. Committee C-9 on Concrete and Concrete Aggregates. (2011). *Standard test method for compressive strength of cylindrical concrete specimens*. ASTM International.

[23] ACI Committee 440. (2017). ACI 440.2 R-17: Guide for the design and construction of externally bonded FRP systems for strengthening concrete structures. *American Concrete Institute.*

[24] ACI Committee. (2014). Building code requirements for structural concrete :(ACI 318-14); and commentary (ACI 318R-14). *American Concrete Institute.*

[25] Rasheed, H. A. (2014). *Strengthening design of reinforced concrete with FRP*. CRC Press.

Chapter 6 - Superior Performance of Reinforced Concrete T Beams Strengthened with CFRP Sheets and Fastened by CFRP Anchors

The use of carbon fiber reinforced polymer (CFRP) anchors has been shown to improve the performance of reinforced concrete (RC) beams strengthened in flexure with (CFRP) sheets. This improvement results from delaying or controlling the debonding of FRP sheets at failure. In this study, five full-scale T beams are prepared and tested to examine the flexural enhancement of anchored beams with CFRP spike anchors. The first T beam was tested as a control beam and the remaining specimens were retrofitted with three unidirectional layers of CFRP sheets and one bidirectional layer of CFRP sheet but with different anchorage arrangements. The second T beam was anchored with 12 anchors of 16 mm diameter at 140 mm spacing along each shear span. The Third T specimen was bonded using 9 anchors of 19 mm diameter positioned at 203 mm per shear span. Four CFRP anchors with diameter of 16 mm were used to secure the CFRP sheets for the forth T specimen. These anchors were spaced at 406 mm on center per shear span. The last T beam was anchored utilizing only one CFRP anchor of 16-mm diameter at the ends of the CFRP sheets. The experimental testing results show that by bonding the flexural CFRP sheets with CFRP anchors extremely enhance the flexural capacity of the RC beams (T beams). This enhancement increases as the number and fiber content of the CFRP anchor increases. Furthermore, the closely spaced anchors, the higher load level can be achieved until gaining the full sectional capacity up to the FRP rupture failure mode.

6.1 Introduction

Despite the fact that FRP materials have been found to be very effective in strengthening and repairing the RC members, premature failure may occur at a strain quite a bit lower than the

ultimate strain of the FRP. For the fully strengthened beams with FRP sheets, the failure caused probably by deboning that limits the load-carrying capacity of the member and prevents gaining the full fiber utilization. The debonding initiates due to the flexural or flexural-shear cracks which is referred to as intermediate induced cracking (also known as IC debonding) [1-2]. After the cracks are developed, premature debonding between the FRP and concrete surface of the beam induces, usually within the shear span. With additional load, the debonding propagates toward the free end of the FRP sheets causing the complete separation of the sheets occurs, Figure 6-1. This type of failure is often dominant in moderately reinforced, moderately strengthened beams with FRP sheets [2].

There are two applicable approaches to avoid this type of failure mode, by limiting the maximum FRP strain below the FRP debonding strain as specified by ACI 440-2R.-17 [3], or by using anchorage technique which is anchoring the flexural FRP of the RC beams with transvers U-wraps or FRP spike anchors. By eliminating the strain design restrictions that restrain achieving the ultimate sectional capacity, FRP anchors have shown an essential solution to increase the tension capacity of the FRP sheets. That will also improve the efficiency use of FRP [4-14].

The aim of this work is to investigate the flexural improvement of the RC beams using different numbers and sizes of CFRP spike anchors. To do so, five identical T beams were prepared (T1-T5). One beam was left unstrengthen as the control, and the remaining four beams were strengthened in flexure with similar CFRP sheets but using different anchorage arrangements. All the CFRP anchors herein were installed along the shear spans only since it was found that the anchors positioned in the constant moment region are ineffective [15]. Additionally, two types of CFRP anchors were considered for beams T2-T3. Dowel-fiber CFRP anchors are applied on one

shear span and bundled-fiber CFRP anchors are installed in the other shear span of the same beams (T2-T3).

Several studies have been conducted using end anchorage techniques to prevent debonding or cover delamination that cause such a premature failure [16-20]. Chahrour et al. [21] investigated the flexural behavior of the strengthened RC beams with end-anchored partially bonded CFRP strips. The authors considered fixing the both ends of the flexural CFRP strips using a mechanical anchor that consisted of top and bottom steel plates with 10 mm thickness and fastened together utilizing two tightened bolts. Oh and Sim [22] evaluated the effect of positioning two FRP anchors at 500 mm centers at the end of a simply supported beam of 2000 mm span. Those two anchors were employed to bond the flexural GFRP plates that were supposed to fail in concrete cover delamination. It was concluded that the anchors did not work successfully in delaying the cover separation. Kalfat et al. [23] reported that by anchoring the ends of the CFRP plates or sheets, a higher bond strength capacity may be achieved before delamination failure occurs.

Still the debonding failure induced by flexural or flexural-shear crack has received very limited attention [1]. The effect of using spike FRP anchors at the ends of CFRP sheets has not been even studied. Accordingly, in this present study, one of the strengthened T-beams was secured at the ends of CFRP sheets with one CFRP anchor on each side to evaluate the flexural performance. The test showed that the end anchors did not successfully improve the flexural capacity.

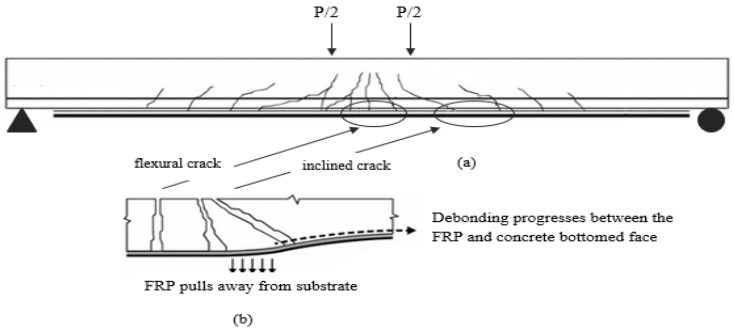

Figure 6-1 Mechanism of debonding failure (a) behavior of flexural member strengthened with FRP on soffit; (b) debonding initiates due to flexural and/or shear cracks

6.2 Specimens Details

All the T-beams had identical cross-sectional areas of 152 mm x 305 mm web dimensions and 406 mm x 102 flange dimensions as observed in Figure 6-2. The beams were reinforced with two Φ 16 mm dimeter bars at the tension zone and four Φ 10 mm bars at compression face. Φ 10 diameter stirrups spaced at 127 mm on center were used for the shear reinforcement. Also, Φ 10 mm hanger bars were positioned at 127 mm longitudinally along the entire span length. The beams had similar total span length of 4877 mm.

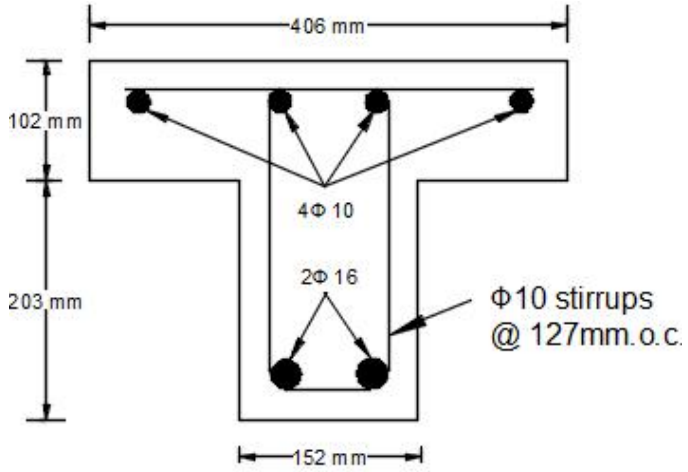

Figure 6-2 Beam cross section details for control beam T1

6.3 Materials

The compressive strength for 28-day was 38 MPa. This value resulted from the average of twelve cylinders of 101.6 mm dimeter and 203.2 height. These cylinders were prepared and tested according to ASTM C39 [24]. The yield strength of the tension steel bars was 488 MPa, and the Young's modulus was 211 GPa. For the compression steel bars, the yield strength and Young's modulus were 470 MPa and 211 GPa, respectively**.** The material properties of the CFRP materials were provided by the manufacturer. Two types of the CFRP sheets were used in this study, unidirectional CFRP (V-Wrap C100) where all the fibers are running in longitudinal direction (0°)

and bidirectional CFRP (V-Wrap 220B) where the fibers are running in longitudinal and transverse directions (0° and 90°). The unidirectional CFRP properties were 0.584 mm thickness, 966 MPa tensile strength, and 66.19 GPa tensile modulus of the cured laminate. The bidirectional CFRP had 0.51 mm thickness in each direction, 1068 MPa tensile strength, and 96.53 GPa tensile modulus. The spike anchors were made of CFRP with 102-mm dowel depth and 150-mm splay length, Figure 6-3 (a-b). The diameters were virous between 16 mm and 19 mm.

(a) (b)

Figure 6-3 CFRP anchors (a) dowel Anchors; (b) bundled fiber anchors

Furthermore, the adhesive used for bonding the CFRP sheets was two component epoxy resin (V-Wrap 770) that were mixed together as specified by the manufacture. The same adhesive was mixed with some silica fume to bond the CFRP anchors into the predrilled holes in the concrete surface.

6.4 Surface Preparation

The bonding surface of the concrete specimens were prepared using water blasting with high pressure of 24 MPa to rough the surface by exposing the coarse aggregate and remove any existing coating. In addition, the bottom corners of the beams were rounded off to approximately a 13-mm radius in order to avoid stress concentration in the FRP as specified in ACI 440.2R-17 [3]. A concrete drill was used to drill the CFRP anchor holes with a minimum hole diameter of 3

mm larger than the anchor diameter. Then, the holes were cleaned with compressed air to clear away the dust and debris. Figure 6-4 shows the beam before and after the surface preparation.

(a) (b) (c)

Figure 6-4 Surface preparation (a) before surface preparation; (b) after rounding and sandblasting the surface; (c) clearing away the dust form the holes

6.5 Experimental Program

6.5.1 Layout and Application of CFRP Sheets to Beams

A series of five T beams were prepared and tested. One of those beams was tested as a control specimen (T1), Figure 6-2. The remaining RC beams (T2, T3, T4, and T5) were strengthened in flexure with similar CFRP sheets but using different anchorage arrangements as elaborated in sections 6.5.1.1-6.5.1.4.

6.5.1.1 Layout and Application of CFRP Sheets and Anchors for T2

The second T beam was strengthened with two layers of unidirectional CFRP applied to the bottom face of beam only, followed by a third layer of CFRP installed to the bottom and wrapped 51 mm up the sides from the soffit, Figure 6-5. Then, a one layer of bidirectional CFRP (V-Wrap C220B) sheet was applied on the top of previous 3 sheets and wrapped 89 mm up the sides, Figure 6-5 section a-a. In addition, the specimen was secured with two types of CFRP anchors of 16 mm-diameter spaced at 140 mm center-to-center along each shear span. This yielded using 12 dowel CFRP anchors per one shear span and 12 bundled- fiber CFRP anchors on the other

shear span (24 total anchors) as laid out in Figure 6-6. The application of CFRP sheets and anchors is presented in Figure 6-7. It is important to note that the purpose of using bidirectional CFRP layer was to provide transverse fibers that support the side anchorage systems. If V-Wrap C100 unidirectional sheets were used for all layers instead, these fibers would have easily separated and detached from the side anchorage prematurely.

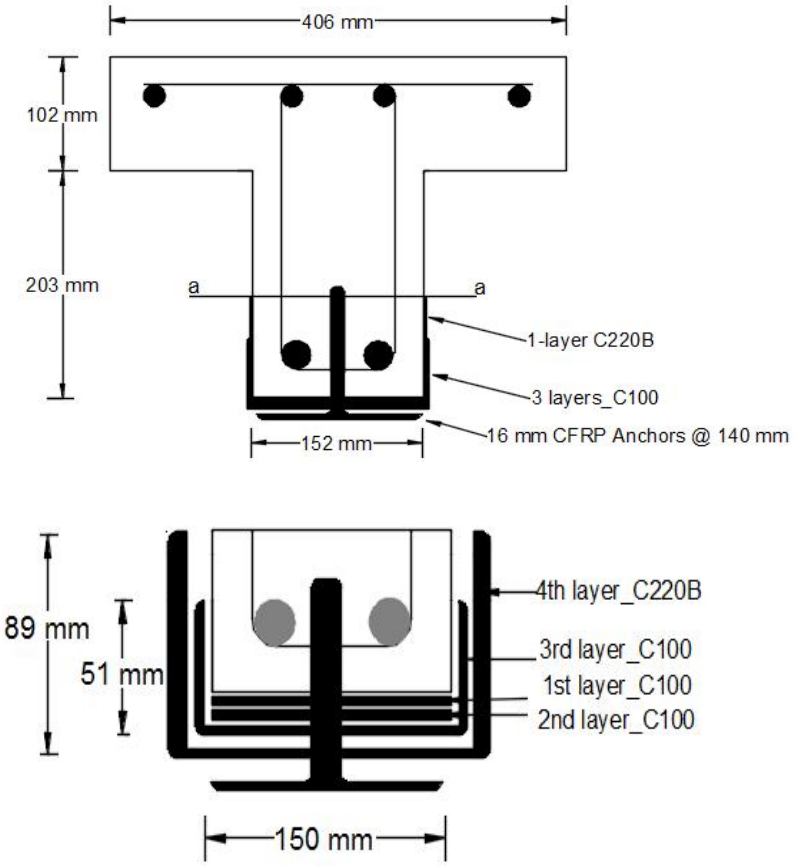

Figure 6-5 Figure 5: Beam cross section details for beam T2

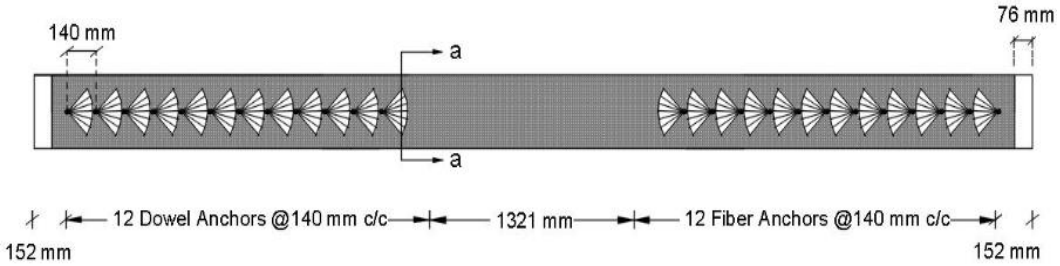

Figure 6-6 Layout of CFRP anchors for T2 beam

(a) (b) (c)

Figure 6-7 Applications of the CFRP sheets and anchors for beam T2 (a) applying the CFRP sheets; (b) installing the CFRP anchors; (c) impregnating the anchors with epoxy resin

6.5.1.2 Layout and Application of CFRP Sheets and Anchors for T3, T4, and T5

T3, T4, and T5 beams were strengthened in flexural with identical CFRP sheets of T2, Figure 6-5. However, the design for beam T3 involved using two types of CFRP spike anchors with diameter of 19 mm spaced at 203 mm. Nine dowel anchors were installed one shear span and nine bundled-fiber anchors applied on the other shear span (18 total anchors), Figure 6-8. For T4 specimen, four bundled-fiber CFRP anchors were installed with diameter of 16 mm spaced at 406 mm per each shear span (8 total anchors), Figure 6-9. The CFRP sheets of the last beam (T5) was bonded with one CFRP anchor on each side of the shear span using 16 mm- diameter anchor positioned at 76 mm from the ends of the CFRP sheets, Figure 6-10. The applications of CFRP sheets and anchors for T3, T4, and T5 are presented in Figure 6-11.

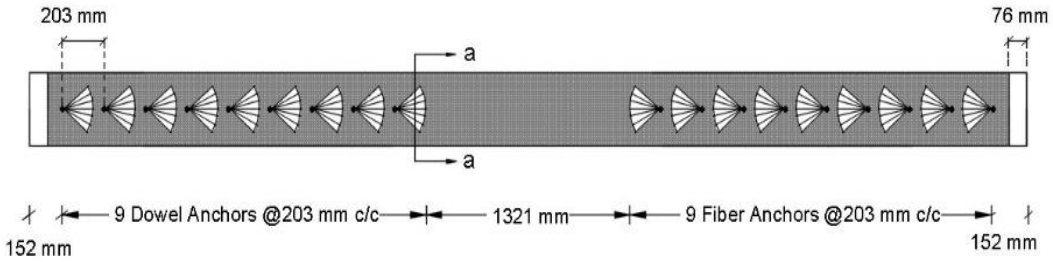

Figure 6-8 Layout of CFRP anchors for T3 beam

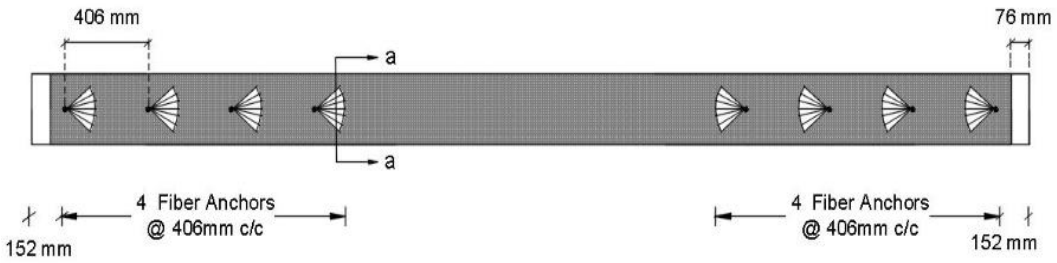

Figure 6-9 Layout of CFRP anchors for T4 beam

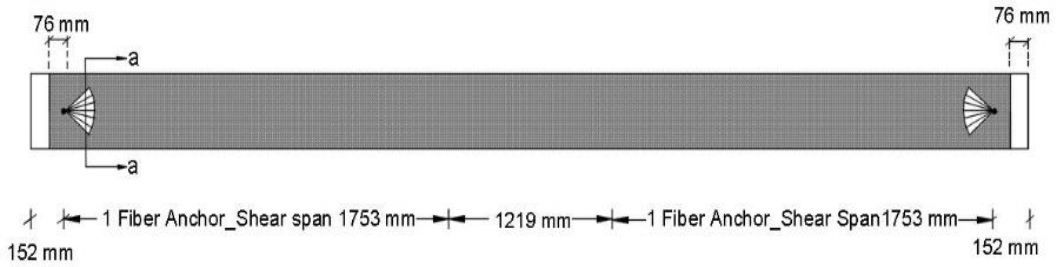

Figure 6-10 Layout of CFRP anchors for T5 beam

(a) (b) (c)

Figure 6-11 Application of CFRP sheets and anchors (a) beam T3; (b) beam T4; (c) beam T5

6.6 Anchorage Design Procedure

Rasheed et al. [24] proposed a design procedure by adapting the ACI 318-14 [25] provisions on shear friction to get a simplified U-wrap design model. This model determines the maximum possible tensile force in the FRP at mid span corresponding to the failure mode of FRP

rupture or concrete crushing and use the shear flow to size the U-wraps, Figure 6-12 a. In this research study, the same proposed procedure is further adapted to design the CFRP spike anchors for both T and rectangular beams. As the debonding crack tends to form, the spike anchors are stretched (force T) since the two faces of the crack move apart. As a result, an equal and opposite clamping force (N) is excerted by the anchors on the crack surface, Figure 6-12 b. The design procedure is explained in the following steps:

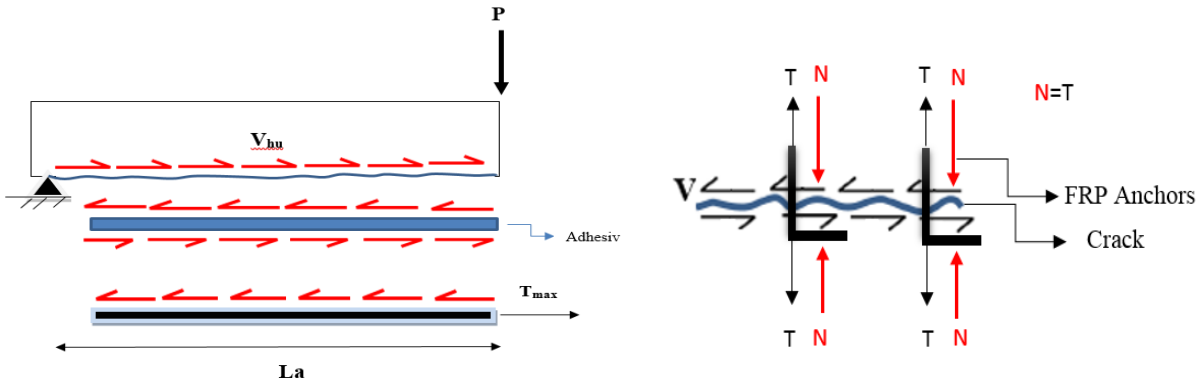

(a) (b)

Figure 6-12 Schematic presenting (a) shear flow distribution (b) stretching the transverse FRP anchors

- Computing the maximum tensile force (Tmax) that is required to develop in the flexural FRP at the location of maximum moment at ultimate sectional failure:

$T_{max} = E_f A_f \varepsilon_{fu}$ (FRP Rupture for T-shaped section)

$T_{max} = E_f A_f \varepsilon_{fe}$ (Concrete Crushing for rectangular section)

$$\varepsilon_{fe} = [\frac{0.003}{c}(h - c) - \varepsilon bi] \quad \text{(Eq 6-1)}$$

$$Tmax = Ef\ Af\ [\frac{0.003}{c}(h - c) - \varepsilon bi] \quad \text{(Eq 6-2)}$$

- Computing the horizontal shear force (V_{hu}) per unit length along the shear span (shear flow):

$$V_{hu} = \frac{Tmax}{La} \quad \text{(Eq 6-3)}$$

- Computing the tension force in the transverse direction of FRP (N):

$V_{hu} = N\,\mu, \longrightarrow N = \frac{Vhu}{\mu}$ (Eq 6-4)

There are two possible failure modes that the FRP anchors may experience. These are pull out and shear failure modes.

Pull out failure mode

$N = \Phi\, Av\, Ef\, \varepsilon_{fe,}$ (Eq 6-5)

$Av * S(spacing) = \frac{\pi}{4} (d_{fiber})^2$ (Eq 6-6)

$S = \frac{\pi}{4\,Av} (d_{fiber})^2$ (Eq 6-7)

Shear-kink failure mode

$V_{hu} = \Phi\, Av\, T_{ult,}$ (Eq 6-8)

$T_{ult} = G_{12}\, \gamma_{ult,}$ (Eq 6-9)

$V_{hu} = \Phi\, Av\, G12\, \gamma_{ult,} \qquad S = \frac{\pi}{4\,Av} (d_{fiber})^2$

Where E_f is tensile modulus of elasticity of FRP, A_f is area of FRP flexural external reinforcement, ε_{fu} is design rupture strain of FRP reinforcement, ε_{fe} is effective strain level in FRP reinforcement attained at failure, h is overall thinness or height of the secion, c is distance from extreme compression fiber to the neutral axis, ε_{bi} is strain level in concrete substrate at time of FRP installation, L_{af} is FRP shear span, μ is Static coefficient of friction, Φ is strength reduction factor Av is area of FRP shear reinforcement per unit length of shear span, d_{fiber} is dimeter of CFRP anchors, T_{ult} is ultimate shear force, G_{12} = shear modules, and γ_{ult} is critical kink angle beyond which the anchor loses its effectiveness.

The shear-kink failure mode was considered for the anchorage design since it is found to be the controlling failure mode.

6.6.1 The Design Calculations

The design calculations of the CFRP spike anchors for T-beams are listed below. The same design results were used for the rectangular specimens. The embedment depth of the anchors was 102 mm for all the beams.

6.6.1.1 General Calculations

For unidirectional V-Wrap C100

Ef = 66.19 GPa, ε_{fu} = 0.011 (rupture strain for C220B), t= 0.584 mm, b (width) = 152 mm

The total width of CFRP sheets are 152 mm for the first 2 layers (applied to bottom face only) and 254 mm for the third layer (installed to the bottom and wrapped 51 mm up from the soffit).

$T_{max1} = E_f A_f \varepsilon_{fu}$ = 66.19 * (0.584 * 152 * 2) * 0.011 = 129.3 kN

$T_{max2} = E_f A_f \varepsilon_{fu}$ = 66.19 * (0.584 * 254 * 1) * 0.011 = 108.0 kN

For bidirectional V-Wrap C220B

Ef = 96.527 GPa, ε_{fu} = 0.011, t= 0.51 mm, b (width) = 152 mm

The total width of the bidirectional CFRP sheet is 330.2 mm (covered the bottom face of the beam and wrapped 89 mm up the sides from the soffit).

$T_{max3} = E_f A_f \varepsilon_{fu}$ = 96.527 * (0.51 * 330.2 * 1) * 0.011 = 108.0 kN

Tmax (total) = 129.3 + 108.0 + 108.0 = 416 kN

$$V_{hu} = \frac{Tmax}{La} = \frac{416}{1.676} = 248.2 \text{ kN/m}$$

G12 = 4.8 kN/mm^2, γ_{ult} = (2.5 degree angle kink) = 0.044 rad

$V_{hu} = \Phi A_v G_{12} \gamma_{ult} \longrightarrow 248.2 = 0.85 * A_v * 4.8 * 0.044 \longrightarrow A_v = 1382.6$ mm^2/m

6.6.1.2 Spacing Calculations using 16 mm- Diameter anchors

Using 16 mm-diameter of CFRP anchors (5/8 inch),

$S = \frac{\pi}{4\ Av} (d_{fiber})^2 = \frac{\pi}{4*1382.6} * (16)^2 = 0.145$ m = 145 mm, Use S= 140 mm (5.5 inches)

This arrangement yields 24 small CFRP anchors. Twelve dowel anchors were applied to one shear span and twelve bundled fiber anchors were installed at the other shear span as shown in Figure 6-6.

6.6.1.3 Spacing Calculations using 19 mm- Diameter anchors

Using 19 mm-dimeter of CFRP anchors (3/4 inch),

$S = \frac{\pi}{4\ Av} (d_{fiber})^2 = \frac{\pi}{4*1382.6} * (19)^2 = 0.205$ m = 205 mm, Use S= 203 mm (8 inches)

That yields 18 big CFRP anchors. Nine dowel anchors were applied to one shear span and nine fiber anchors were installed at the other shear span as shown in Figure 6-8.

It is important to note that no anchors were used in the constant moment region since it was found to be ineffective to apply, Smith et al. [15].

6.7. Test Setup and Data Acquisition

All the beams were simply supported with 4877 mm of total span length and 4724 mm as a clear span. The shear span on each side of the applied load was 1753 mm, Figure 6-13. The specimens were tested in four-point bending in the structural testing lab at Kansas State University. Two linear variable displacement transducers (LVDTs) were placed at mid-span to measure the deflection. Two strain gauges of 5 mm gauge length were mounted on the main flexural bars at mid-span that were embedded into the concrete before casting to measure the strains for steel reinforcement. Two strain gauges of 25 mm gauge length were installed on the compression face

of beams to monitor the strain at top of concrete. In addition, two strain gages were fixed at the bottom to measure the strain on the CFRP sheets. To capture the propagation of debonding in the CFRP sheets and anchors along the entire span length, six more strain gauges were applied between the CFRP anchors, three on each shear span. Displacement control system was followed throughout the testing process at a rate of 2.54 mm per minute.

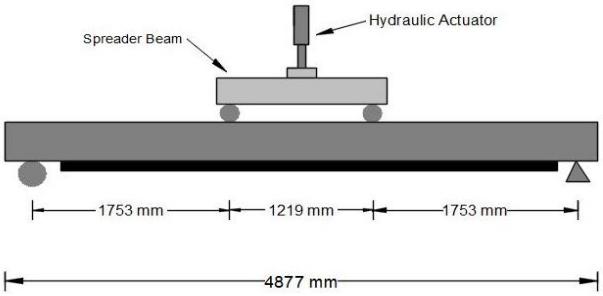

Figure 6-13 Beam details and experimental test setup

6.8. Numerical Analysis

6.8.1 Computer Program

The experimental results are compared with the numerical values that obtained using an Excel analysis program, developed earlier at Kansas State University. For this program, the properties of concrete and the beam section properties are entered. Also, the program gives the option to select the type of the FRP materials and steel reinforcement such as prestressed, mild steel, glass bars, or FRP sheets, Figure 6-14. The program assumes perfect bond to determine the load deflection response, ultimate carrying load capacity, the flexural response, the flexural failure mode, and moment curvature relationship. Moreover, the program accounts for the nonlinearity of concrete in compression by using the Hognestad's parabola. Tension stiffening effect is also considered after concrete cracking.

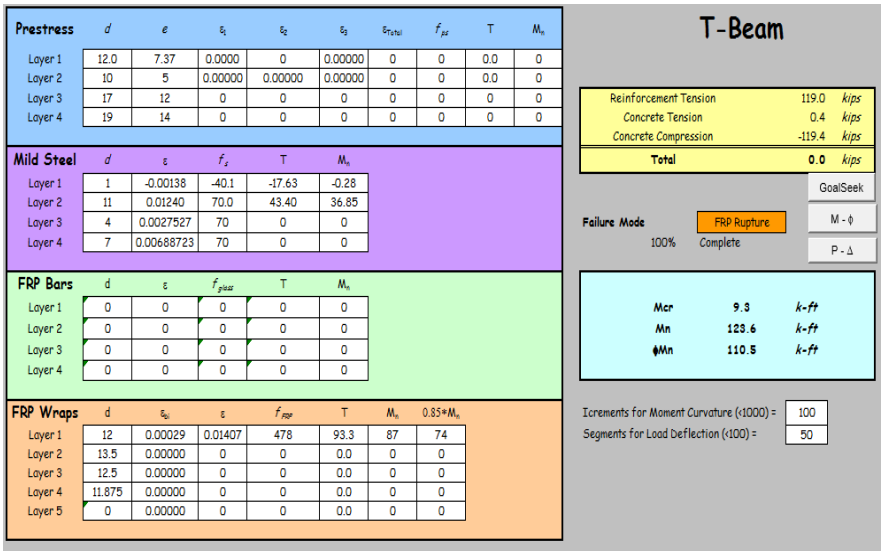

Figure 6-14 Output interface for the analysis program

6.9. Results and Discussion

The results of this study are also compared with the RC beam strengthened using equivalent flexural CFRP sheets but anchored with distributed U-wrap anchorage (Beam T6). The latter beam was prepared and tested by Rasheed et al. [26]. The specimen with U-wrap anchors was reinforced in flexure utilizing five layers of CFRP (V-Wrap C100) applied to the bottom face of the beam and bonded with U-wrap anchorage. Two layers of transverse U-wraps with 127 mm width spaced at 305 mm on center were applied along the span length. The geometry, properties, and the contribution of flexural CFRP sheets (the five layers only) of the beam tested by Rasheed et al. [26] are equivalent to the strengthened T beams (T2-T5) with four flexural CFRP sheets composed of 3 layers of V-Wrap C100 and one layer of C220B that used in this study (Appendix A). As a result, it is so beneficial to compare between the results of T2-T5 (presented herein) and the results of T6. [26].

6.9.1 Control Beam (T1)

The first T specimen was prepared and tested as a control beam. From the analysis program, the ultimate carrying load capacity was determined to be 57.70 kN with a mid-span deflection of

269.7 mm. The beam failed at a load of 71.0 kN with a maximum deflection of 178 mm. As predicted by the program, the failure mode for the tested beam was concrete crushing in compression after steel yielding, Figure 6-15. It can be noticed that the theoretical program is very accurate in evaluating the failure mode. The load-deflection comparison between the analysis program and the experimental results are shown in Figure 6-16. Both curves are in good agreement up to the steel yielding level, while the experimental results showed stiffer response after yielding. Figures 6-17 indicates the load-strain comparisons between the theoretical and experimental values at top concrete surface. Unexpectedly, the strain gauge readings for the main tension rebars were lost during the test.

Figure 6-15 Control beam T1 after the test

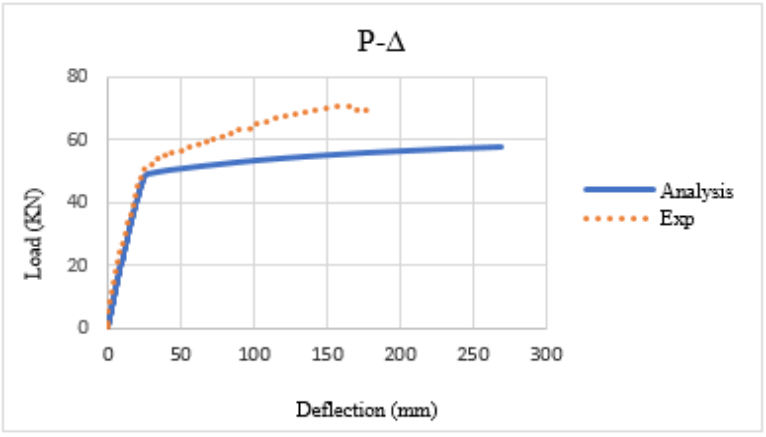

Figure 6-16 Comparison of test and analysis response of control beam T1

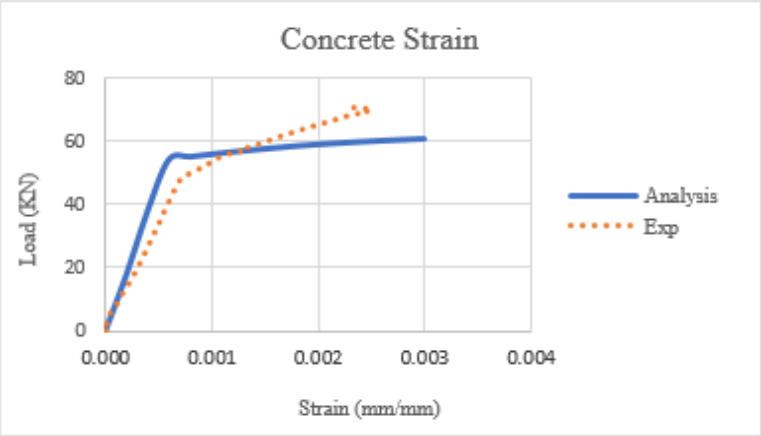

Figure 6-17 Comparison of the load-strain at the top concrete surface of T1

6.9.2 Beam T2 with Flexural CFRP Sheets and 24 CFRP Anchors

The second T specimen was strengthened with flexural CFRP sheets on the bottom face and anchored with total 24 CFRP anchors along the shear spans of the beam. According to the theoretical analysis, the strengthened beam (assuming perfect bond) would have an ultimate load capacity of 173.1 kN, which corresponded to a mid-span deflection of 88.6 mm. The test results showed that the beam reached 193.4 kN of peak load with a maximum deflection of 89.4 mm. This significant increase in load carrying capacity was due to the use of CFRP anchors that bonded the CFRP sheets in place to the point of rupture failure of CFRP sheets. The failure mode was debonding plus partial rupture occurred where the bundled-fiber CFRP anchors were located (the north side**),** Figure 6-18. The obtained load capacity from the analysis (173.1 kN) presents the maximum theoretical value (assuming perfect bond) that the strengthened beam can carry at the ultimate sectional capacity before the failure. To reach this level, an anchorage system is required in order to control the premature debonding. Still, the results of beam T2 show about 11.7% greater strength than the analyzed specimen. This is attributed to the increase in the amount of carbon fiber that added by the anchors, which was not included in the analysis.

Figure 6-19 shows the load deflection comparisons between the numerical results of the T2 versus the experimental values for, the control beam T1, the beam T2 with CFRP spike anchors, and the beam T6 with distributed CFRP U-wraps. It is evident from this graph that the experimental results for beam T2 (using closely spaced CFRP spike anchors) show more strength than the analyzed beam and the one with distributed U-wrap anchors. Figure 6-20 shows the experimental and analytical comparison of the load versus strain results at the upper concrete surface. After steel yielding level, the experimental curve diverts due to the proximity to a flexural crack. Excellent agreement was observed between the experimental and analytical responses of the load versus strain results in the steel rebars, Figure 6-21. The experimental and analytical comparison of the load versus strain results in the CFRP at mid-span is shown in Figure 6-22. Up to the steel yielding both curves are very similar, while after yielding the experimental curve became stiffer indicating that the strain gauge locations are relatively far from the induced flexural cracks.

Furthermore, the propagation of debonding in the CFRP sheets was tracked using three more strain gauges fixed on each shear span at different locations as presented in Figure 6-23. The load-strain comparisons between the experimental and numerical values for these locations are observed in Figure 6-24. The strain gauge readings for T2 beam at locations 8, 10, 12 (on the north side) where the CFRP fiber anchors were installed are greater and more ductile than the experienced strains at the other shear span where the CFRP dowel anchors were applied (7, 9, and11). That was expected since the failure was due to the complete deboning and partial rupture occurred on the bundled fiber anchors side. The strains at 7 and 8 experienced higher deformations than 9, 10, 11, and 12 which was expected because they were located closer to the applied loads. Similarly, the strains at 9 and 10 had greater values than strains at 11 and 12 for the same reason. Also, there were good agreements between the theoretical and the test results of load-strain at 7,8, 9,10,11, and 12.

Figure 6-18 Failure of the beam T2

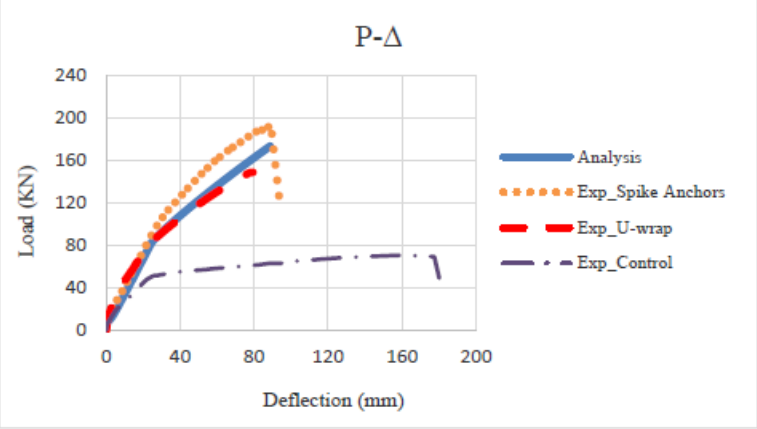

Figure 6-19 Comparison of test and analysis response of beam T2 and comparable beams

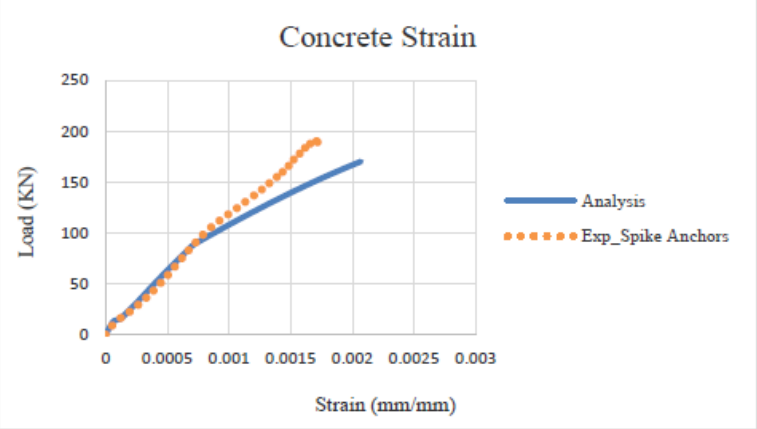

Figure 6-20 Comparison of the load-strain at the top concrete surface of T2

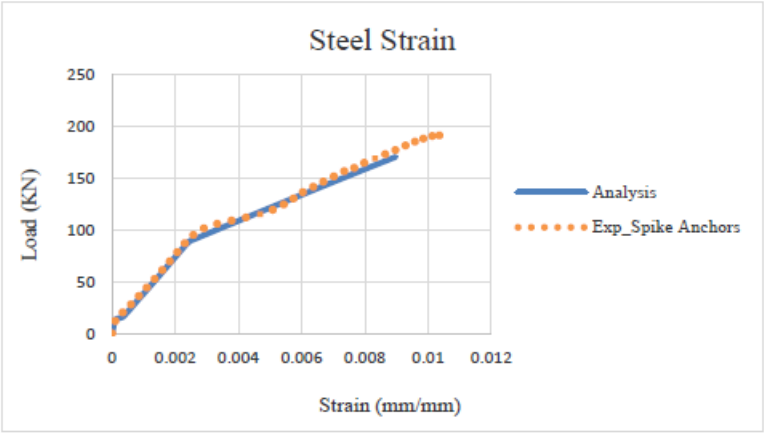

Figure 6-21 Comparison of the load-strain in the main rebars of T2

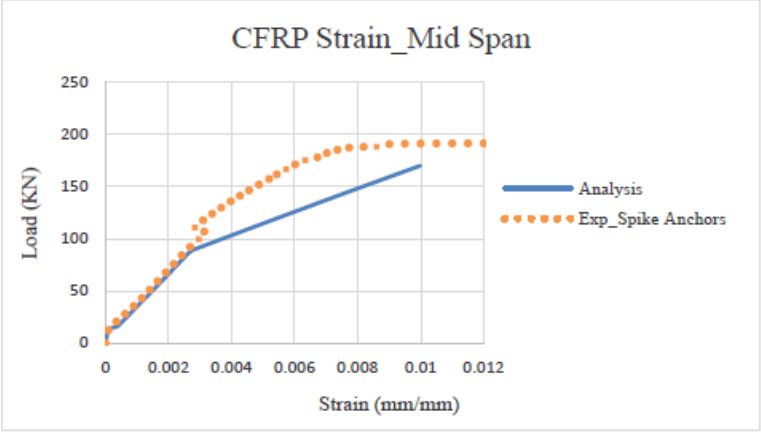

Figure 6-22 Comparison of the load-strain in the CFRP sheets of T2

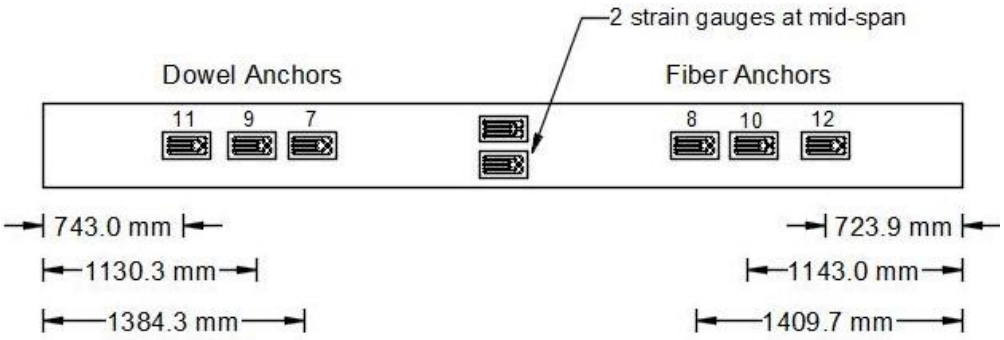

Figure 6-23 Strain gauge details for beam T2

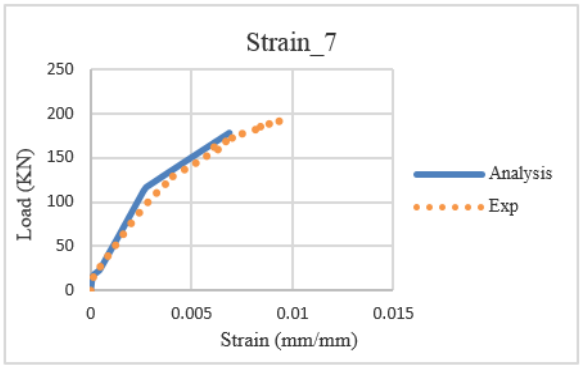

(a)

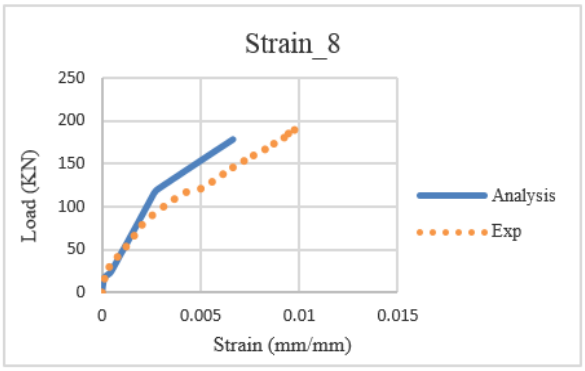

(b)

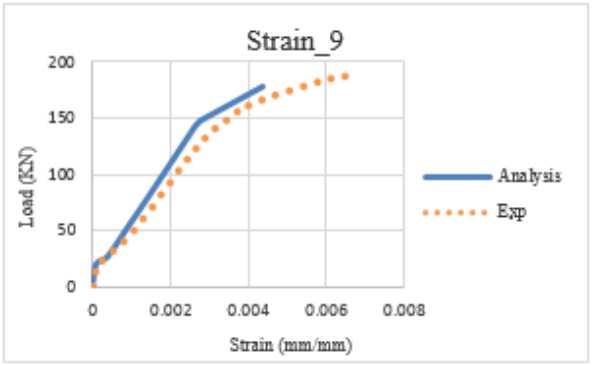

(c)

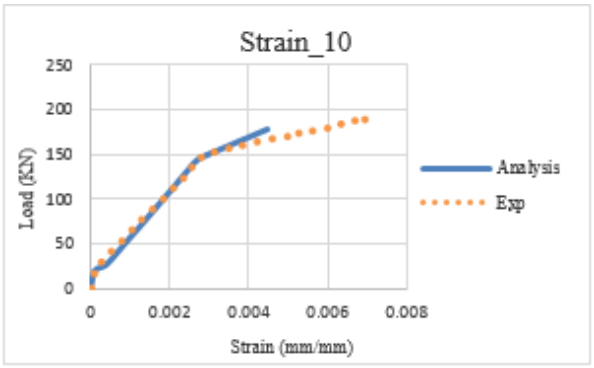

(d)

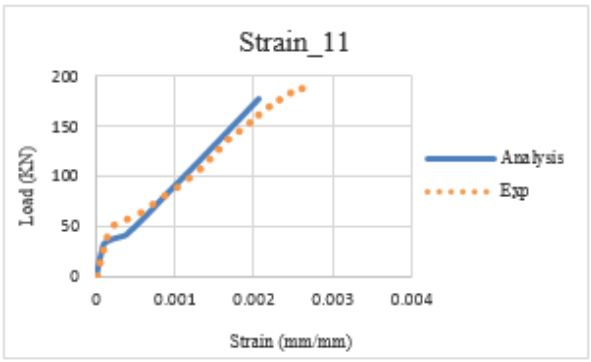

(e)

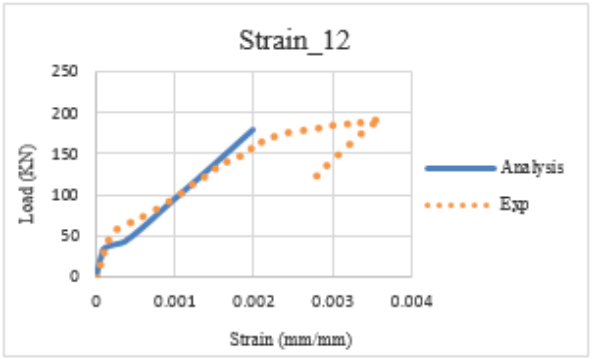

(f)

Figure 6-24 Comparisons of the load- strain (a); (b); (c); (d); (e); and (f) strain results in the CFRP sheets at different location along the shear spans of the beam T2

6.9.3 Beam T3 with Flexural CFRP Sheets and 18 CFRP Anchors

This strengthened beam was anchored with total 18 CFRP spike anchors (Figure 6-8) with a diameter of 19 mm, spaced at 203 mm. The amount of the carbon fiber in these 18 anchors with

19mm-diameter is the same as the amount of carbon fiber in 24 anchors with 16 mm- diameter used in specimen T2, as explained in the following,

Area distribution of CFRP anchors with 16 mm diameter

$$= \frac{\pi}{4} (16 \text{ mm})^2 / 140 \text{ mm (spacing)} = 1.4 \text{ mm}^2/\text{mm (T2)}$$

Area distribution of CFRP anchors with 19 mm diameter

$$= \frac{\pi}{4} (19 \text{ mm})^2 / 203 \text{ mm (spacing)} = 1.4 \text{ mm}^2/\text{mm (T3)}$$

The goal behind using large anchors (19 mm diameter) at wider spacing (203 mm) versus smaller anchors (16 mm diameter) at shorter spacing (140 mm) is to examine their effect on performance. This beam failed at a load of 178.0 kN with central deflection of 87.6 mm. The failure mode was debonding from the south side of specimen (Figure 6-25) where the bundled fiber CFRP anchors had been installed. Figure 6-26 shows the load deflection comparisons between the numerical results of the T3 versus the experimental values for, the control beam T1, the beam T3 with CFRP spike anchors, and the beam T6 with U-wrap CFRP [26]. It is obvious from the graph that the experimental (T3) and theoretical responses are in very good agreement.

The effect of anchorage arrangement in this beam (T3) reduced the strength to about 8% in comparison with T2 specimen. Still, the behavior of the tested beam T3 with CFRP anchors showed more strength than both the analyzed specimen and the beam with U-wrap anchorage due to the use of the CFRP anchors. The first local debonding initiates at a load of 170.9 kN then several localized debonding episodes occurred, until the complete failure of the beam at a maximum load of 178.0 kN, as shown form the drop in the load-deflection response, Figure 6-26.

The experimental and numerical comparison of the load versus strain results at the top concrete surface, in the steel rebars, and in the CFRP at mid-span are presented in Figures 6 (27-29), respectively. There are excellent agreements between the experimental and numerical relationship of the load versus strains in both the tension rebars and the CFRP sheets at mid-span.

Whereas, the experimental curve of the concrete strain diverted after steel yielding due to the proximity to a flexural crack. Figure 6-30 presents the details of other six strain gauges that were applied per shear span. Moreover, the load-strain comparisons between the experimental and numerical values along the shear spans (strain 7, 8, 9, 10, 11, and 12) are shown in Figure 6-31. The strain gauges that were installed on the bundled-fiber anchor side (number 8, 10, and 12) had higher strains and more ductility than those installed on the dowel anchors side. Again, the closer installed strain gauges to the applied load, the greater strain was experienced by the CFRP sheets.

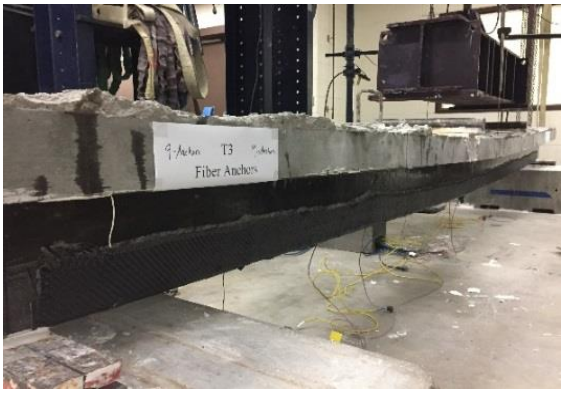

Figure 6-25 Beam T3 after the failure

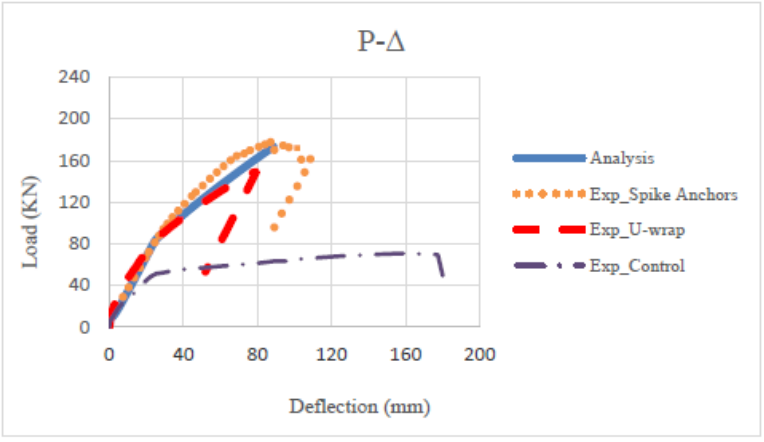

Figure 6-26 Comparison of test and analysis response of beam T3 and comparable beams

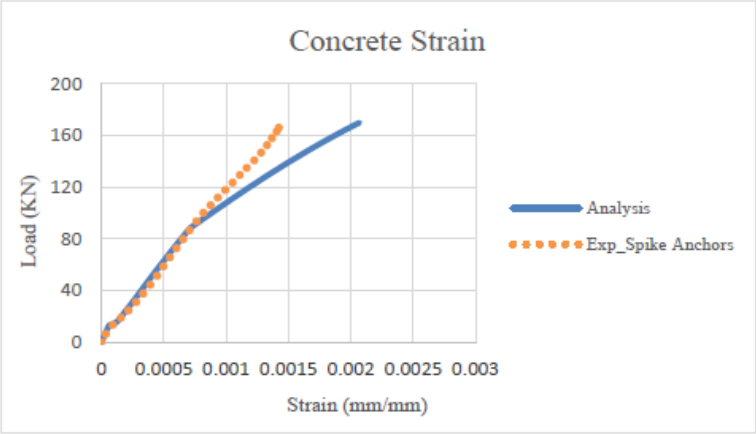

Figure 6-27 Comparison of the load-strain at the top concrete surface of T3

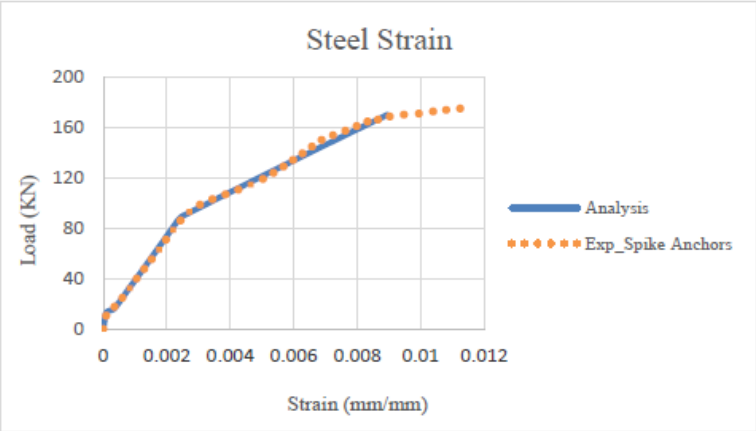

Figure 6-28 Comparison of the load-strain in the main rebars of T3

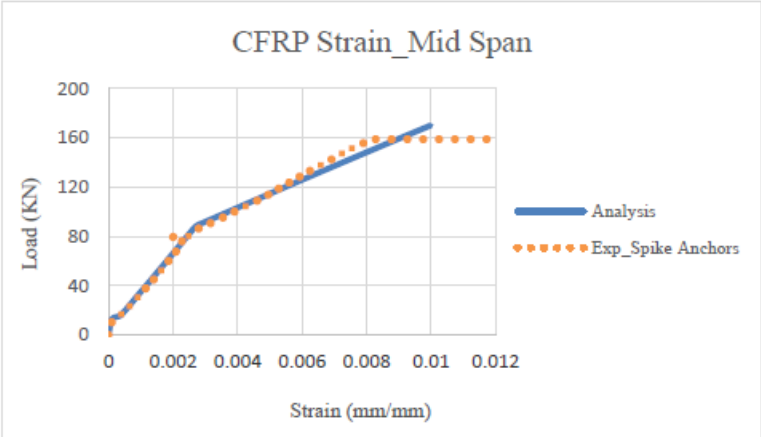

Figure 6-29 Comparison of the load-strain in the CFRP sheets of T3

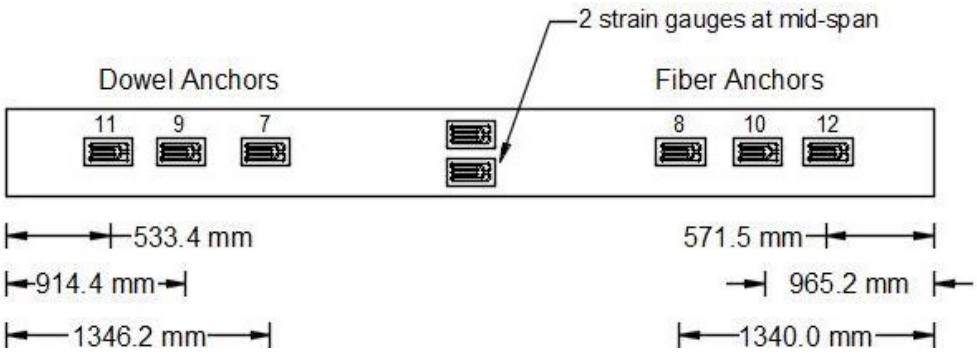

Figure 6-30 Strain gauge details for beam T3

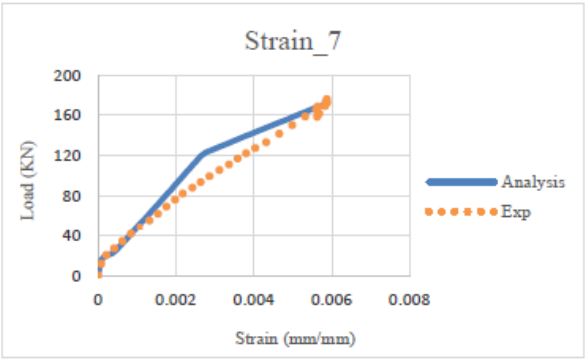

(a)

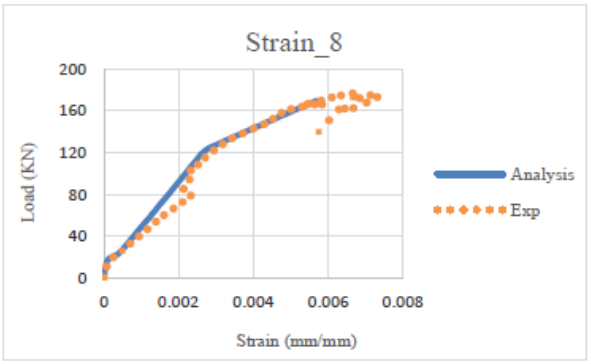

(b)

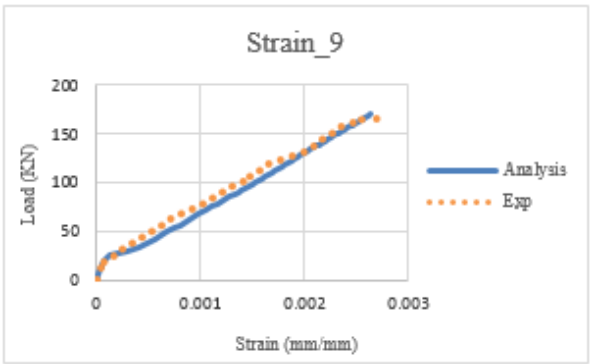

(c)

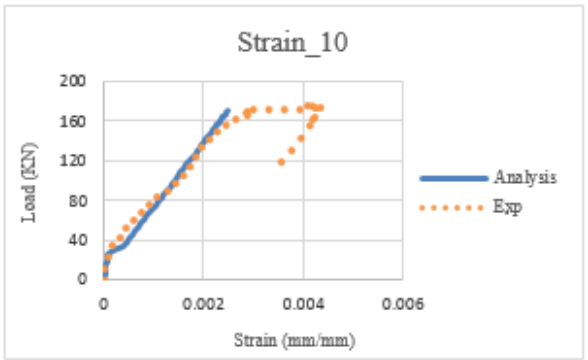

(d)

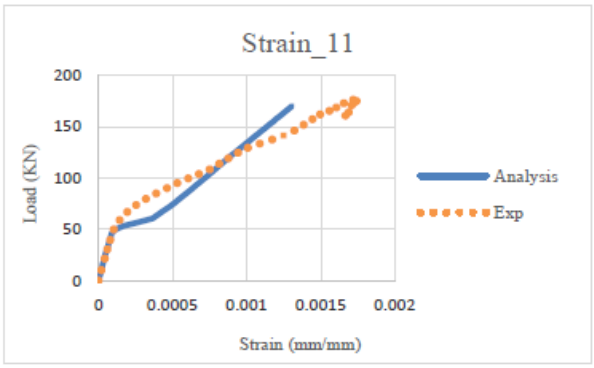

(e)

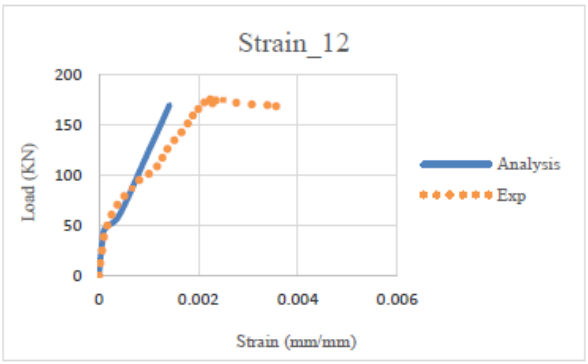

(f)

Figure 6-31 Comparisons of load- strain (a); (b); (c); (d); (e); and (f) strain results in the CFRP sheets at different location along the shear spans of the beam T3

6.9.4 Beam T4 with Flexural CFRP Sheets and 8 CFRP Anchors

To evaluate the performance with fewer number of anchors, four bundled-fiber CFRP spike anchors with 16 mm-dimeter were considered per shear span to bond the CFRP sheets of beam T4. The specimen had 33.3% of the number of CFRP anchors as beam T2. These four anchors were spaced at 406 mm, which is almost triple of the spacing of beam T2 (140 mm). From the experimental test, the beam failed in debonding as clearly observed in Figure 6-32 at a peak load of 150.3 kN and 87.9 mm as a mid-span deflection. Figure 6-33 shows the load-deflection comparisons between the numerical results versus the experimental values for, the control beam T1, the beam T4 with CFRP spike anchors, and the beam T6 with CFRP U-wraps [26]. It can be noticed from this graph that the theoretical curve is stiffer than the experimental one, with spike anchors, since the beam failed in debonding before reaching the ultimate sectional capacity (unlike beam T2 that failed in rupture). Using this arrangement (4 CFRP anchors per span length), the strength reduced about 22.3% over beam T2. Nevertheless, the capacity of beam T4 (150.3 kN) is very similar to the capacity of beam T6, that bonded with 2 layers of distributed U-wrap anchors (149.0 kN).

There are good agreements between the experimental and numerical comparison of the load versus strain results at the top concrete surface, in the steel rebars, and in the CFRP at mid-span as presented in Figures 6-34, 6-35, and 6-36. However, the analytical curves (concrete, steel, and CFRP at mid-span) are stiffer than the experimental ones, due to the premature failure of the CFRP sheets. Details of the strain gauges that were fixed along the shear spans for T4 beam is shown in Figure 6-37. Also, the load-strain comparisons between the experimental and theoretical values at these locations (strain 7, 8, 9, 10, 11, and 12) are shown in Figure 6-38. The experimental strain responses show more ductility than the those in T2 and T3 specimens. That it could be due to the high strain were experienced by the CFRP anchors and sheets.

Figure 6-32 Beam T4 after the failure

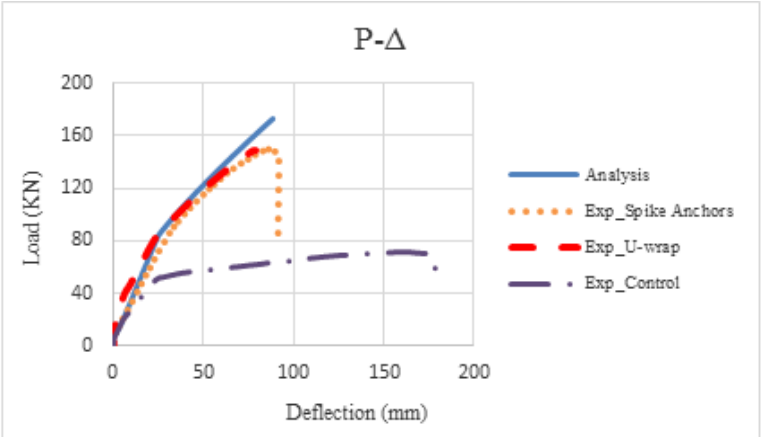

Figure 6-33 Comparison of test and analysis response of beam T4 and comparable beams

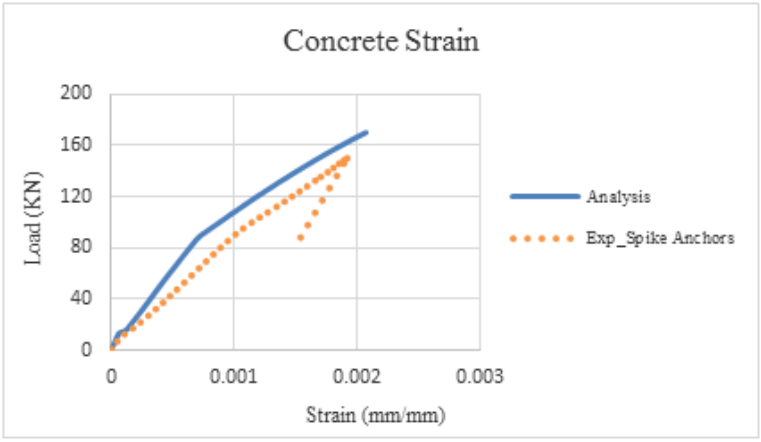

Figure 6-34 Comparison of the load-strain at the top concrete surface of T4

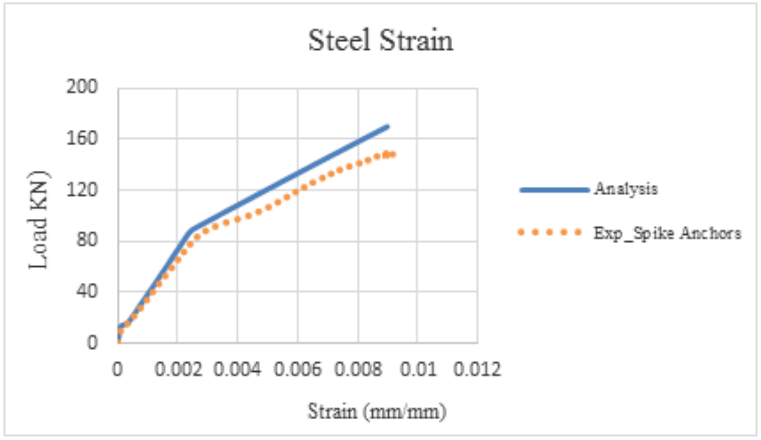

Figure 6-35 Comparison the load-strain in the main rebars of T4

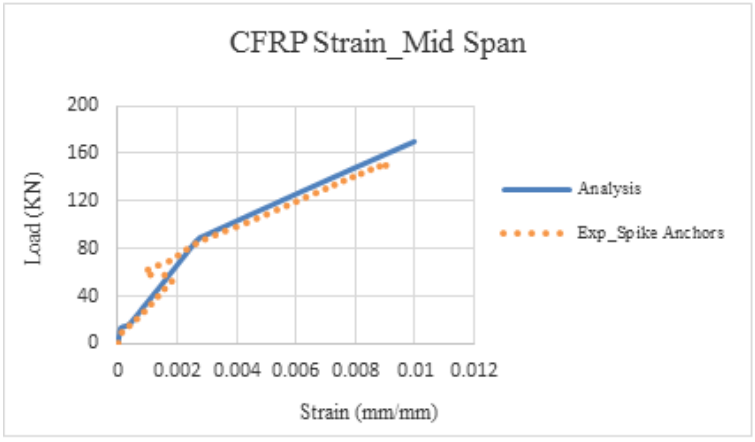

Figure 6-36 Comparison of the load-strain in the CFRP sheets of T4

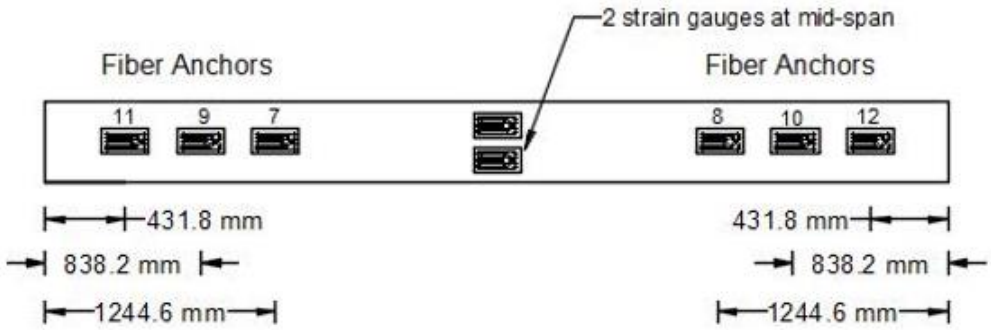

Figure 6-37 Strain gauge details for beam T4

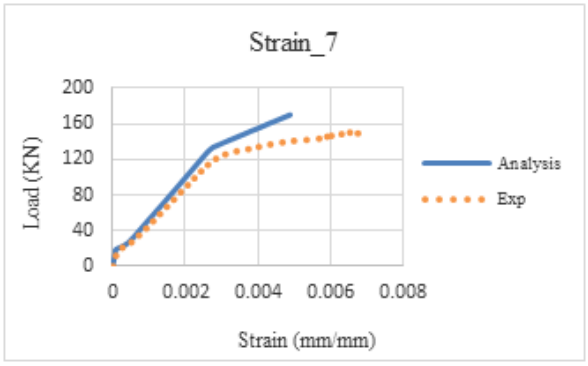

(a)

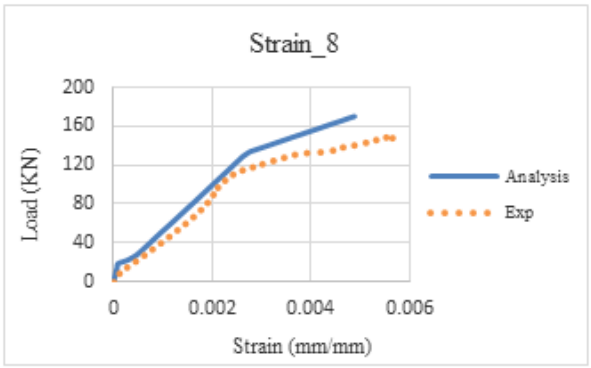

(b)

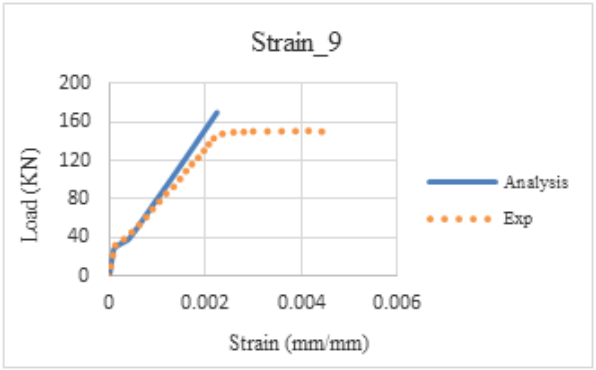

(c)

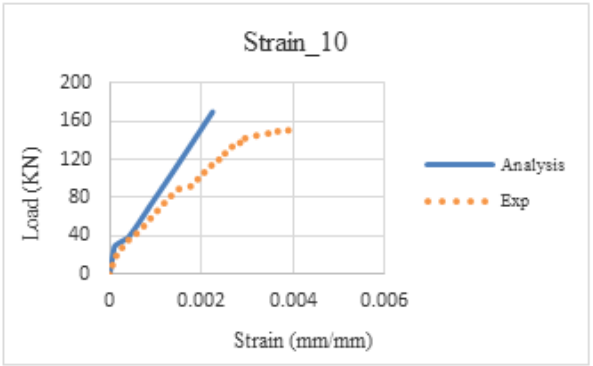

(d)

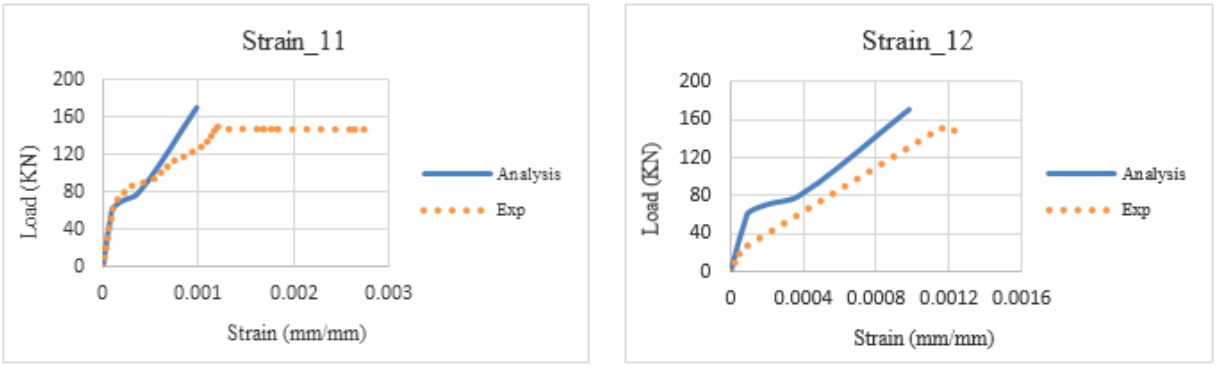

(e) (f)

Figure 6-38 Comparisons of the load- strain (a); (b); (c); (d); (e); and (f) strain results in the CFRP sheets at different location along the shear spans of the beam T4

6.9.5 Beam T5 with Flexural CFRP Sheets and End CFRP Anchor

It was interesting to secure the CFRP sheets of the last T beam with one CFRP spike anchor per each span length to study the effect of the end anchorage on load carrying capacity. The end anchorage technique has been utilized to control the cover delamination failure mode [22-23] that initiates at the end of the FRP plates or sheets bonded to the concrete substrate due to the high stress concentration. In this paper; on the other hand, the end bundled-fiber CFRP anchor system was used (for T5) to evaluate whether it would improve the flexural performance by controlling the debonding or not. This beam (T5) failed at an ultimate load of 138.7 kN with a maximum deflection of 69.0 mm caused by the debonding of CFRP sheets, Figure 6-39. The debonding started from the critical region (mid-span) and propagated through the shear spans. It was observed and recorded that the load capacity dropped down before the debonding of CFRP sheets reaching the end installed CFRP anchor. Thus, one end spike anchor on each side just held the edge layers of the CFRP sheets from being sagging without providing any strength.

Figure 6-40 shows the load-deflection comparisons between the numerical versus the experimental results for, the control beam T1, the beam T5 with end CFRP spike anchor, and the beam T6 with

distributed CFRP U-wraps [26]. Even though both the experimental and numerical curves are matching up very well, the analyzed beam shows more strength than the tested specimen. This was attributed to the premature debonding of the CFRP sheets that limited the ultimate capacity of T5. Good agreements can be observed for the load-strain comparison between the experimental and analytical results at the top concrete surface, in the main tension rebars, and in the CFRP at mid-span, Figures 6-41, 6-42, and 6-43. The installed strain gauges details along the shear spans is shown in Figure 36. Furthermore, the relationship between the experimental and numerical values of load-strain are presented in Figure 6-44. It is obvious from the graphs that the experimental stain responses are softer than the analytical curves since the beam failed in debonding before achieving the ultimate sectional capacity.

Figure 6-39 Beam T5 after the failure

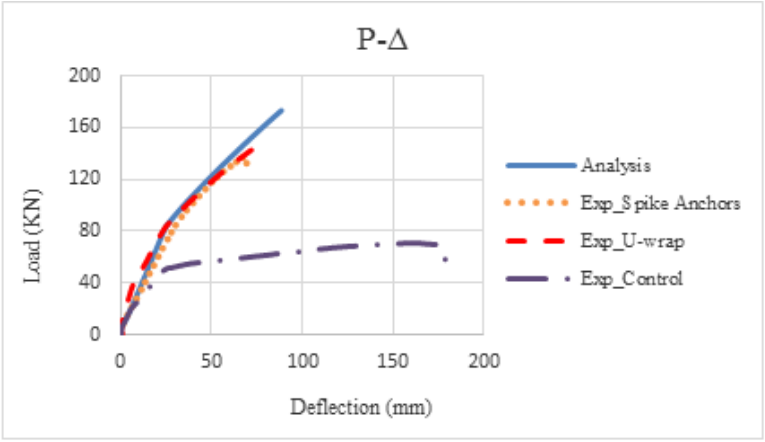

Figure 6-40 Comparison of test and analysis response of beam T5 and comparable beams

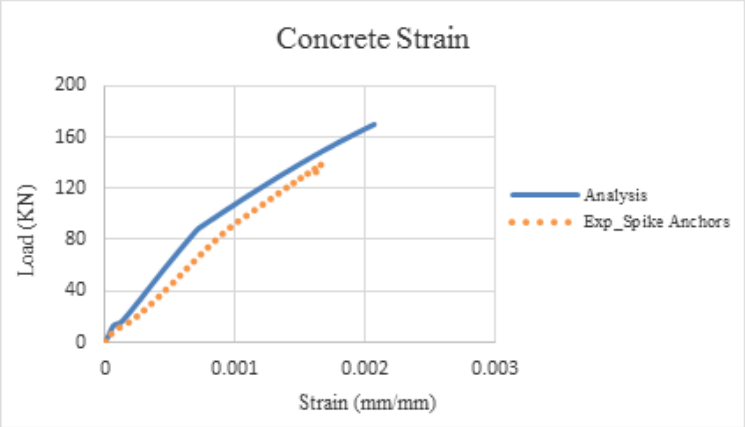

Figure 6-41Comparison of the load-strain at the top concrete surface of T5

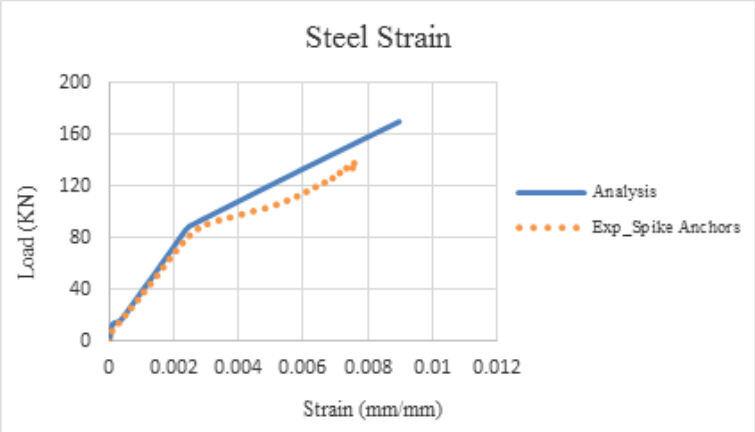

Figure 6-42 Comparison of the load-strain in the main rebars of T5

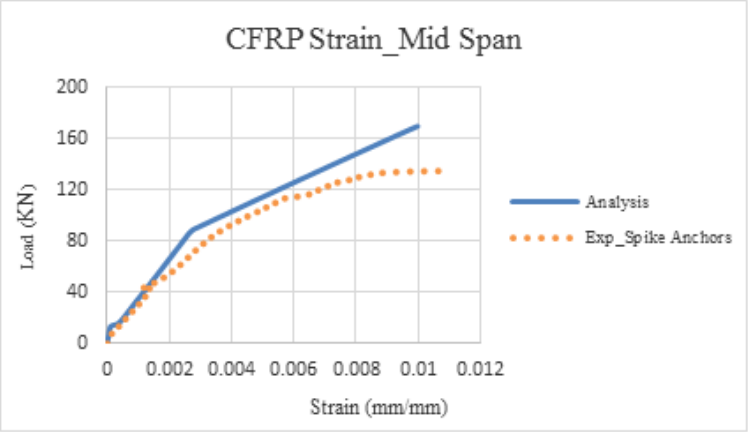

Figure 6-43 Comparison of the load-strain in the CFRP sheets of T5

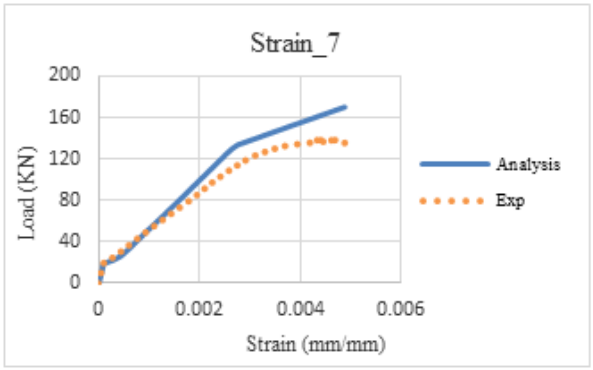

(a)

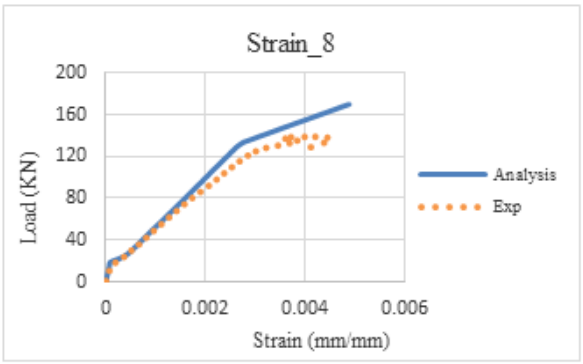

(b)

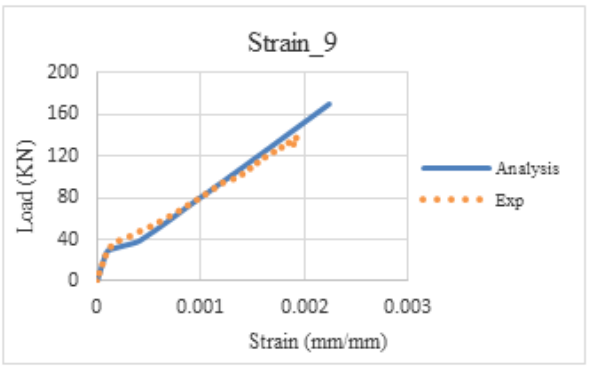

(c)

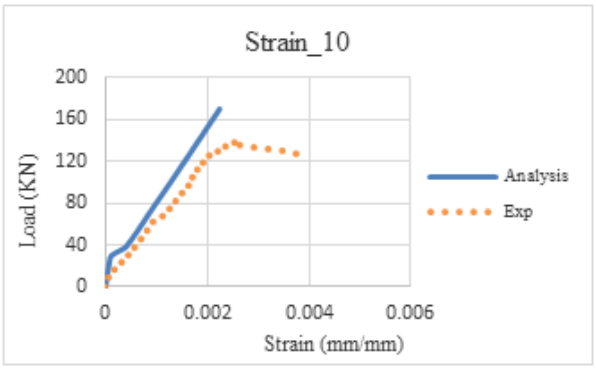

(d)

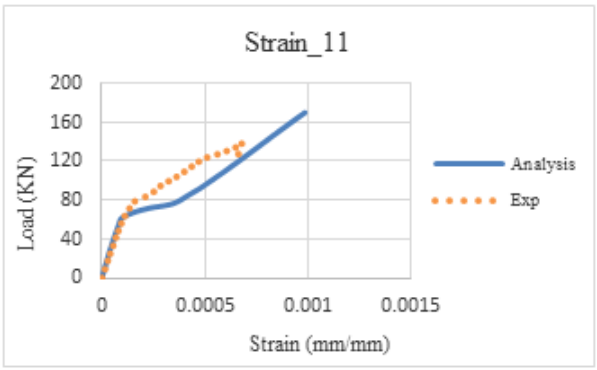

(e)

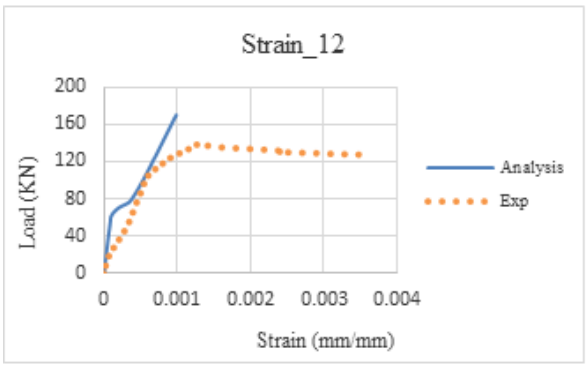

(f)

Figure 6-44 Comparisons of the load- strain (a); (b); (c); (d); (e); and (f) strain results in the CFRP sheets at different location along the shear spans of the beam T5

6.10 Summary

The summary of the experimental load-deflection results for the all T beams is shown in Figure 6-45 and Table 6-1.

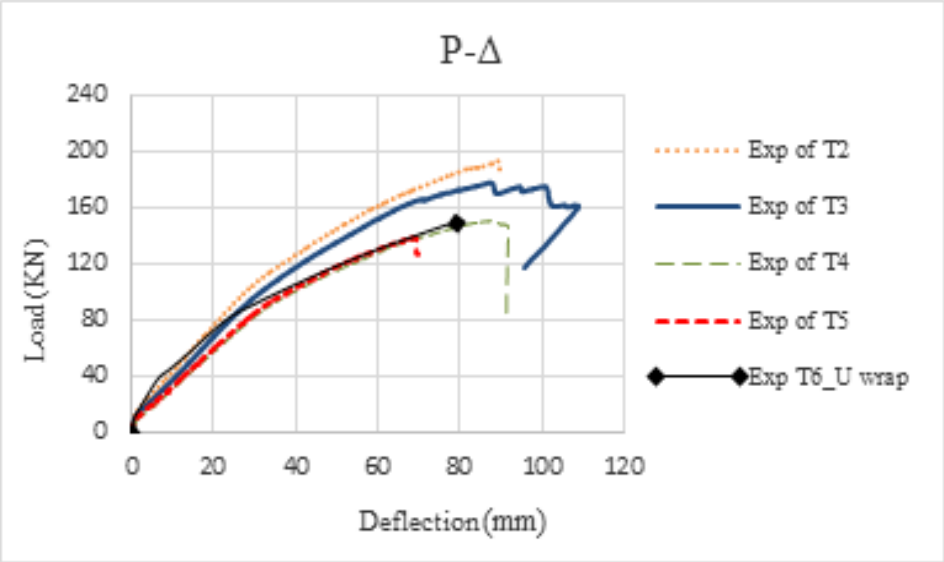

Figure 6-45 Comparison of experimental results for beams T2- T6

Table 6-1 Summary of the results for T1-T6

Beam	Diameter of CFRP anchors (mm)	Nu of CFRP anchors per span length	Spacing (mm)	Ultimate Experimental load capacity (kN)
T1	Control	Control	Control	71.0
T2	16	12	140	193.4
T3	19	9	203	178.0
T4	16	4	406	150.3
T5	16	1	End anchor	138.7
U-wraps (T6)	U-wraps with127 mm width	2 layers of Distributed U-wrap	127 along the entire beam	148.6 Rasheed et. al [26]

6.11 Conclusions

The performance of the RC beams strengthened with CFRP sheets and bounded using different anchorage arrangements of CFRP anchors is reported in this paper. The summary of the anchorage results is listed in the Table 6-1. Beam T2 showed the greatest enhancement in flexural strength. The flexural capacity increased by 39.4% over beam T5 (with end anchors only). This proves the effectiveness of close spaced CFRP anchors. Also, there was no drop in the load-deflection response for beams T2 (Figure 6-44) since the CFRP anchors were positioned behind each other (small spacing) without any free region to initiate local debonding between the installed CFRP anchors. As a result, the anchors were successfully bonded the CFRP sheets and prevented the premature debonding up to complete failure caused by rupture of the CFRP sheets.

Even though the total CFRP anchors in beam T3 had the same amount of carbon fiber as beam T2, the strength in beam T3 reduced due to the bigger spacing and a smaller number of anchors that were utilized. The strength capacity of beam T3 was about 92% of that in beam T2. Furthermore, there were several drops in the load-deflection response (down-up) for beam T3 before the failure. These drops in load-deflection response caused by local debonding of CFRP sheets between the applied anchors. However, the CFRP anchors delayed the propagation of the debonding to the higher load level, before the failure of specimen. The dowel CFRP anchors showed better performance than the bundled-fiber CFRP anchors since the beams failed in debonding and/or fiber rupture from where the bundled-fiber anchors were installed. That could be attributed to the fact that the fibers in the dowel anchors perform as a unit bundle to resist the applied shear forces. Some fibers in the bundle-fiber anchors, on the other hand, might be sheared, pulled, or torn individually due to the shear forces.

Using widely spaced anchors arrangement as in beam T4 significantly reduced the flexural capacity over the strength of T2. Nevertheless, utilizing four CFRP spike anchors per shear span (T4) could be a great replacement of the two layers of distributed U-wrap anchors along the entire span length (T6). The load carrying capacity for beam T4 was very similar to the capacity of beam T6 with distributed U-wraps. Lastly, it was found that the use of an end CFRP spike anchor is ineffective to shift or delay the premature debonding. The beam (T5) failed in debonding of CFRP sheets along the critical regions (mid-span and shear spans) before the propagation of debonding reaching to the end of CFRP sheets and anchor.

6.12 References

[1] Teng, J. G., Smith, S. T., Yao, J., & Chen, J. F. (2003). Intermediate crack-induced debonding in RC beams and slabs. *Construction and building materials*, *17*(6-7), 447-462.

[2] Rasheed, H. A. (2014). *Strengthening design of reinforced concrete with FRP*. CRC Press.

[3] ACI Committee 440. (2017). ACI 440.2 R-17: Guide for the design and construction of externally bonded FRP systems for strengthening concrete structures. *American Concrete Institute.*

[4] Khalifa, A., Alkhrdaji, T., Nanni, A., & Lansburg, S. (1999). Anchorage of surface mounted FRP reinforcement. *CONCRETE INTERNATIONAL-DETROIT-*, *21*, 49-54.

[5] Chahrour, A., & Soudki, K. (2005). Flexural response of reinforced concrete beams strengthened with end-anchored partially bonded carbon fiber-reinforced polymer strips. *Journal of Composites for Construction, 9*(2), 170-177.

[6] Al-Amery, R., & Al-Mahaidi, R. (2006). Coupled flexural–shear retrofitting of RC beams using CFRP straps. *Composite Structures, 75*(1-4), 457-464.

[7] Pham, H. B., & Al-Mahaidi, R. (2006). Prediction models for debonding failure loads of carbon fiber reinforced polymer retrofitted reinforced concrete beams. *Journal of composites for construction, 10*(1), 48-59.

[8] Ceroni, F., Pecce, M., Matthys, S., & Taerwe, L. (2008). Debonding strength and anchorage devices for reinforced concrete elements strengthened with FRP sheets. *Composites Part B: Engineering, 39*(3), 429-441.

[9] Orton, S. L., Jirsa, J. O., & Bayrak, O. (2008). Design considerations of carbon fiber anchors. *Journal of Composites for Construction, 12*(6), 608-616.

[10] Kalfat, R., & Al-Mahaidi, R. (2010). Investigation into bond behaviour of a new CFRP anchorage system for concrete utilising a mechanically strengthened substrate. *Composite structures, 92*(11), 2738-2746.

[11] Kim, S. J., & Smith, S. T. (2010). Pullout strength models for FRP anchors in uncracked concrete. *Journal of composites for construction, 14*(4), 406-414.

[12] Maghsoudi, A. A., & Bengar, H. A. (2011). Acceptable lower bound of the ductility index and serviceability state of RC continuous beams strengthened with CFRP sheets. *Scientia Iranica, 18*(1), 36-44.

[13] Kalfat, R., Al-Mahaidi, R., & Smith, S. T. (2011). Anchorage devices used to improve the performance of reinforced concrete beams retrofitted with FRP composites: State-of-the-art review. *Journal of Composites for Construction, 17*(1), 14-33.

[14] Smith, S. T., Rasheed, H. A., & Kim, S. J. (2017). Full-range load-deflection response of FRP-strengthened RC flexural members anchored with FRP anchors. *Composite Structures, 167*, 207-218.

[15] Smith, S. T., Hu, S., Kim, S. J., & Seracino, R. (2011). FRP-strengthened RC slabs anchored with FRP anchors. *Engineering Structures, 33*(4), 1075-1087.

[16] Jones, R., Swamy, R. N., & Charif, A. (1988). Plate separation and anchorage of reinforced concrete beams strengthened by epoxy-bonded steel plates. *Structural Engineer, 66*(5).

[17] Sharif, A., Al-Sulaimani, G. J., Basunbul, I. A., Baluch, M. H., & Ghaleb, B. N. (1994). Strengthening of initially loaded reinforced concrete beams using FRP plates. *Structural Journal, 91*(2), 160-168.

[18] Spadea, G., Bencardino, F., & Swamy, R. N. (1998). Structural behavior of composite RC beams with externally bonded CFRP. *Journal of Composites for Construction, 2*(3), 132-137.

[19] Ritchie, P. A., Thomas, D. A., Lu, L. W., & Connelly, G. M. (1990). External reinforcement of concrete beams using fiber-reinforced plastics.

[20] Nurchi, A., Matthys, S., Taerwe, L., Scarpa, M., & Janssens, J. (2003). Tests on RC T-beams strengthened in flexure with a glued and bolted CFRP laminate. In *Fibre-Reinforced Polymer Reinforcement for Concrete Structures: (In 2 Volumes)* (pp. 297-306).

[21] Chahrour, A., & Soudki, K. (2005). Flexural response of reinforced concrete beams strengthened with end-anchored partially bonded carbon fiber-reinforced polymer strips. *Journal of Composites for Construction, 9*(2), 170-177.

[22] Oh, H. S., & Sim, J. (2004). Interface debonding failure in beams strengthened with externally bonded GFRP. *Composite Interfaces, 11*(1), 25-42.

[23] Kalfat, R., & Al-Mahaidi, R. (2010). Investigation into bond behaviour of a new CFRP anchorage system for concrete utilising a mechanically strengthened substrate. *Composite structures*, *92*(11), 2738-2746.

[24] American Society for Testing and Materials. Committee C-9 on Concrete and Concrete Aggregates. (2011). *Standard test method for compressive strength of cylindrical concrete specimens*. ASTM International.

[25] ACI Committee. (2014). Building code requirements for structural concrete :(ACI 318-14); and commentary (ACI 318R-14). American Concrete Institute.

[26] Rasheed, H. A., Decker, B. R., Esmaeily, A., Peterman, R. J., & Melhem, H. G. (2015). The influence of CFRP anchorage on achieving sectional flexural capacity of strengthened concrete beams. *Fibers*, *3*(4), 539-559.

Chapter 7 - Flexural Behavior of Reinforced Concrete Rectangular Beams Strengthened with CFRP Sheets and Secured Using CFRP Anchors

In this present paper, five full-scale rectangular beams are prepared and tested. The first specimen was tested as a control beam. The second rectangular beam was strengthened with CFRP sheets and anchored with 16 mm diameter anchors at 140 mm spacing along the shear span. The third beam was strengthened with CFRP sheets and anchored with 19 mm diameter anchors at 203 mm spacing along the shear span. Four CFRP anchors with 16mm- diameter spaced at 406 mm were utilized to secure the flexural CFRP sheets for the fourth beam. An end CFRP anchorage technique was considered for the last rectangular beam, which included installing one CFRP spike anchor spaced at 76 mm form the edge of CFRP sheets (152 mm from the support). Experimental testing and nonlinear analysis showed improvement in the flexural performance of anchored beams by attaining the concrete crushing failure mode. The results prove that anchors offer an effective solution against premature debonding failure.

7.1 Introduction

Due to several advantages of using fiber reinforced polymer (FRP) materials, the externally bonded FRP composite system has been considered in the strengthening of reinforced concrete (RC) members. However, the efficiency of the FRP strengthening is vulnerable to the premature debonding failure that occurs at strains below the strain capacity of the FRP. It was found that the FRP sheets debond at 50% of their average tensile capacity [1]. Thus, half of the FRP strength and strain capacity are ineffective. Since the debonding failure limits the strength of the RC structures and causes a brittle failure, numerous studies have been conducted to investigate some solutions

against this premature failure. It has been observed that FRP anchorage system is one of the very effective techniques that might be used to prevent or control the debonding [2-22]. The FRP anchorage reinforces the externally bonded FRP sheets to achieve a full fiber utilization or to reach a higher level of the desirable strength. In addition, using FRP anchors increase the ductility by transferring the stress between CFRP sheets and concrete surface [23]

This paper presents the experimental study carried out to investigate the flexural improvement of strengthened RC beams with CFRP sheets and anchored utilizing CFRP spike anchors. Five rectangular beams were prepared and tested (R1, R4-R7). One the beams was tested as a control beam, while the remaining four specimens were strengthened with carbon fiber reinforced polymer (CFRP) sheets and anchored using CFRP spike anchors. The design included using identical CFRP sheets for all strengthened beams but with different anchorage arrangements. Additionally, two types of CFRP anchors were considered for two out of the five RC beams (R4-R5). These types are dowel CFRP anchors, which are employed on one shear span, and bundle-fiber CFRP anchors (Figure 7-1) that are installed on the other shear span of the same beams. The purpose of utilizing these various types of CFRP anchors, to assess their performance as well as the ease of installation. The results of the all specimens are evaluated and the comparisons between the experimental and numerical results are also discussed. Furthermore, the outcome is compared with the results of the RC beams (R2-R3) that were prepared and tested by Rasheed et al. [24]. In 2015, Rasheed et al. [24] conducted a study on improving the flexural capacity of RC beams. One of the beams was strengthened with five layers of flexural CFRP sheets only. Another specimen was retrofitted using five layers of flexural CFRP sheets and anchored with distributed U-wraps. It is interesting to note that the beam geometry, material properties, and contribution of flexural CFRP only (without anchorage) for specimens tested earlier [24] and the specimens in the current study are equivalent

(Appendix A). Accordingly, the performance of strengthened RC beams and bonded with CFRP spike anchors that presented herein is envaulted and compared with strengthened RC beams with and without distributed U-wrap anchorage, Rasheed et al [24].

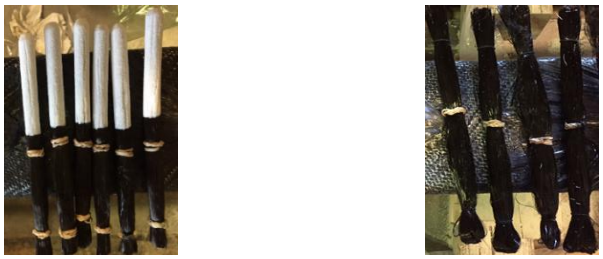

(a) (b)

Figure 7-1 CFRP anchors (a) dowel CFRP anchors; (b) bundled-fiber CFRP anchors

7.2 Beam Geometry

All the beams had the same web dimensions of 152 mm x 305 mm Figure 7-2. Two Φ 16 mm diameter of steel bars was used for tension zone, and two Φ 10 mm diameter bars were utilized for the compression steel. Steel reinforcement stirrups of Φ 10 mm are placed vertically at 127 mm on center, Figure 7-2. The concrete cover around the core was 25.5 mm. Each beam had a total span length of 4877 mm.

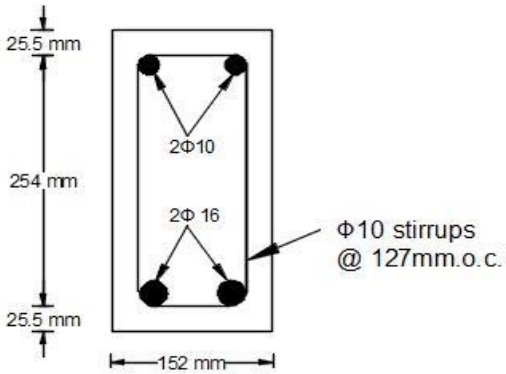

Figure 7-2 Beam cross section details

7.3 Materials

7.3.1 Concrete and Steel Reinforcement

The five specimens were cast in one batch using concrete ready mix. During concrete pouring, twelve cylinders were prepared then tested at 28 days. The average compressive strength was 38 MPa and the modulus of elasticity was 29 GPa. The flexural steel reinforcement had 211 GPa as modulus of elasticity and 488 MPa of a yield strength. While, the modulus of elasticity was 200 GPa for the top steel bars with a yield strength of 470 MPa. The tensile testing was performed by research lab at Kansas Department of Transportation (KDOT).

7.3.2 FRP Properties

The material properties of the CFRP sheets were provided by the manufacturer. Unidirectional CFRP (V-Wrap C100) and bidirectional CFRP (V-Wrap 220B) are the two types of the CFRP sheets that were used in this study. The Unidirectional CFRP properties were 0.584 mm thickness, 966 MPa tensile strength, and 66.19 GPa tensile modulus of the cured laminate. The bidirectional CFRP had 0.51 mm thickness in each direction, 1068 MPa tensile strength, and 96.53 GPa tensile modulus. For the C100 sheets, the CFRP fibers are oriented longitudinally a long one direction of the beam axis only (0°). On the other hand, the CFRP fibers for the C220B sheets are oriented in both direction longitudinally and transversely (0° and 90°). Furthermore, two parts (A and B) of the epoxy resin (V-Wrap 770) were mixed together according to manufacture proportions to form high strength bonding between the CFRP sheets and the tension face of the RC beams. A silica fume was mixed with the same resin (V-Wrap 770) to bond the CFRP anchors.

7.4 Surface Preparation

Since the procedure of concrete surface preparation and FRP application has a big impact on the performance and strength, some considerations were taking into account before installing

the CFRP sheets and anchors. All sharp corners were rounded to a minimum 13 mm radius in order to prevent stress concentrations in the FRP sheets during the loading. The bonding surface was also prepared using high pressure water-blasting technique (24 MPa) to expose the coarse aggregate and to clear away any laitance, dust, and existing coating, Figure 7-3 (a). Furthermore, a concrete drill was employed to drill the holes into the concrete at certain locations. Then, the predrilled holes were cleaned with compressed air to remove the dust and debris before inserting the CFRP anchors, Figure 7-3 (b).

(a) (b)

Figure 7-3 Surface preparation for the beams (a) roughening the surface; (b) drilling and cleaning the predrilled holes

7.5 Experimental Program

7.5.1 Layout and Application of CFRP Sheets and Anchors to Beams

The cross-sectional area for the control beam (R1) is presented in Figure 7-2. The layout and cross-sectional details of the RC specimens R2-R7 are explained in section 7.5.1.1- 7.5.1.3 and shown in Figures 7 (4-6), 7 (8-10).

7.5.1.1 Layout and Application of CFRP Sheets with and without U-warp Anchorage (R2-R3)

Rasheed et al. [24] strengthened the beam R2 with flexural five layers of unidirectional V-Wrap C100 only (Figure 7-4) and strengthened the beam R3 with flexural five layers plus distributed CFRP U-wrap anchors. One layer of transverse distributed U-wraps with 140 mm width spaced at 305 mm on center was used along the entire span length, Figure 7-5. The purpose of

using U-wrap anchorage was to anchor the bottom layers of CFRP and prevent the separation of CFRP sheets. Figures 7-4 and 7-5 show the layouts and cross-section details for specimens R2 and R3.

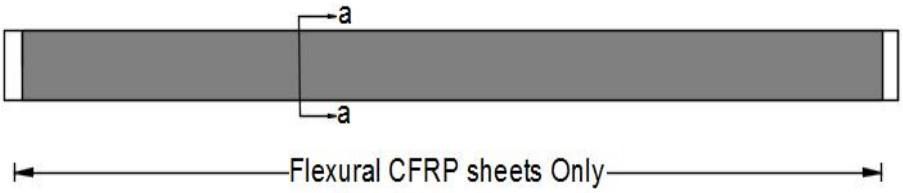

Figure 7-4 Layout of beam R2

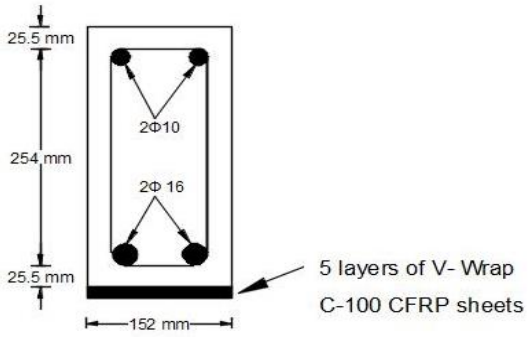

Section a-a

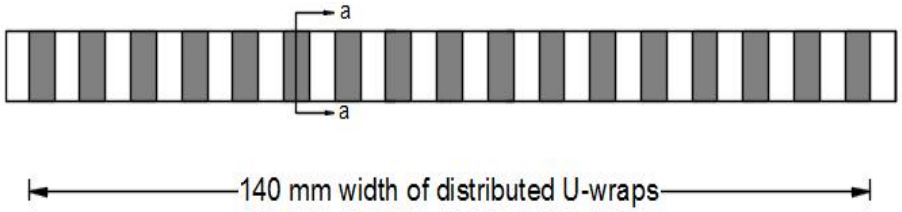

Figure 7-5 Layout of beam R3

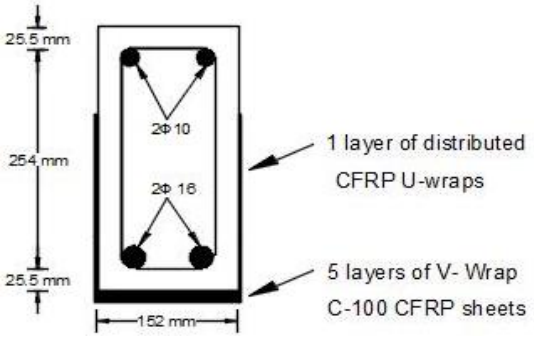

Section a-a

7.5.1.2 Layout and Application of CFRP Sheets and Anchors for Beam R4

The specimen R4 was strengthened in flexural with three sheets of unidirectional CFRP (V-Wrap C-100). The first two layers installed on the bottom face of the beams only and the third layer was applied to the bottom and wrapped 51 mm up the sides from the soffit. One more layer of bidirectional CFRP (C220B) was placed on the top of the preinstalled three layers (C100) and wrapped 89 mm up the sides, Figure 7-6**.** In addition, the beam was reinforced with 16 mm-diameter CFRP spike anchors spaced at 140 mm on center. This yielded using twelve large dowel CFRP anchors on one shear span and twelve large bundled-fiber CFRP anchors on the other shear span. The layout and details of CFRP sheets and CFRP anchors is showing in Figure 7-6, section a-a and section b-b. Figure 7-7 presents the application procedure of CFRP sheets and anchors.

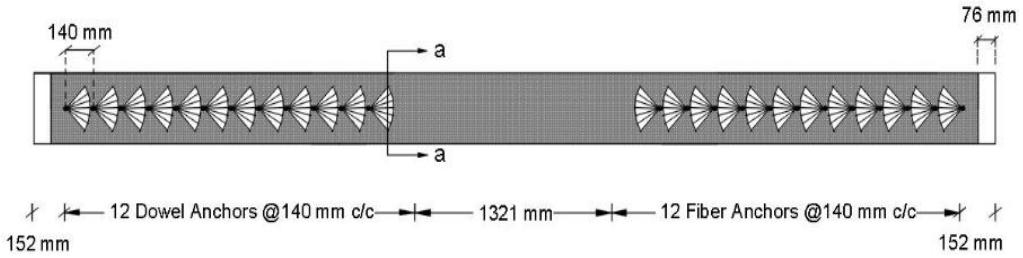

Figure 7-6 Layout of beam R4

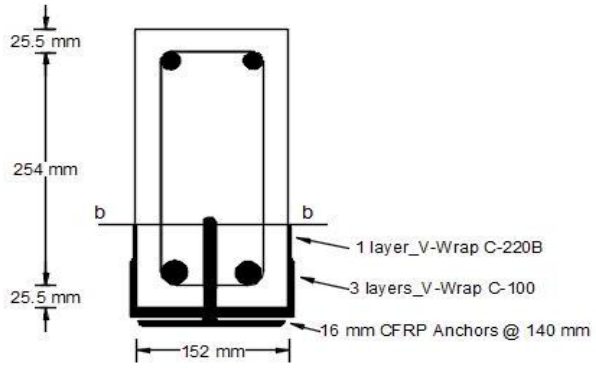

Section a-a

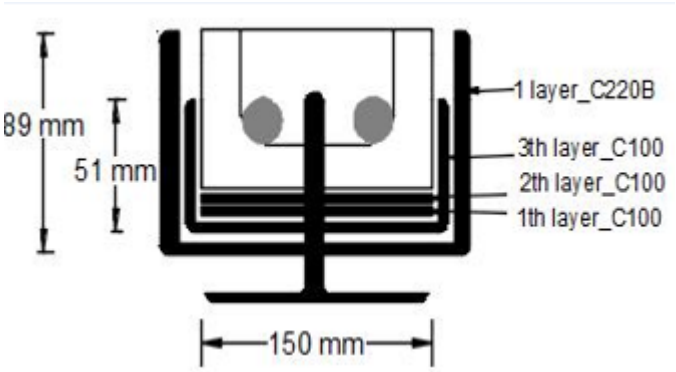

Section b-b

(a)

(b)

(c)

Figure 7-7 Application procedure of series 2 (a) installing CFRP anchors; (b) installing the CFRP sheets; and (c) impregnating the CFRP anchors with epoxy resin

7.5.1.3 Layout and Application of CFRP Sheets for Beams R5, R6, and R7

The specimens R5, R6, and R7 were flexurally strengthened with the same four layers of CFRP sheets that were installed for beam R4 (R2 and R3, Rasheed et al. [24] had equivalent contribution of CFRP sheets of R4-R7). This includes three layers of CFRP C100 and one layer of CFRP C220B. However, various anchorage arrangements were considered. The design of beam R5 involved using total of 18 CFRP spike anchors with diameter of 19 mm spaced at 203 mm per each shear span, Figure 7-8. Thus, nine dowel CFRP anchors placed on one shear span and nine bundled-fiber CFRP anchors installed on the other shear span. The total amount of the carbon fiber in the CFRP anchors of beam R4 and R5 are equivalent. For R6 specimen, four CFRP anchors were installed with diameter of 16 mm spaced at 406 mm per each shear span (8 total anchors),

Figure 7-9. The CFRP sheets of the last beam (R7) was bonded with one CFRP anchor (end anchorage system) on each side of the shear span positioned at 76 mm from the ends of the CFRP sheets (152 mm from the support), Figure 7-10. The applications of CFRP sheets and anchors for R5, R6, and R7 are presented in Figure 7-11.

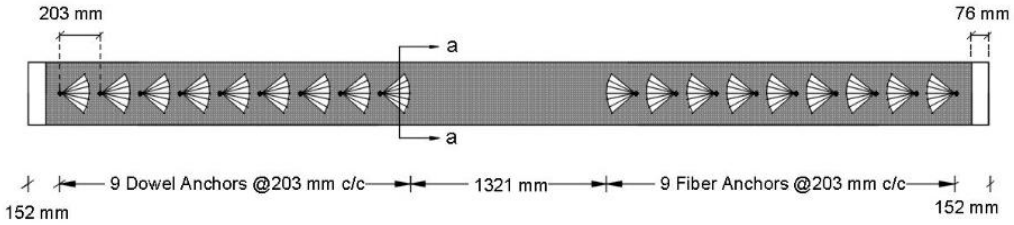

Figure 7-8 Layout of beam R5

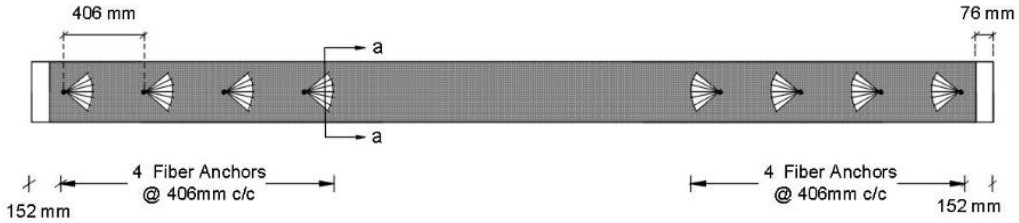

Figure 7-9 Layout of beam R6

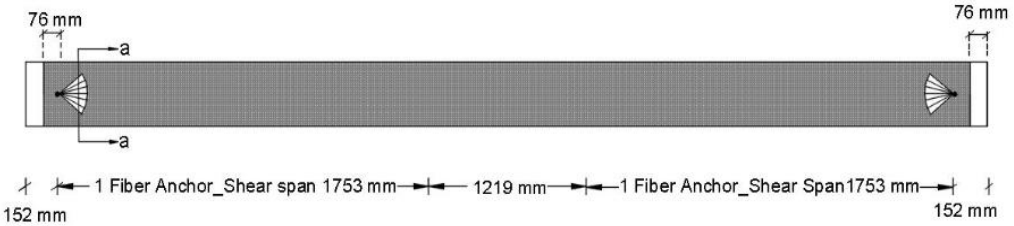

Figure 7-10 Layout of beam R7

(a) (b) (c)

Figure 7-11 Application of CFRP sheets and anchors for (a) R5; (b) R6; (c) R7

7.6 Test Setup and Data Acquisition

All the specimens were simply supported and tested in four-point bending in the structural testing lab at Kansas State University. The shear span on each side was 1753 mm, and the distance between the applied loads was 1219 mm, Figure 7-12. The total and clear span lengths are 4877mm and 4724 mm, respectively. It is important to note that the supports were placed at 76 mm from the edges of the beams and the CFRP sheets were installed at 152 mm from the edges (74 from the supports) to avoid being touched by the supports, Figure 7-12. Two linear variable displacement transducers (LVDTs) were installed at mid-span to measure the deflection. Two strain gauges had already been mounted on the main flexural bars at mid span that were embedded into the concrete before casting the concrete to measure the strains for steel reinforcement. Other two strain gauges were placed on the top of beams to monitor the strain at top of concrete. In addition, two strain gauges were applied at the bottom to measure the strain on the CFRP sheets. To capture the propagation of debonding in the CFRP sheets and anchors along the entire span length, six more strain gages were installed between the CFRP anchors. Three of these strain gauges were placed on one shear span, and three strain gauges were installed on the other shear span. Displacement control system was followed throughout the testing process at a rate of 2.54 mm per minute.

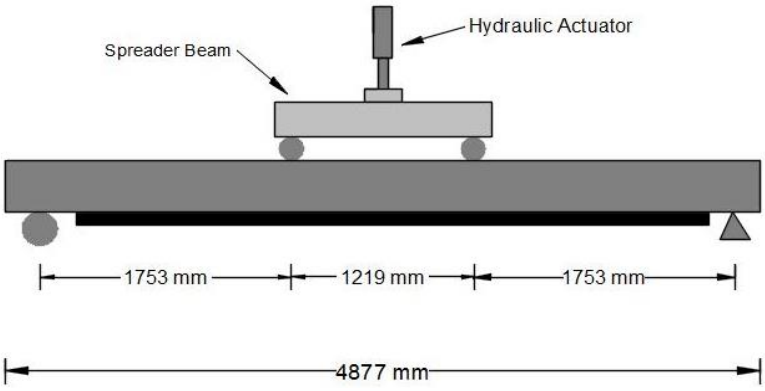

Figure 7-12 Beam details and experimental test setup

7.7 Numerical Analysis

7.7.1 Computer Program

In order to assess the obtained experimental results, an Excel numerical program was considered to calculate the theoretical values of each beam. This program was developed earlier at Kansas State University to compare the experimental load-deflection and load-strain response to numerical predictions. This program can also determine the flexural response, ultimate flexural capacity, and the flexural failure mode, Figure 7-13. Additionally, the program is capable of evaluating the moment curvature relationship and it uses the Hognestad's parabola to account for the nonlinearity of concrete in compression.

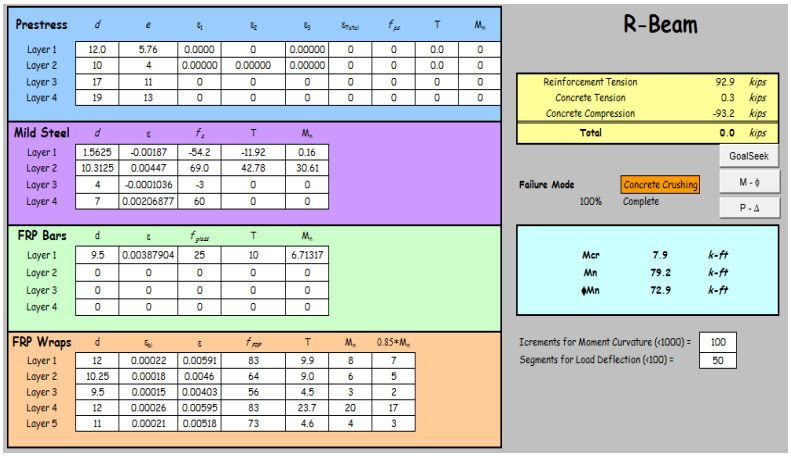

Figure 7-13 Output interface for the analysis program

7.8 Results and Discussion

7.8.1 Control Beam R1

One of the specimens was tested as a control beam (R1). The numerical program determined the ultimate load would be 50.0 kN with a central deflection of 70.9 mm. The experimental test results showed that the specimen reached 54.7 kN (almost similar to theoretical values) before the failure caused by concrete crushing after steel yielding, as observed in Figure

7-14. The experimental mid-span deflection was 79.7 mm. Figure 7-15 presents the load deflection comparison between the analytical and the experimental results that were found to be very similar. Moreover, there were good agreements between the numerical and experimental results of the load versus strain in top concrete surface and in steel rebars, Figures 7-16 and 7-17

Figure 7-14 Control beam CBR after the test

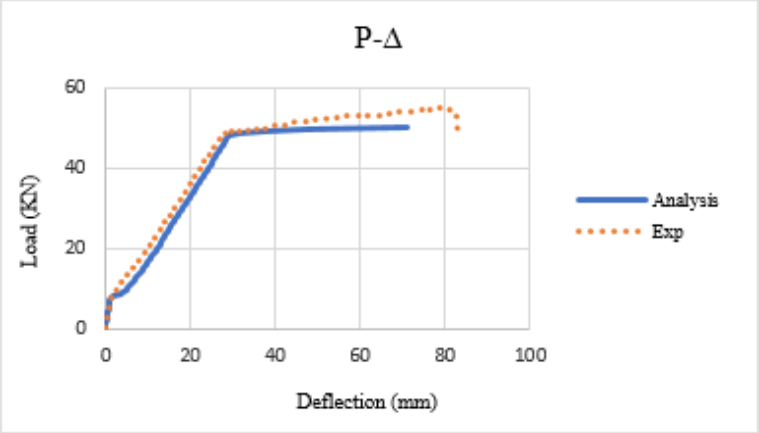

Figure 7-15 Comparison of test and analysis response of control beam R1

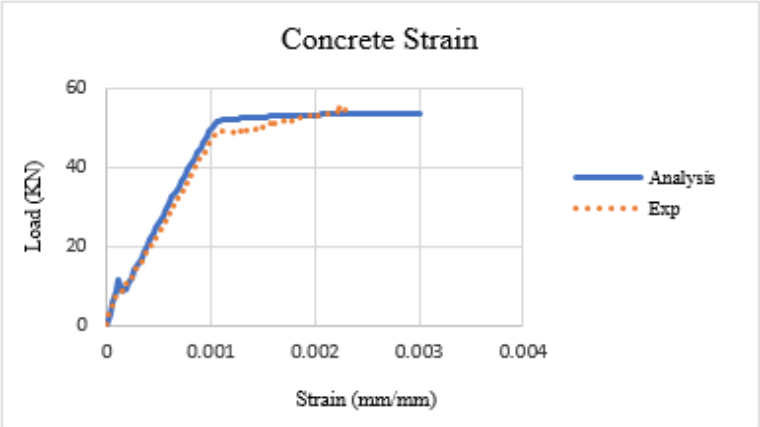

Figure 7-16 Comparison of the load-strain in the top concrete surface of R1

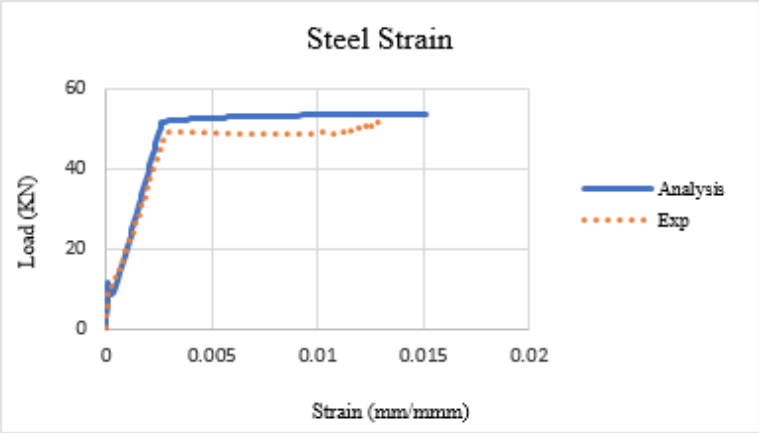

Figure 7-17 Comparison of the load-strain in the main rebars of R1

7.8.2 Beam R2 with Flexural CFRP Sheets only

This beam (R2) was prepared and tested by Rasheed et al. [24]. In that study, the researchers used five layers of CFRP sheets (V-Wrap C-100) to strength the rectangular RC beam in flexure. Rasheed et al. [24] reported that the specimen R2 failed at an ultimate load of 109.4 kN with a maximum deflection of 60.20 mm. The experimental results are reasonably close to the analytical values that were predicted to reach 97.32 kN of maximum load capacity and 51. 71 mm deflection at mid-span, based on ACI440.2R-17 debonding strain. The failure mode was mostly debonding that occurred between the CFRP sheets and the concrete substrate (Figure 7-18). The

load-deflection response for the numerical and experimental results is shown in Figure 7-19, and they are in very good agreement.

Figure 7-18 Beam R2 after the failure

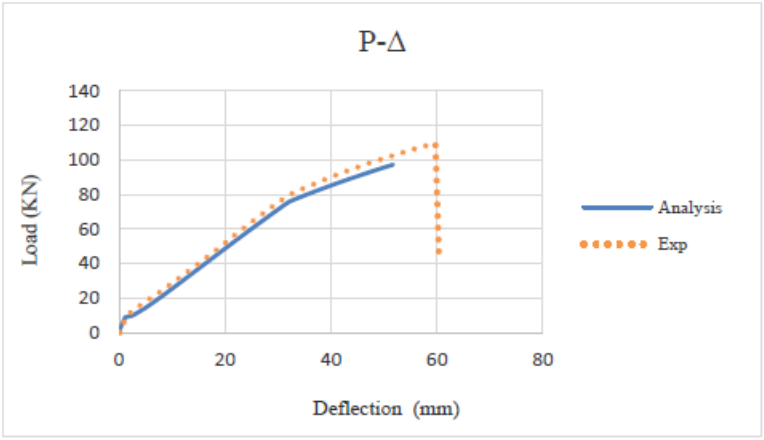

Figure 7-19. Comparison of test and analysis response of beam R2

7.8.3 Beam B3 with Flexural CFRP and U-wrap Anchorage

The beam R3 was also prepared and tested by Rasheed et al. [24]. The researchers used five layers of CFRP sheets (V-wrap C-100) to strength the bottom face of the specimen in flexure. In addition, the beam was anchored with one layer of the distributed U-wrap with 140 mm width spaced on 305 mm on center. The rationale behind using U-wrap anchorage was to anchor the bottom layers of CFRP and prevent the separation of CFRP sheets. Rasheed. et al. [24] outlined

that the test specimen reached an ultimate load of 120.5 kN before the rupture of CFRP occurred by concrete crushing and excessive curvature at the critical region, Figure 7-20. There was excellent agreement between the analytical and experimental results as observed in the load-deflection response graph, Figure 7-21. It is important to note that the specimen geometry, material properties, and the contribution of CFRP sheets of R2 [24] and R3 [24] are identical to those strengthened RC beams with CFRP sheets but unanchored (R4-R7) that presented in this paper (Appendix A). Therefore, the results of beams R2 and R3 are directly compared herein with the values of strengthened beams using CFRP sheets and secured with CFRP anchors (R4-R7).

Figure 7-20 Beam R3 after the test

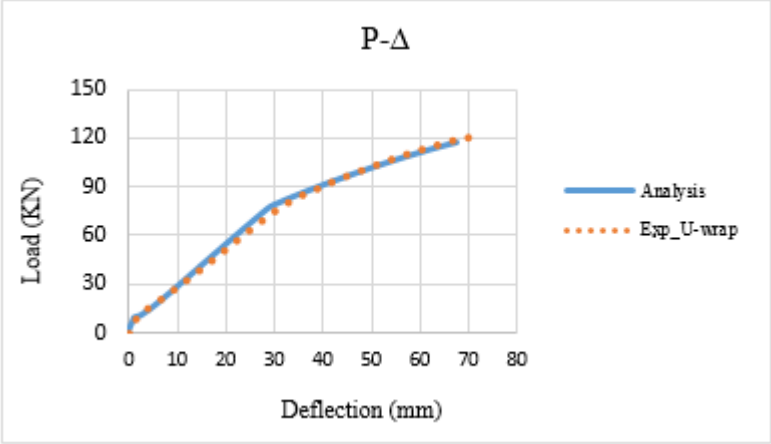

Figure 7-21 Comparison of test and analysis response of beam R3

7.8.4 Beam R4 with Flexural CFRP and 16 mm-Diameter of Spike Anchors

The specimen R4 was strengthened with CFRP sheets and anchored using two types of CFRP anchors with 16-mm diameter. A 112.6 kN was the expected ultimate load from the analysis, with a central deflection of 63.8 mm. The experimental test shows that the beam failed in concrete crushing after steel yielding (Figure 7-22) at a load of 125.0 kN and 69.3 mm as a mid-span deflection. The load deflection comparison between the numerical response versus experimental results for the control beam R1, the beam R3 with CFRP U-wraps [24], and the beam R4 with CFRP spike anchors is shown in Figure 7-23**.** It is noticeable that the experimental and theoretical response correlate very well. Whereas, the behavior of the tested beam with spike CFRP anchors showed greater capacity than the analyzed specimen due to the use of the CFRP anchors.

An excellent agreement can be clearly observed between the experimental versus numerical values for the load-strain at top concrete surface and in the bottom tensile rebars, Figures 7 (24-25). Additionally, there is good agreement between the load-strain responses in CFRP sheets at mid-span except for the local debonding at the critical region where the experimental graph deviated from the analysis after the cracking level at a load of 63 kN, Figure 7-26**.** The details and layout of other six stain gauges is clarified in Figure 7-27. Lastly, the load-strain comparison between the experimental and numerical relationship for the strains along the shear span from each side of the specimen are presented in Figure 7-28. Good agreement can be observed from these graphs (a-f, Figure 7-28) between the theoretical and experimental responses except for location 12 (on the north side). No ductility was noticed from the strain gauge readings since the beam failed in concrete crushing and did not reach the full utilization of the fiber. However, the shear span on the north side (at 8,10, and 12), where the bundled-fiber CFRP anchors were installed, experienced higher strain in the CFRP sheets than the south side (at 7,9, and 11), Figure 7-28.

Figure 7-22 Failure of the beam R4

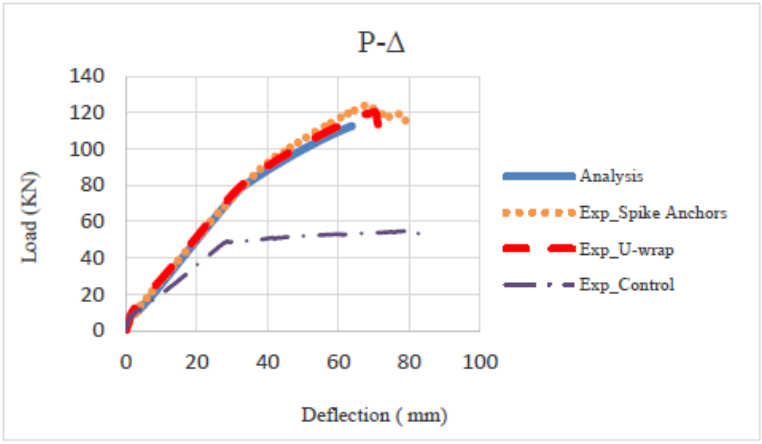

Figure 7-23 Comparison of test and analysis response of beam R4 and comparable beams

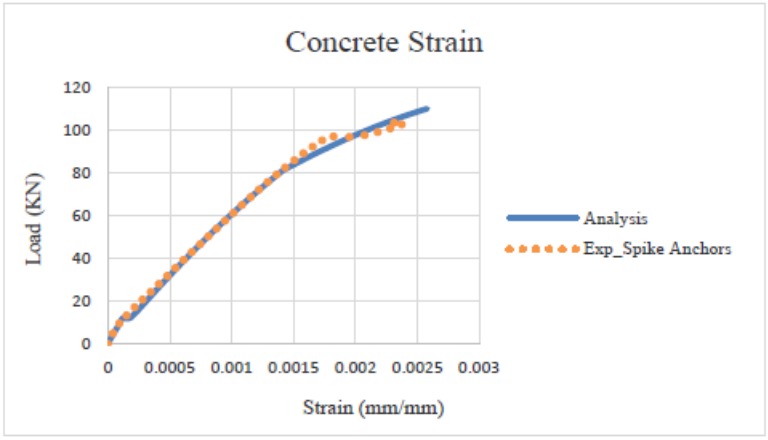

Figure 7-24 Comparison of the load-strain of R4 at the top concrete surface

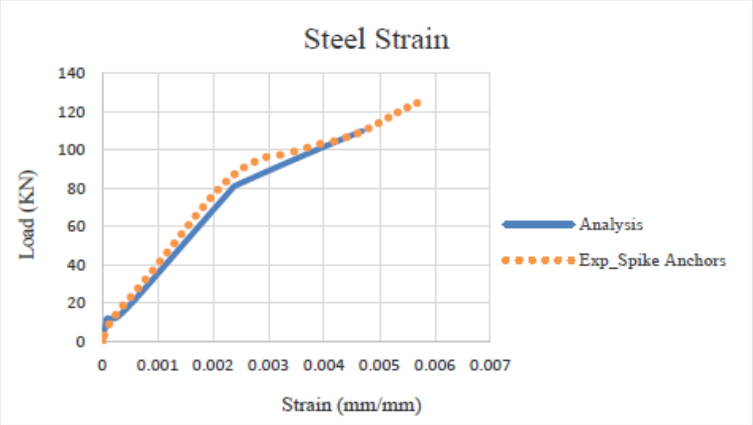

Figure 7-25 Comparison of the load-strain of R4 in the main rebars

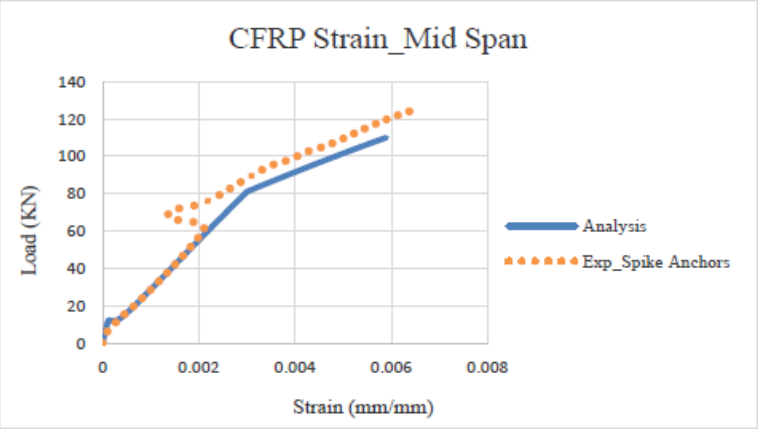

Figure 7-26 Comparison of the load-strain of R4 in the CFRP sheets

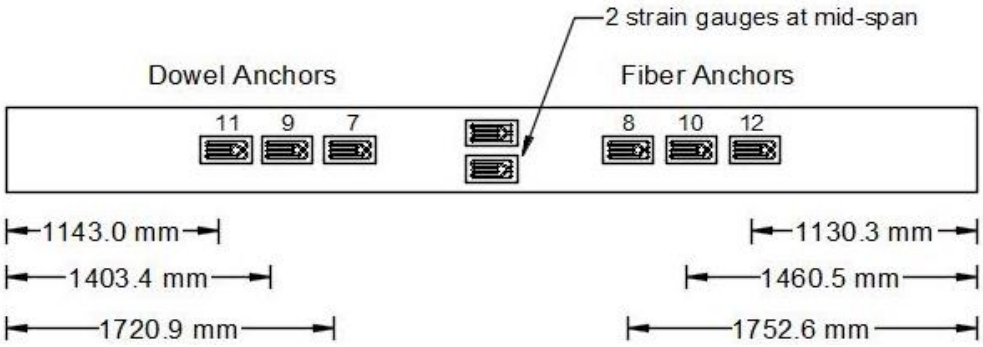

Figure 7-27 Strain gauge details for beam R4

Dowel anchors

Fiber anchors

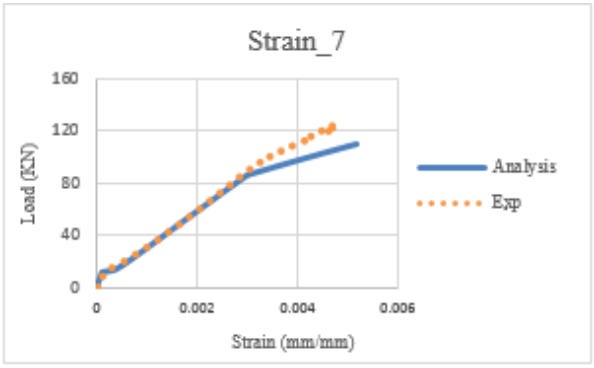

(a)

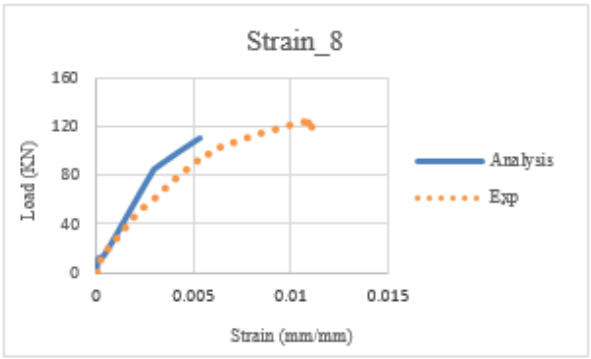

(b)

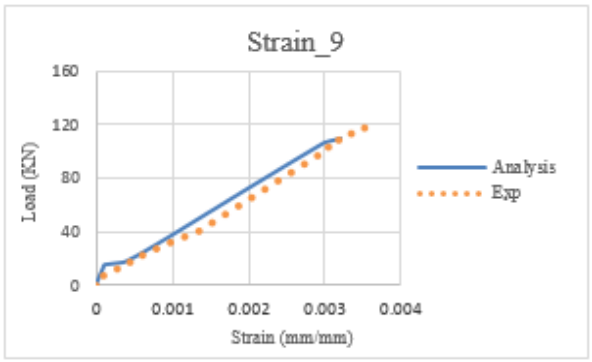

(c)

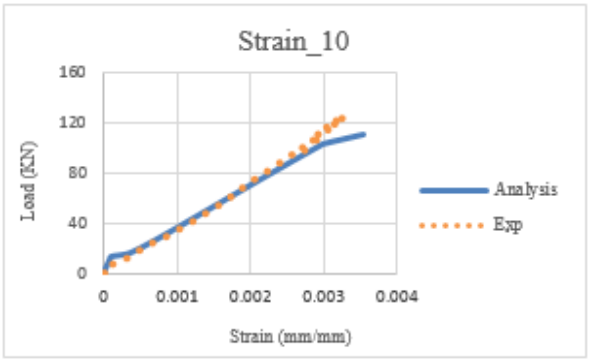

(d)

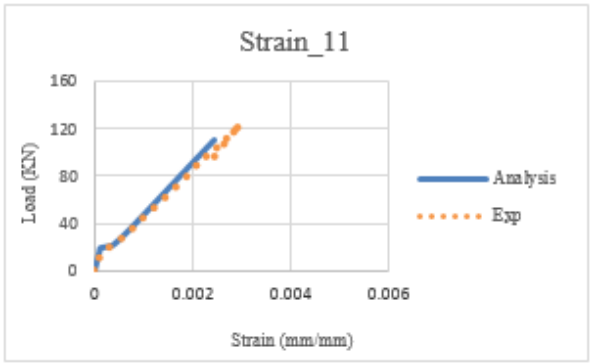

(e)

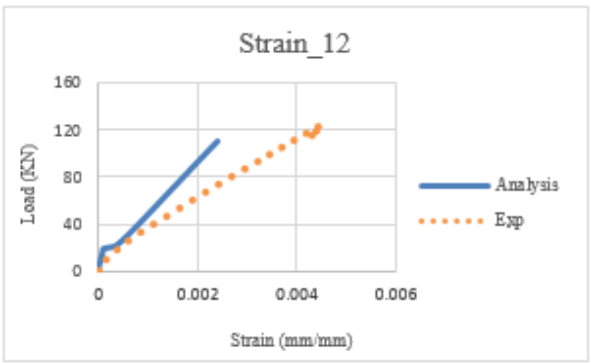

(f)

Figure 7-28 Comparisons of the load-strain (a); (b); (c); (d); (e); and (f) strain results in the CFRP sheets at different location along the shear spans of the beam R4

7.8.5 Beam R5 with Flexural CFRP and 19 mm-Diameter of Spike Anchors

The specimen R5 was strengthened with flexural CFRP sheets and secured with 19-mm diameter of CFRP anchors. An ultimate load of 120.5 kN was obtained from the experimental test with a maximum deflection of 77.5 mm. The failure mode was concrete crushing after the yielding of steel reinforcements, Figure 7-29. The strength of this beam was a bit reduced over the beam R4. However, R5 specimen was able to achieve about 12% increase in the peak deflection (Figure 7-30), compared to specimen R4**.** Also, the R4 had no drop in the load-deflection response (Figure 7-23) as beam R5 since the anchors were positioned behind each other without any free region to initiate local debonding between the installed CFRP anchors. That proves the close spaced anchors were successfully bonded the CFRP sheets and prevented the premature debonding up to complete failure caused by concrete crushing.

Similar load capacity of 120.5 kN was obtained using distributed U-wrap anchors [24]. Figure 7-30 shows the load deflection comparison between the numerical results of the strengthened beam (assuming perfect bond) versus the experimental values for the control beam R1, the beam R3 with CFRP U-wraps [24], and the beam R5 with CFRP spike anchors. It is obvious from the graph that the theoretical and both the experimental responses of the beam with spike anchors and the beam with U-wrap anchorage are identical. On the other hand, the behavior of the tested beam with CFRP spike anchors showed more capacity than the analyzed specimen. This is attributed to the use of anchors and the increase in the amount of carbon fiber added by the CFRP anchors, which was not included in the analysis.

There are very good agreements between the numerical and experimental results of the load-strain at the top concrete surface, in the tension rebars, and in the CFRP sheets at mid-span as observed in Figures 7(31-33). Moreover, the details of the other six stain gauges in the CFRP sheets and the layout of CFRP anchor types is shown in Figure 7-34. The load-strain comparisons

between the experimental and numerical relationship for the strains along the shear span from each side of the specimen are presented in Figure 7-35. From the graphs, no ductility can be seen from the experimental response of stain gauges readings along the shear spans. That because the beam also failed in concrete crushing and so that could not utilize the full advantage of the CFRP fibers. Still, the strains in the CFRP sheets on the bundled-fiber anchors side (at 8, 10, and 12) showed bigger strain than the dowel anchor side (at 7,9, and 11).

Figure 7-29 Beam R5 after the failure

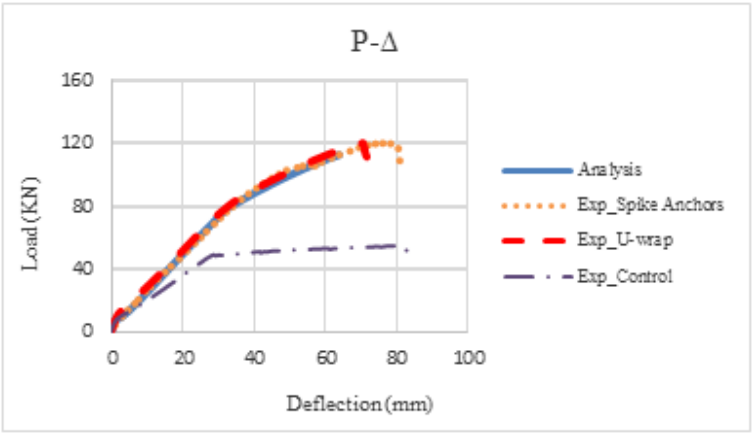

Figure 7-30 Comparison of test and analysis response of beam R5 and comparable beams

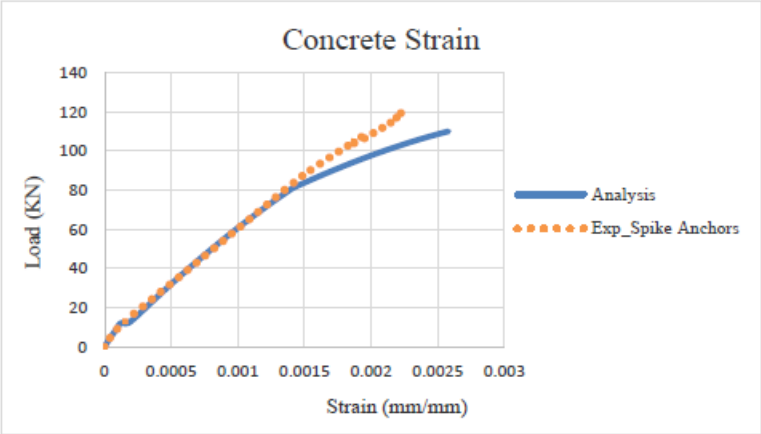

Figure 7-31 Comparison of the load-strain at the top concrete surface of R5

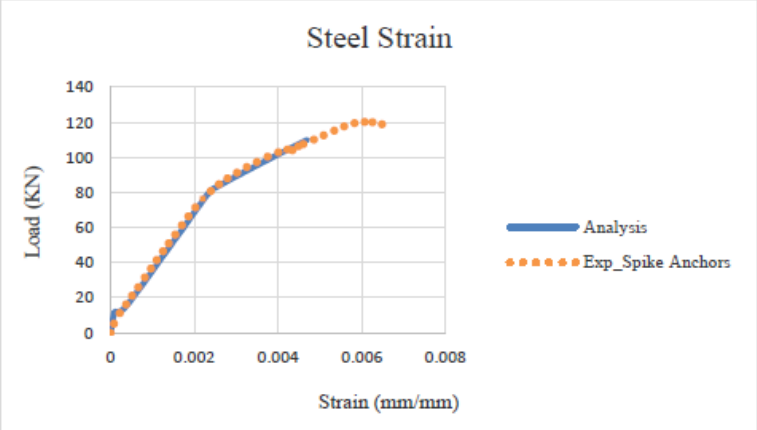

Figure 7-32 Comparison of the load-strain in the main rebars of R5

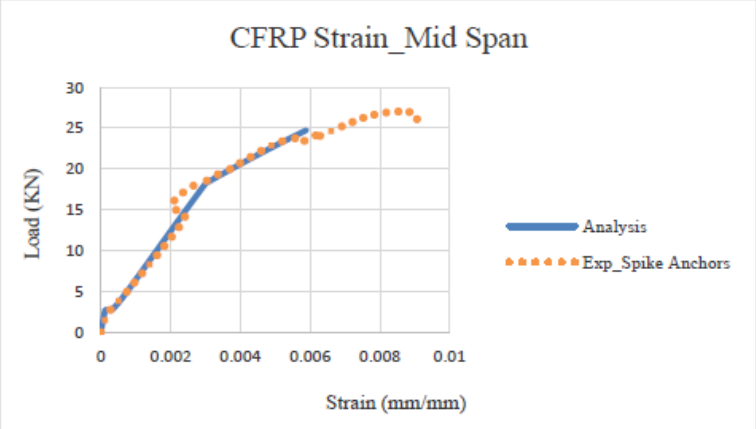

Figure 7-33 Comparison of the load-strain in the CFRP sheets of R5

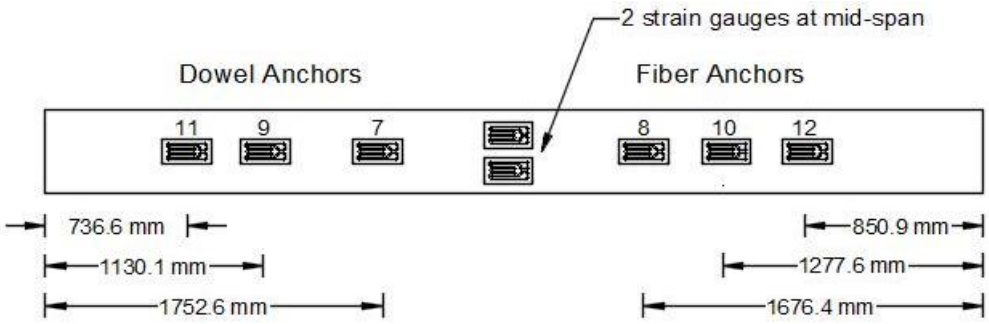

Figure 7-34 Strain gauge details for beam R5

Dowel anchors

Fiber anchors

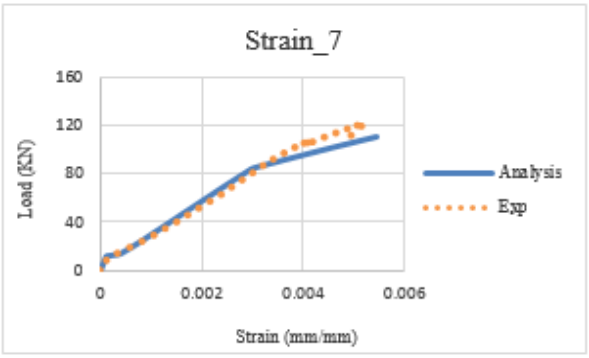

(a)

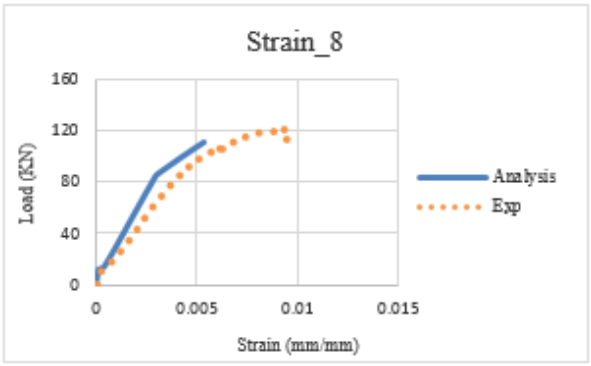

(b)

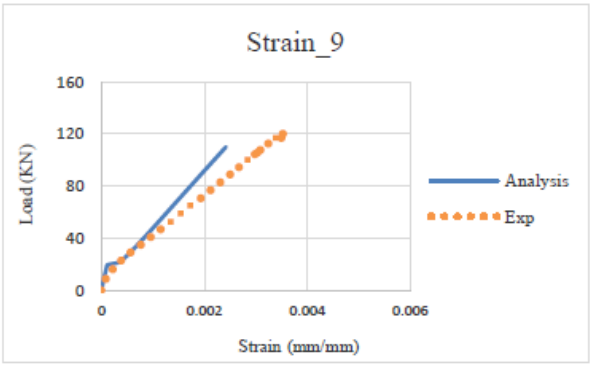

(c)

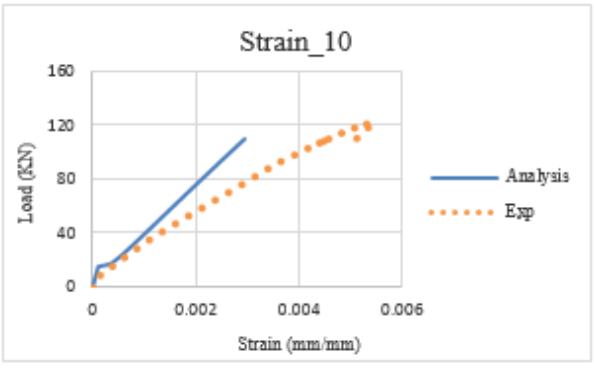

(d)

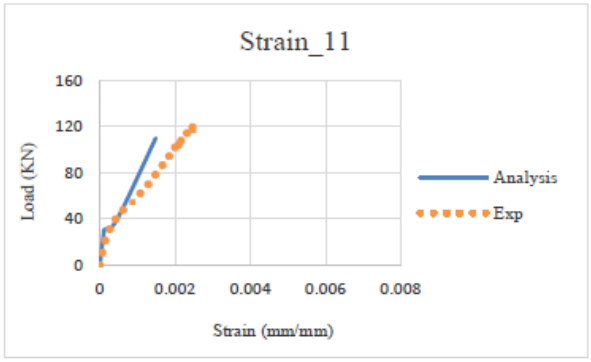

(e)

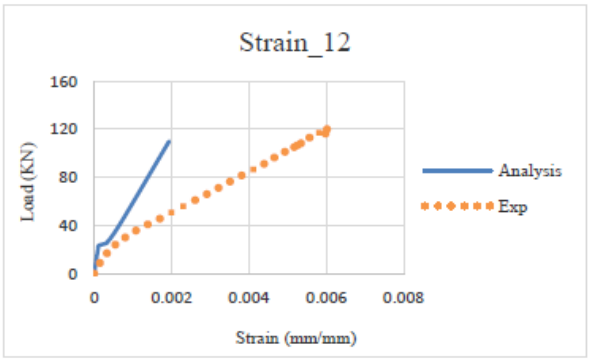

(f)

Figure 7-35 Comparisons of the load-strain (a); (b); (c); (d); (e), and (f) strain results in the CFRP sheets at different location along the shear spans of the beam R5

7.8.6 Beam R6 with Flexural CFRP and 16 mm-Diameter of Spike Anchors

Four bundled-fiber CFRP spike anchors with 16 mm-dimeter were utilized along the shear spans to secure the CFRP sheets of beam R6. These 4 anchors were spaced at 406 mm, which is almost triple of the spacing of beam R5 (140 mm). The specimen had 33.3% of the number of CFRP anchors as beam R5. From the experimental test, the beam failed early in concrete crushing at a load of 106.6 kN which corresponded to a mid-span deflection of 70.1, Figure 7-36. The experimental load capacity (106.6 kN) was lower than the ultimate peak load that obtained from the analysis**.** This early failure within the constant moment region caused by a void in concrete because of poor vibration near the top surface. Figure 7-37 shows the load-deflection comparisons between the numerical results of R6 versus the experimental responses for, the control beam R1, the beam R3 with CFRP U-wraps [24], and the beam R6 with CFRP spike anchors. It can be noticed from this graph that the theoretical curve is stiffer than the experimental one (with spike anchors) since the beam failed early in crushing at the top surface before reaching the ultimate sectional capacity.

Furthermore, the experimental response of the load-strain at the top concrete surface (at mid-span) is softer than the analytical curve, Figure 7-38. This proves there was a defect at that section (constant moment region). Very good agreement is noticed between the experimental and numerical comparison of the load versus strain results, in the steel rebars and in the CFRP at mid-span as presented in Figures 7 (39-40). Details of the strain gauges that were fixed along the shear spans for R6 beam is showing in Figure 7-41. Also, the load-strain comparisons between the experimental and theoretical responses at these locations (strain 7- 12) are shown in Figure 7-42. It can be clearly observed from these graph that the numerical response is stiffer than the experimental curves.

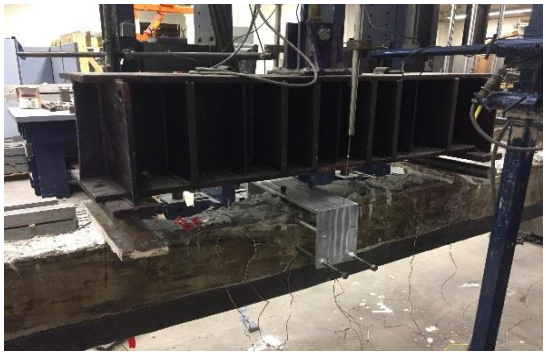

Figure 7-36 Beam R6 after the failure

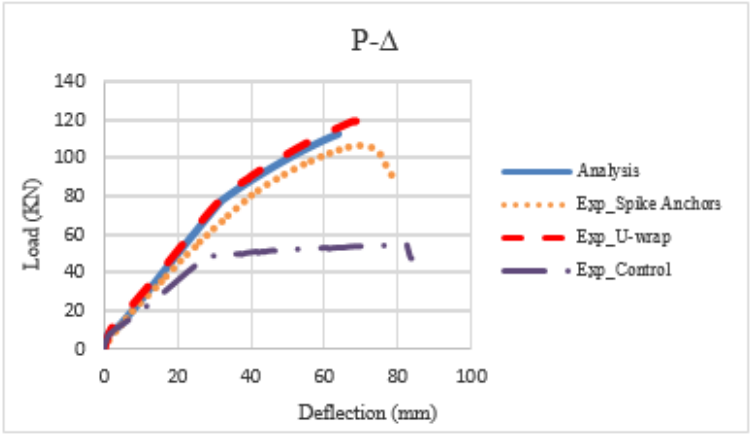

Figure 7-37 Comparison of test and analysis response of beam R6 and comparable beams

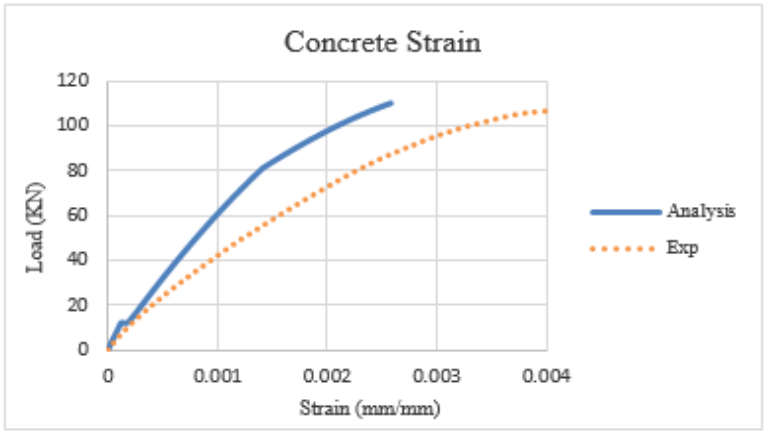

Figure 7-38 Comparison of the load-strain at the top concrete surface of R6

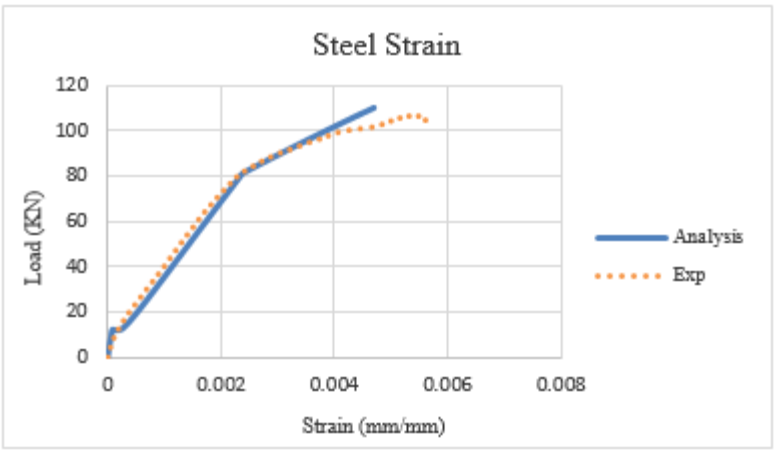

Figure 7-39 Comparison the load-strain in the main rebars of R6

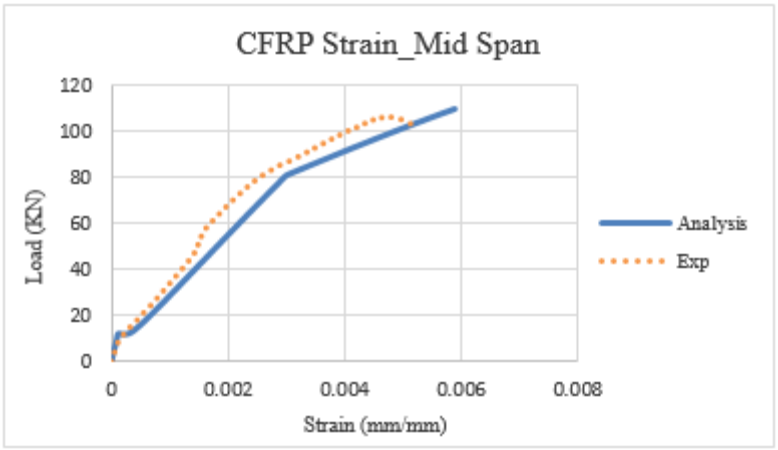

Figure 7-40 Comparison of the load-strain in the CFRP sheets of R6

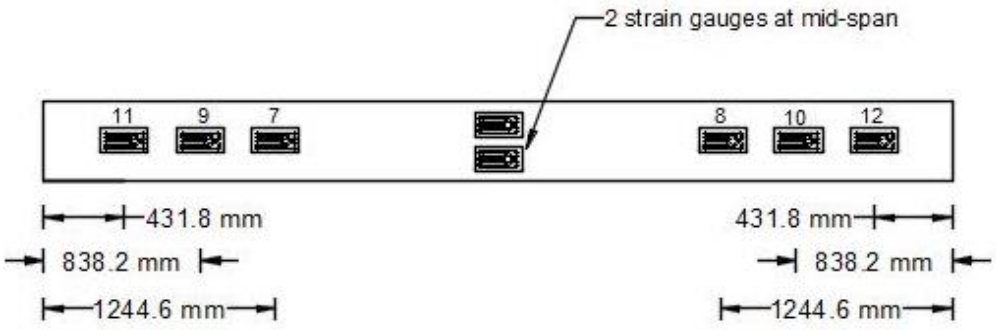

Figure 7-41 Strain gauge details for beam R6

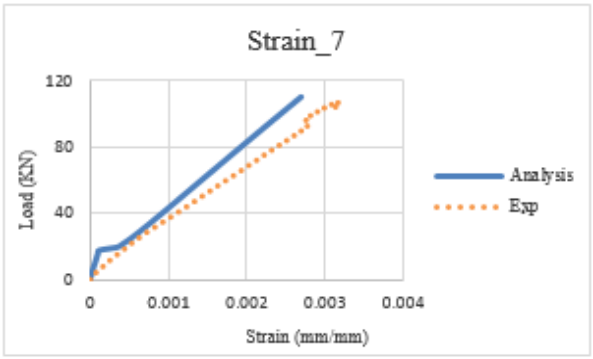

(a)

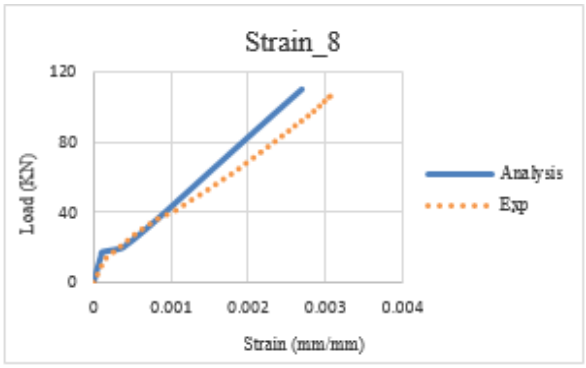

(b)

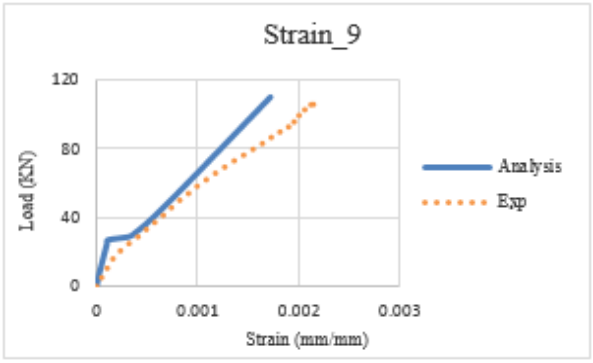

(c)

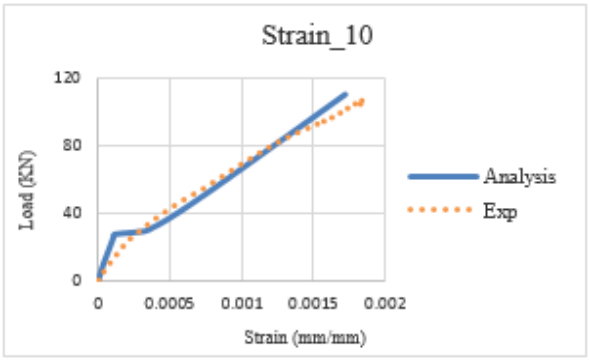

(d)

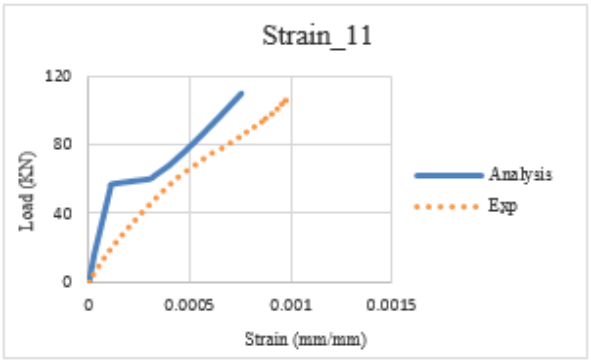

(e)

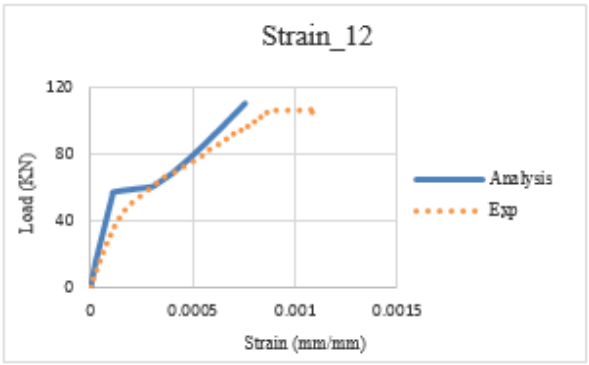

(f)

Figure 7-42 Comparisons of load-strain (a); (b); (c); (d); (e); and (f) strain results in the CFRP sheets at different location along the shear spans of the beam R6

7.8.7 Beam R7 with Flexural CFRP and End CFRP Anchor

For the last rectangular beam; the end anchorage system was used to evaluate whether it would improve the flexural performance by controlling the debonding or not. This beam (R7) failed at an ultimate load of 112.0 kN with a maximum deflection of 57.4.0 mm caused by the debonding of CFRP sheets, Figure 7-43. The debonding started from the critical region (mid-span) and propagated through the shear spans. It was observed and recorded that the load capacity dropped down before the debonding of CFRP sheets reached the end installed CFRP anchor. Accordingly, the peak load capacity of R7 (112.0 kN) is very close to the load capacity of beam R2 (109.4 kN) that strengthened with 5 layers of CFRP sheets only [24]. Thus, the end CFRP spike anchor did not successfully control the debonding of the CFRP sheets and did not provide any extra strength to the strengthened beam.

Figure 7-44 shows the load-deflection comparisons between the numerical response of R7 versus the experimental results for, the control beam R1, the beam R3 with distributed CFRP U-wraps [24], and the beam R7 with end CFRP spike anchor. The experimental and numerical responses of beam R7 are in excellent agreement.

Furthermore, good agreement can be observed for the load-strain comparison between the experimental and numerical results at the top concrete surface, in the main tension rebars, and in the CFRP at mid-span, Figures 7 (45-47). The installed strain gauges details along the shear spans is showing in Figure 7-36. The relationship between the experimental and numerical values of load-strain are presented in Figure 7-48. The experimental and analytical load-strain curves at locations 7-10 show good agreement, while there is little miss match for the load-strain at location 11. The readings of the strain gauge at location 12 was unexpectedly lost during the test.

Figure 7-43 Beam R7 after the failure

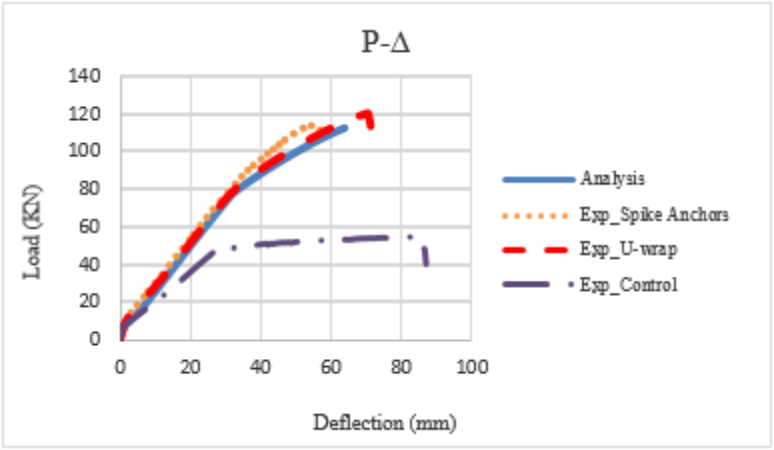

Figure 7-44 Comparison of test and analysis response of beam R7 and comparable beams

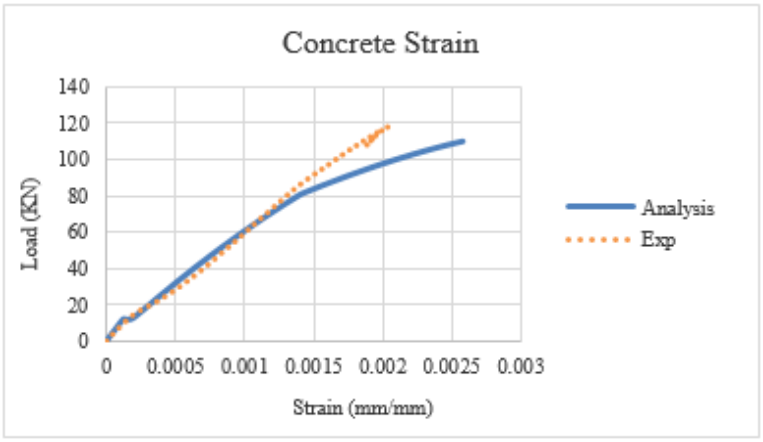

Figure 7-45 Comparison of the load-strain at the top concrete surface of R7

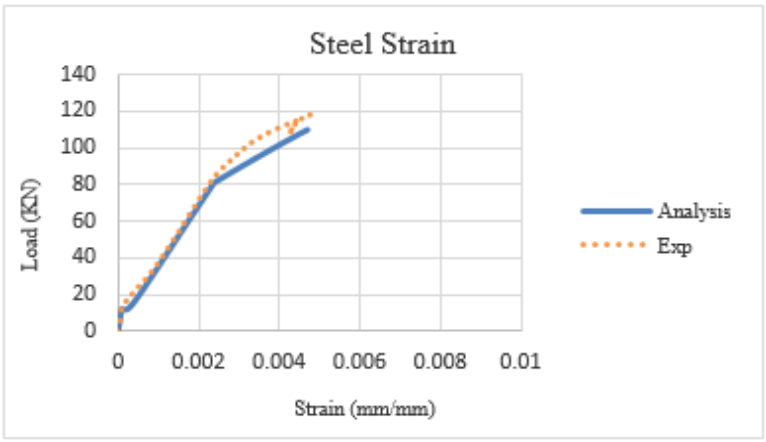

Figure 7-46 Comparison the load-strain in the main rebars of R7

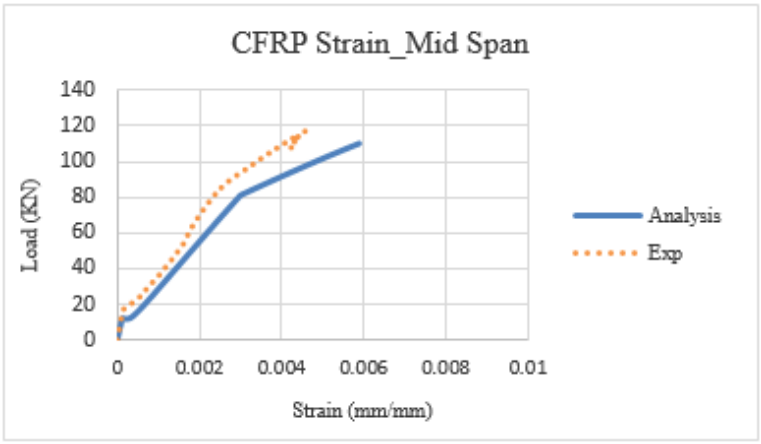

Figure 7-47 Comparison of the load-strain in the CFRP sheets of R7

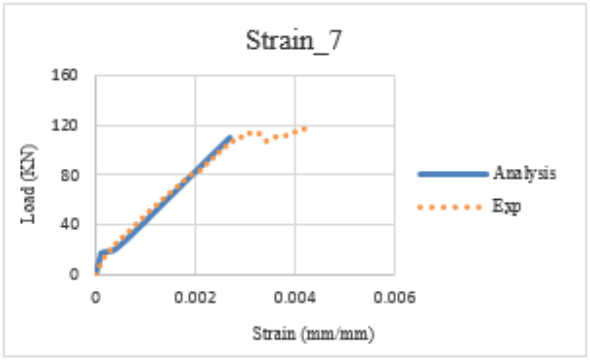

…… ….(a)

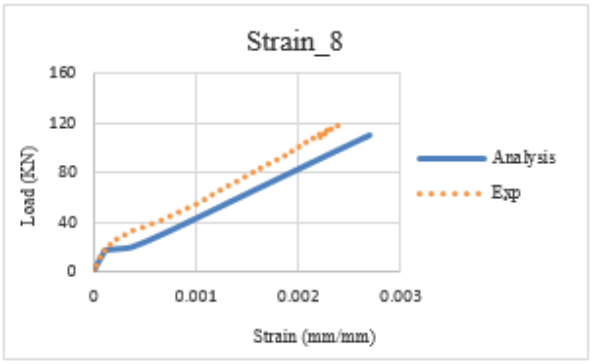

(b)

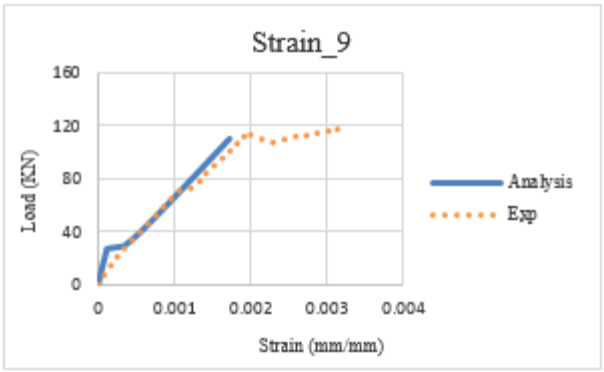

……(c)

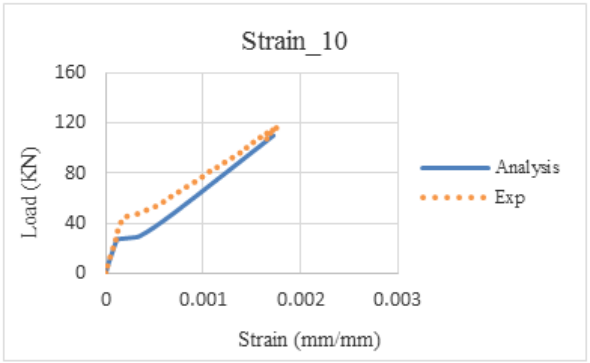

. (d)

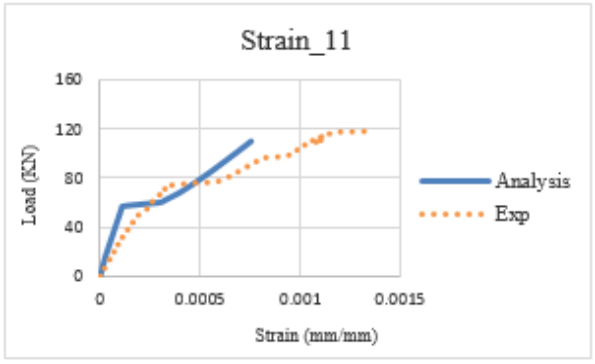

(e)

Figure 7-48 Comparisons of load- strain (a); (b); (c); (d); and (e) strain results in the CFRP sheets at different location along the shear spans of the beam R7

7.9 Conclusions

This paper investigates the use of CFRP spike anchors with various anchorage arrangements. Two different types of CFRP anchors with equivalent fiber density were also considered to study their effect on performance (R4 and R5). The following conclusions are drawn based on the experimental and analytical results.

- The anchorage arrangements of specimens R4 and R5 increased the flexural strength for the rectangular beams up to the ultimate sectional capacity (concrete crushing).

- Utilizing the distributed U-wrap anchorage technique enhanced the strength for rectangular beam. However, the strengthened specimen and secured with 12 CFRP spike anchors along shear spans (R4) gained more strength than the U-wrap anchors (R3).

- The use of nine CFRP anchors per shear span (R5) showed similar strength as the beam R3 that anchored with distributed U-wraps.

- The close spaced anchors (R4) showed greatest flexural improvement.

- It was found that the use of an end CFRP spike anchor is ineffective to shift or delay the premature debonding. The beam R7 failed in debonding of CFRP sheets along the critical regions (mid-span and shear spans) before the propagation of debonding reached to the end of CFRP sheets and the installed anchor.

- The dowel anchors were easier to insert by hand in the predrilled holes into the concrete (without the need to any tool). On the other hand, the fiber anchors need a rigid tool like a

solid metal stick to insert the anchors into the holes and to force them as straight as possible inside the holes.

- Dowel CFRP anchors showed better performance than the fiber CFRP anchors since the stain responses on the dowel CFRP anchors side experience lower strains than the other side of beam were the bundle-fiber anchors were installed.

7.10 References

[1] Bonacci, J. F., & Maalej, M. (2001). Behavioral trends of RC beams strengthened with externally bonded FRP. *Journal of Composites for Construction, 5*(2), 102-113.

[2] Khalifa, A., Alkhrdaji, T., Nanni, A., & Lansburg, S. (1999). Anchorage of surface mounted FRP reinforcement. *CONCRETE INTERNATIONAL-DETROIT-*, *21*, 49-54.

[3] Smith, S. T., & Teng, J. G. (2003). Shear-bending interaction in debonding failures of FRP-plated RC beams. *Advances in Structural Engineering*, *6*(3), 183-199.

[4] Oh, H. S., & Sim, J. (2004). Interface debonding failure in beams strengthened with externally bonded GFRP. *Composite Interfaces, 11*(1), 25-42.

[5] Chahrour, A., & Soudki, K. (2005). Flexural response of reinforced concrete beams strengthened with end-anchored partially bonded carbon fiber-reinforced polymer strips. *Journal of Composites for Construction, 9*(2), 170-177.

[6] Eshwar, N., Ibell, T. J., & Nanni, A. (2005). Effectiveness of CFRP strengthening on curved soffit RC beams. *Advances in Structural Engineering*, *8*(1), 55-68.

[7] Al-Amery, R., & Al-Mahaidi, R. (2006). Coupled flexural–shear retrofitting of RC beams using CFRP straps. *Composite Structures, 75*(1-4), 457-464.

[8] Pham, H. B., & Al-Mahaidi, R. (2006). Prediction models for debonding failure loads of carbon fiber reinforced polymer retrofitted reinforced concrete beams. *Journal of composites for construction, 10*(1), 48-59.

[9] Yalim, B., Kalayci, A. S., & Mirmiran, A. (2008). Performance of FRP-strengthened RC beams with different concrete surface profiles. *Journal of composites for construction, 12*(6), 626-634.

[10] Orton, S. L., Jirsa, J. O., & Bayrak, O. (2008). Design considerations of carbon fiber anchors. *Journal of Composites for Construction, 12*(6), 608-616.

[11] Ozbakkaloglu, T., & Saatcioglu, M. (2009). Tensile behavior of FRP anchors in concrete. *Journal of Composites for Construction, 13*(2), 82-92.

[12] Kalfat, R., & Al-Mahaidi, R. (2010). Investigation into bond behaviour of a new CFRP anchorage system for concrete utilising a mechanically strengthened substrate. *Composite structures, 92*(11), 2738-2746.

[13] Kim, S. J., & Smith, S. T. (2010). Pullout strength models for FRP anchors in uncracked concrete. *Journal of composites for construction, 14*(4), 406-414.

[14] Micelli, F., Rizzo, A., & Galati, D. (2010). Anchorage of composite laminates in RC flexural beams. *Structural Concrete, 11*(3), 117-126.

[15] Maghsoudi, A. A., & Bengar, H. A. (2011). Acceptable lower bound of the ductility index and serviceability state of RC continuous beams strengthened with CFRP sheets. *Scientia Iranica, 18*(1), 36-44.

[16] Kalfat, R., Al-Mahaidi, R., & Smith, S. T. (2011). Anchorage devices used to improve the performance of reinforced concrete beams retrofitted with FRP composites: State-of-the-art review. *Journal of Composites for Construction, 17*(1), 14-33.

[17] Smith, S. T., Hu, S., Kim, S. J., & Seracino, R. (2011). FRP-strengthened RC slabs anchored with FRP anchors. *Engineering Structures, 33*(4), 1075-1087.

[18] Zhang, H. W., & Smith, S. T. (2012). FRP-to-concrete joint assemblages anchored with multiple FRP anchors. *Composite Structures, 94*(2), 403-414.

[19] Zhang, H. W., & Smith, S. T. (2012). Influence of FRP anchor fan configuration and dowel angle on anchoring FRP plates. *Composites Part B: Engineering, 43*(8), 3516-3527.

[20] Grelle, S. V., & Sneed, L. H. (2013). Review of anchorage systems for externally bonded FRP laminates. *International Journal of Concrete Structures and Materials, 7*(1), 17-33.

[21] Llauradó, P. V., Ibell, T., Gómez, J. F., & Ramos, F. J. G. (2017). Pull-out and shear-strength models for FRP spike anchors. *Composites Part B: Engineering, 116*, 239-252.

[22] Smith, S. T., Rasheed, H. A., & Kim, S. J. (2017). Full-range load-deflection response of FRP-strengthened RC flexural members anchored with FRP anchors. *Composite Structures, 167*, 207-218.

[23] Ceroni, F., Pecce, M., Matthys, S., & Taerwe, L. (2008). Debonding strength and anchorage devices for reinforced concrete elements strengthened with FRP sheets. *Composites Part B: Engineering, 39*(3), 429-441.

[24] Rasheed, H. A., Decker, B. R., Esmaeily, A., Peterman, R. J., & Melhem, H. G. (2015). The influence of CFRP anchorage on achieving sectional flexural capacity of strengthened concrete beams. *Fibers, 3*(4), 539-559.

[25] ACI Committee. (2014). Building code requirements for structural concrete :(ACI 318-14); and commentary (ACI 318R-14). American Concrete Institute.

[26] American Society for Testing and Materials. Committee C-9 on Concrete and Concrete Aggregates. (2011). *Standard test method for compressive strength of cylindrical concrete specimens*. ASTM International.

[27] ACI Committee 440. (2017). ACI 440.2 R-17: Guide for the design and construction of externally bonded FRP systems for strengthening concrete structures. *American Concrete Institute*.

[28] Rasheed, H. A. (2014). *Strengthening design of reinforced concrete with FRP*. CRC Press.

Chapter 8 - Summary and Conclusions

8.1 Summary

Tables 8-1 and 8-2 present the overall summary of the twelve tested RC beams. These beams were strengthened with CFRP sheets and anchored using different techniques, arrangements, and types of FRP anchors.

Table 8-1 A detailed summary of the results for all tested T-beams

T- Beams					
No	**Anchorage Technique /Type of anchors**	**No of layers or anchors**	**load capacity Any, Ex (kN)**	**Deflection Any, Ex (mm)**	**Failure mode**
T	-	Control beam	57.7, 71.0	269.7, 178.0	concrete crushing
T1	Side GFRP bars	1 on each side	199.6, 197.2	93.0, 88.4	debonding + cover separation
T2	Side GFRP patches	2 per one each side	182.4, 178,2	86.9, 80.3	debonding of CFRP
T3	CFRP Spike anchors (dowel+ bundled fiber)	12 per shear span	173.1, 193.4	88.6, 89.4	debonding + rupture of CFRP
T4	CFRP Spike anchors (dowel+ bundled fiber)	9 per shear span	173.1, 178.0	88.6, 87.6	debonding of CFRP
T5	CFRP Spike anchors	4 per shear span	173.1, 150.3	88.6, 87.9	debonding of CFRP
T6	End anchorage CFRP Spike anchors	1 per shear span	173.1, 138.7	88.6, 69.0	debonding of CFRP
T	Flexural CFRP layers only (Rasheed et al)	-	- 113.7	- 50.1	debonding of CFRP
T	Flexural CFRP layers +U-wraps (Rasheed et al)	2 layers of distributed U-wraps	- 148.6	- 78.7	rupture of CFRP sheets

Table 8-2 A detailed summary of the results for all tested rectangular specimens

Rectangular Beams					
No	**Anchorage Technique /Type of anchors**	**No of layers or anchors**	**load capacity Any, Ex (kN)**	**Deflection Any, Ex (mm)**	**Failure mode**
R	-	Control beam	50.0, 54.7	76.2 79.7	concrete crushing
R1	Side GFRP bars	1 on each side	119.1, 103.5	58.2, 69.9	concrete crushing
R2	Side GFRP patches	1 per one each side	115.3, 97.1	60.9,	concrete crushing
R4	CFRP Spike anchors (dowel+ bundled fiber)	12 per shear span	112.6, 125.0	63.8, 69.3	concrete crushing
R4	CFRP Spike anchors (dowel+ bundled fiber)	9 per shear span	112.6, 120.0	63.8, 77.5	concrete crushing
R5	CFRP Spike anchors	4 per shear span	112.6, 106.0	63.8, 70.1	debonding of CFRP
R6	End anchorage CFRP Spike anchors	1 per shear span	112.6, 112.0	63.8, 57.4	debonding of CFRP
R	Flexural CFRP layers only (Rasheed et al)	-	- 109.4	- 59.7	debonding of CFRP
R	Flexural CFRP layers plus U-wraps (Rasheed et al)	1 layers of distributed U-wraps	- 120.4	- 68.6	concrete crushing

8.2 Conclusions

An investigation for the performance of strengthened RC beams anchored with innovative and different anchorage techniques was conducted in this research study. Six T beams and six rectangular beams were strengthened with identical flexural CFRP sheets. Then, different anchorage systems were applied identically to one of each of the beam types (set 1 – set 6). The first and second sets were secured using side GFRP bars and side GFRP patches, respectively. The third and fourth sets were secured with the same amount of CFRP fibers but with various anchorage

arrangements in terms of anchor diameter and spacing. Also, two types of CFRP anchors (i.e. dowel and bundled fiber anchors) were utilized for these two beam sets (sets 3-4). The fifth beam set had less amount and number of CFRP anchors (4 anchors per shear span) with significantly larger spacing in comparison with sets 3 and 4. An end anchorage system (one CFRP anchor at the end of each shear span) was applied to the last set (set 6).

The experimental results and nonlinear analysis finding showed that the use of side GFRP bars and side GFRP patches significantly increased the load carrying capacity of the T beams to achieve the ultimate predicted strength from the sectional analysis (assuming perfect bond). While, the flexural strength for the rectangular beams did not show noticeable improvement since the beams failed in concrete crushing. Closely spaced-smaller diameter CFRP spike anchors as in set 3 were found to delay the premature debonding by attaining the full flexural sectional capacity up to FRP rupture failure mode for T beam and concrete crushing failure mode for rectangular beam. However, the T beam in set 4 (with same amount of carbon fiber but using larger diameter-larger spacing) failed in debonding with slightly less strength than T beam in set 3. Similarly, the rectangular beam of set 4 gained slightly less strength than the one in set 3, while failing in concrete crushing after steel yielding.

Widely spaced CFRP anchors (set 5) enhanced the strength for the T beam but did not reach the full sectional capacity since the beam failed in premature debonding. Interestingly, the use of U-wrap technique (Rasheed et al. 2015) resulted almost in the same strength as the T beam in set 5. On the other hand, the rectangular specimen for this set failed early in concrete crushing caused by a defect in the top concrete surface of the cast beam. Utilizing the end anchorage technique (set 6) did not successfully improve the strength for both T and rectangular beams.

Dowel CFRP anchors showed stiffer response than the fiber CFRP anchors installed in the same beams. Thus, the T beams in sets 3 and 4 failed in debonding and/or fiber rupture at the shear span side where the fiber anchors were installed. Even though the dowel anchor-shear span side experienced some debonding, it was not as extensive as the fiber anchor-shear span side. That was proved clearly from the strain response on the fiber anchor side that reported higher strains than the other side of the beam where the dowel anchors were applied. Furthermore, the fiber anchor side for the rectangular beams (in sets 3 and 4) had also experienced greater strains than the dowel anchor side. Accordingly, the stiffer dowel anchors may be concluded to offer slightly higher anchoring strength while the more flexible fiber anchors are found to yield slightly more ductility.

8.3 Recommendations

The results and conclusions of this research posed some recommendations for my future work.

1. Extending this study to include applying the same anchorage techniques on bridge girders to examine the flexural improvement in deeper beams.
2. Using closely spaced anchors with small diameters near to the applied loads (from the applied load to the half of shear span) and installing large diameter anchors spaced far apart near to the supports (from the edge of the CFRP sheets to the half of the shear span).
3. Installing the spike CFRP anchors on the beam side to anchor the wrapped CFRP sheets since it was noticed from this research that the debonding starts form the side FRP sheets.
4. Considering one CFRP anchor near the applied load instead of at the end of the CFRP sheets.

Appendix A - Determination of the CFRP Equivalency

Rasheed et. al. (2015) used V-Wrap C100 CFRP sheets in their experiments. In this study, two different CFRP sheet types are used. These are V-Wrap C100 and V-Wrap C220B. The cured laminate properties of these CFRP sheets are:

Thickness of the C100 layer = 0.584 mm
Thickness of the C220B layer = 0.504 mm
Modulus of Elasticity of C100 = 66,180 MPa
Modulus of Elasticity of C220B = 96,500 MPa
Rupture Strain of C100 (tested experimentally) =0.013
Rupture Strain of C220B (from manufacturer) =0.011

A.1 Determination of CFRP Ultimate Strength for Reasheed et al. (2015)

The five CFRP sheets were applied at the bottom face of the beam in this study.
Web width (b) = 152 mm, number of CFRP sheets (C100) = 5 layers

A.1.1 T-beam

$E_f \varepsilon_{fu} A_f$ = 66.18 kN/mm^2 × 0.013 ×152 mm× 0.584 mm× 5 (layers) = 382 kN (Figure A-1)

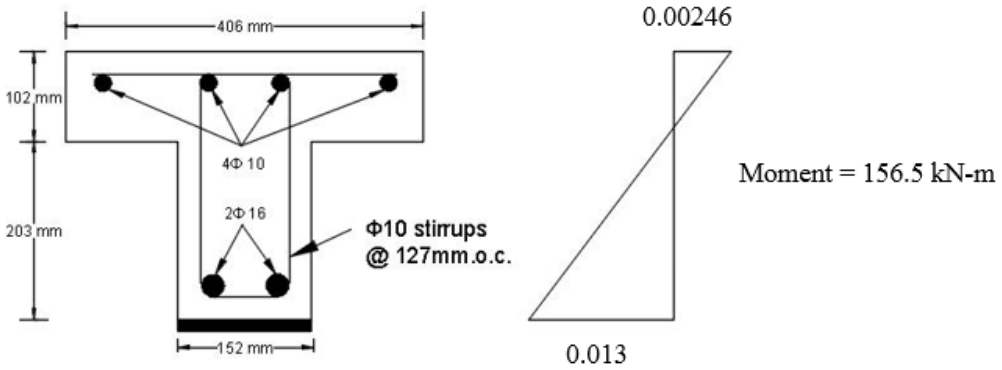

Figure A-1: Ultimate strain profiles for T-beam

A.1.2 Rectangular beam

$E_f \varepsilon_f A_f$ = 66.18 kN/mm^2 × 0.00754 ×152 mm × 0.584 mm × 5 (layers) = 221.5 kN (Figure A-2)

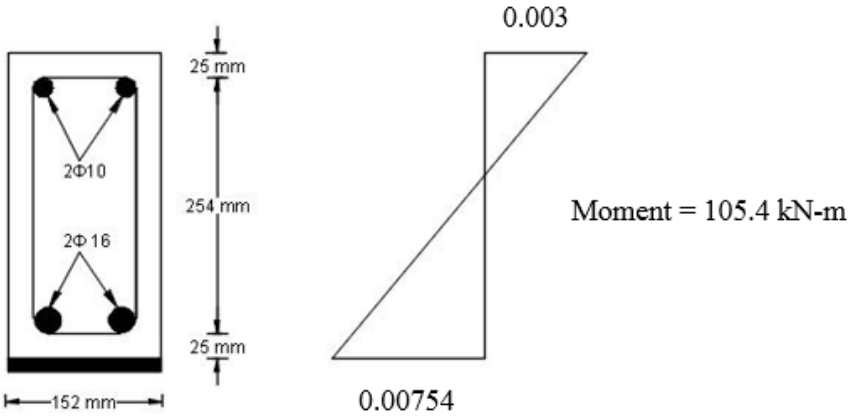

Figure A-2: Ultimate strain profiles for rectangular beam

A.2 Determination of CFRP Ultimate Strength for the Current Work

The strain at extreme tension face is 0.011 and 0.00682 for the T-beam and rectangular beams, respectively. The strain at the center of the 51 mm height (of wrapped C100 layer) up the sides is 0.00985, which 90% of the ultimate strain (0.011) for the T beam, Figure A-3. Also, the strain at the center of the 89 mm height (of wrapped C220B layer) up the sides is 0.00921, which is 84% of the ultimate strain (0.011). For the rectangular beam, the strain at the center of 51 mm height up the sides is 0.00593, which 87% of the ultimate strain (0.011), and it`s 0.00532 at the center of the 89 mm height up the sides for C220B, Figure A-4. The web width (b) is 152 mm, and the number of CFRP sheets is 4 layers (3 of C100 and one layer of C220B) layers as explained earlier.

A.2.1 T-beam

A.2.1.1 Unidirectional V-Wrap C100

The total width of CFRP sheets are 152 mm for the first 2 layers (applied to bottom face only) and 254 mm for the third layer (152 mm was installed to the bottom and wrapped 51 mm up the sides from the soffit).

$E_f\ \varepsilon_{fu}\ A_f$ = 66.18 kN/mm^2× 0.011 × 152 mm × 0.584 mm× 3 (layers) = 193.8 kN

$E_f\ \varepsilon_{fu}\ A_f$ = 66.18 kN/mm^2× (0.011× 0.9) × 51 mm× 0.584 mm × 2 (sides) = 39.0 kN

A.2.1.2.b. Bidirectional V-Wrap C220B

The total width of the bidirectional CFRP sheet is 330.2 mm (152 mm covered the bottom face of the beam and wrapped 89 mm up the sides from the soffit).

$E_f \varepsilon_{fu} A_f$ = 96.5 kN/mm^2× 0.011× 152 mm× 0.508 mm× 1 (layer) = 81.6 kN

$E_f \varepsilon_{fu} A_f$ = 96.5 kN/mm^2× (0.011× 0.84) × 89 mm× 0.508 mm × 2 (sides) = 80.6 kN

Total = 193.8+39.0+39.0+ 81.6+ 80.6 = 395 kN ≈ 382 kN from Rasheed et al. (2015)

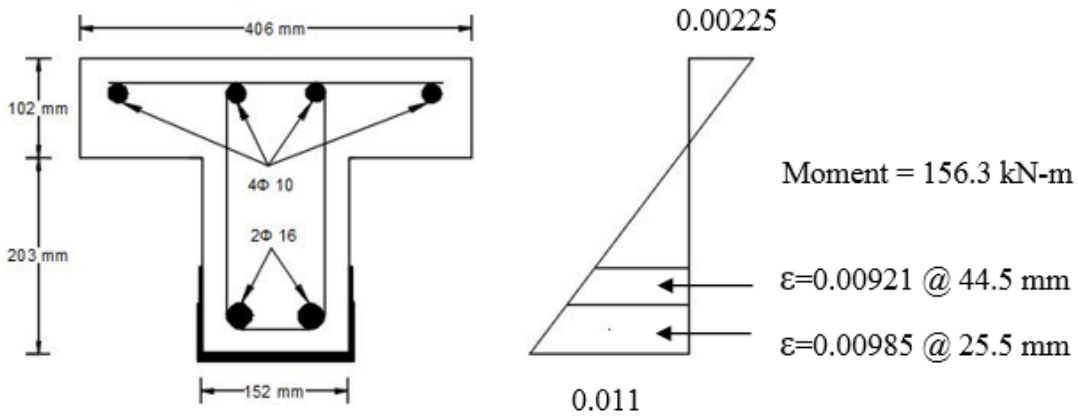

Figure A-3: Ultimate strain profiles for T-beam

A.2.2 Rectangular beam

A.2.2.1. Unidirectional V-Wrap C100

The total width of CFRP sheets are 152 mm for the first 2 layers (applied to bottom face only) and 254 mm for the third layer (152 mm was installed to the bottom and wrapped 51 mm up the sides from the soffit).

$E_f \varepsilon_f A_f$ = 66.18 kN/mm^2× 0.00682× 152 mm × 0.584 mm × 3 (layers) = 120.1 Kips

$E_f \varepsilon_f A_f$ = 66.18 kN/mm^2× (0.00682×0.87) × 51 mm ×0.584 mm × 2 (sides) = 23.3 Kips

A.2.2.2. Bidirectional V-Wrap C220B

The total width of the bidirectional CFRP sheet is 330.2 mm (152 mm was covered the bottom face of the beam and wrapped 89 mm up the sides from the soffit).

$E_f\ \varepsilon_f\ A_f$ = 96.5 kN/mm^2× 0.00682 × 152 mm × 0.508 mm × 1 (layer) = 50.8 Kips

$E_f\ \varepsilon_f\ A_f$ = 96.5 kN/mm^2 × (0.00682× 0.78) × 89 mm × 0.508 mm × 2 (sides) = 46.4 Kips

Total = 120.1+23.3+50.8+46.4 = 241 kN ≈ 222 kN from Rasheed et al. (2015)

Figure 18 shows the strain profiles and maximum moment values for both T and rectangular beams for the specimens that were tested herein.

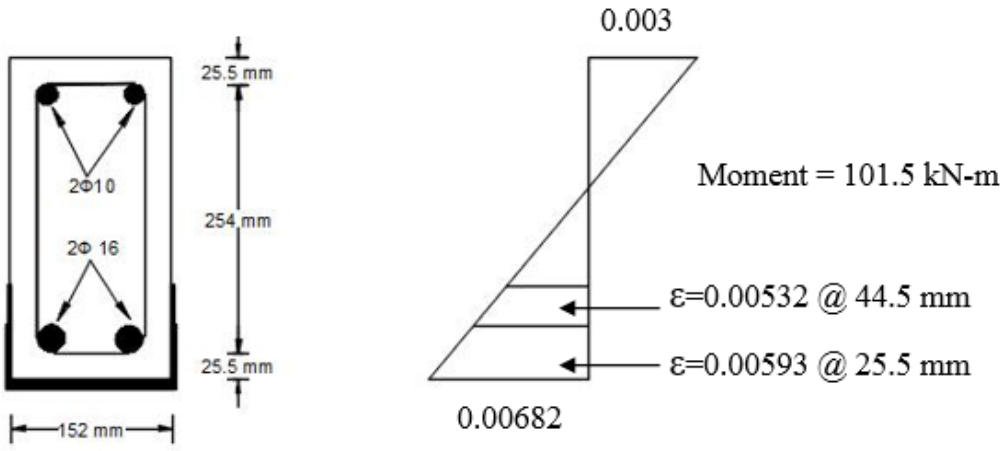

Figure A-2: Ultimate strain profiles for rectangular beam

Appendix B - Strain Gauge Installations

Following are the installation procedures of the strain gauges on the top concrete surface, on the external applied FRP sheets, and on steel rebars. These producers are based on the author's experience and instructions from some specialized strain gauge suppliers such as TML (Tokyo Sokki Kenkyujo Co., Ltd), VPG (Micro Measurements), and HBM strain gauges.

B.1 Strain Gauge Installation on Concrete surface.

Since the strain gauge is used herein only for short-term loading test indoors, coating over the strain gauge is not required. The below steps may be followed to properly install the stain gauges on concrete surface.

B.1.1 Concrete Surface Preparation

a. Remove any paint, particles, or other soiling from gauge installation area on the test specimen to provide a clean contact surface.

b. Use a grinder or an abrasive paper (grade 80 to 120 abrasive paper should be used to finish the surface) any appropriate tool to sooth the installation area.

c. Clean the abraded surface with industrial tissue or cloth dampened with a small amount of an acetone or distilled water.

d. Make sure the installation area is fully dry by removing any moisture since the adhesive may not harden if the gauge installation area on the test specimen is wet.

e. It is recommended to prepare an installation area with 5 mm-perimeter wider than the strain gauge area.

B.1.2 Applying the Adhesive and the Gage into the Place

a. Remove the gage from the transparent envelope by grasping the edge of the gage backing with a tweezer. Then, place the bonding side down on an empty gage box.

b. Use 100-150 mm of PCT-2M gage tape to mask the strain gauge area roughly 20mm larger on each side than the gauge area, Figure B-1a.

c. Position the gage/tape assembly longitudinally on the specimen, Figure B-1b.

d. Lift one end of the tape at about 45degree angle until the gage becomes free of the specimen surface, Figure B-1c.

e. Apply the required adhesive (by manufacture) to the back of the gage and on the specimen (installation area), Figure B-1d.

f. Lay the gage onto the adhesive by pressing it into place gradually from one end so that no air bubbles are trapped under the binder. Press down lightly the gage with a piece of gauze or a tissue to expel any excess adhesive and air bubbles. Pressing should be done utilizing firm pressure with fingers, Figure B-1e.

g. Remove the tape once the adhesive has hardened and the gage being solidly bonded in place. To do that, pull the tape directly over itself, peeling it slowly off the surface to prevent any possible installation damage.

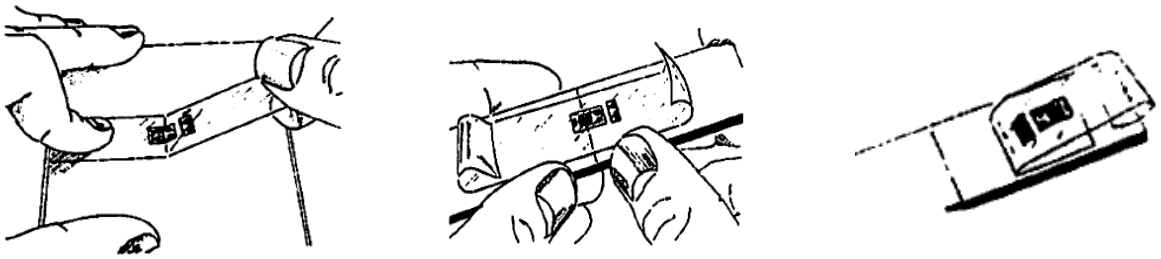

(a) (b) (c)

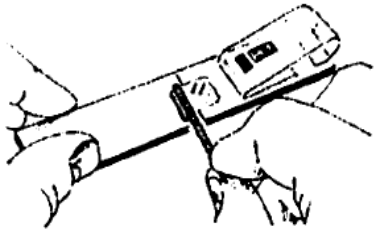

(d)

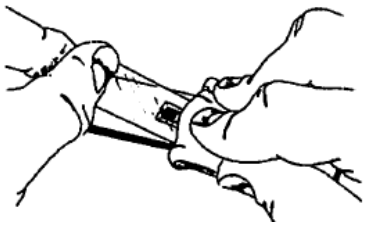

(e)

Figure B-1: Installation of the strain gauges (a); applying a piece of PCT-2M tape (b); position the gage into the place (c); letting up the tape (d); applying the adhesive and (e) laying down gage onto the adhesive.

B.1.3 Soldering the Leadwires.

Some strain gauges are not prewired gages (do not include the leadwirs). Therefore, it is required to install the leadwires after the application of the strain gauges (last step).

a. Place the exposed core of the leadwires on the gauge terminal and apply solder so that the metal foil of terminal will be covered with solder.

b. Make sure to solder the end of leadwires to the terminal and do not extremely heat the terminal to peel off the meatal foil. Figure B-2 shows installed strain gauges on concrete surface for a T beam.

c. Tape the installed wires to the surface of the specimen to avoid any possible damage during the test process (moving the specimen, hooking the wires in the gage reading machine)

Figure B-2: After soldering the leadwires on a T beam surface

B.2 Strain Gauge Installation on FRP surface

B.2.1 Surface Preparation

The installation of the strain gauges on the FRP surface is not needed for the surface preparation as in the concrete's surface. Only a one step may consider to prepare the FRP surface

a. Remove any dust or debris from the FRP sheet surface to have a clean surface area.

B.2.2 Applying the adhesive

a. Repeat steps b-g for applying the adhesive and the strain gauges into to the concrete surface (section B.1.2).

If the adhesive/epoxy is the same as the resin that was used to install the FRP sheets on the concrete surface, the following steps must be considered.

- ❖ Make sure to not press the gage into the adhesive so that will not lose the needed amount of the adhesive to hold the strain gauges in place after curing.
- ❖ Wait a minimum of 24- hours (curing time for the resin) before removing the tape or soldering the leadwires.

B.2.3. Soldering the Leadwires.

If it is needed, the procedure of soldering the leadwires is the same as soldering the leadwires to the concrete strain gages (explained above, section B.1.3). Figure B-3 shows the installation of strain gauges on the FRP sheets.

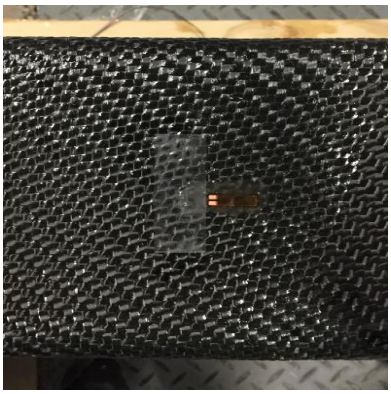

(a)

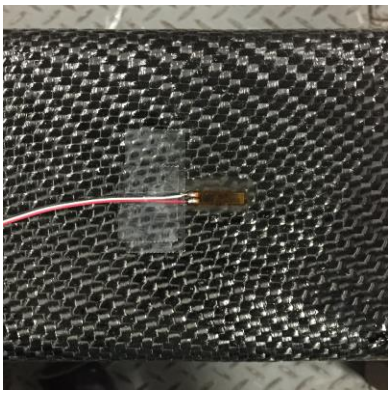

(b)

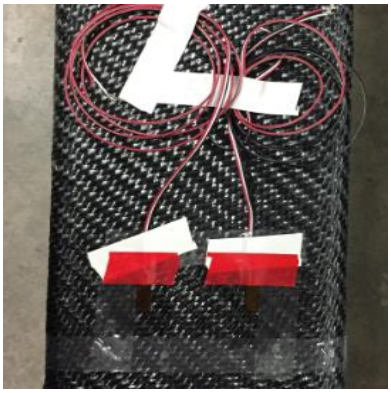

(c)

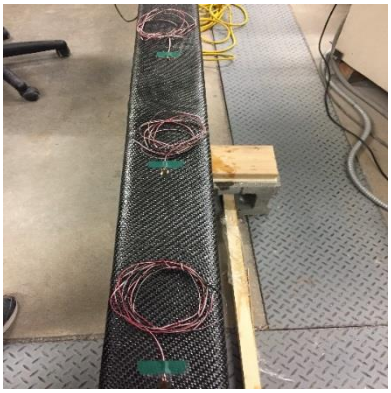

(d)

Figure B-3: Installation of the strain gauges (a); applying the gage on the FRP sheets (b); position the leadwires to the gage terminal (c); Soldering the leadwires (d); taping and wrapping the gage wires (final tough) .

B.3 Strain Gauge Installation on Steel Rebars

B.3.1 Surface Preparation

a. Remove all grease, rust, paint, or any other materials from the bonding area to provide a shiny metallic surface.

b. Use an abrasive paper or a grinder to abrade an area with a 5 mm -perimeter lager than the bonding area.

c. Clean the abraded surface with industrial tissue or cloth soaked with some acetone (chemical solvent). This step mush be repeated until a new tissue or cloth comes completely free of contamination.

d. Clean the bonding area with distilled water and dry the area up.

B.3.2 Applying the Adhesive

a. Repeat steps b-g for applying the adhesive and the strain gauges into to the concrete surface (section B.1.2).

B.3.3 Soldering the Leadwires

Again, the procedure of soldering the leadwires is the same as soldering the leadwires to the concrete / FRP strain gages (explained above in sections A.1.3 and B.2.3).

B.3.4 Protecting the Gages

If the steel rebars are to be embedded in the structural member before casting the concrete, it is extremely important to protect the guage from any moisture and water. Accordingly, some special considerations are required, which include using coated materials and/or waterproof tape. Special kinds of tapes such as SB tape, VM tape or any other suitable tapes may be used for this purpose. However, taping the gage with duct tape, packing tape, or any inappropriate tapes will be insufficient to protect the installed gages from moisture. The application procedure must be performed as stated by the manufacture. Figure B-4 shows the SB tape and the coating material provided by TML (Tokyo Sokki Kenkyuio Co., Ltd) and used in this research to protect the strain gauges of the steel rebars.

(a)

(b)

Figure B-4: Water proves (a) SB tape to cover the gages; (b) coating material

(a)

(b)

Figure B-5: Gage Installation on the steel rebars (a) After the application of SB type; (b) taping the wires outside the specimen before casting